DISSERTATION

MONITORING HETEROGENEITY AND CARBON SEQUESTRATION OF RESTORED RIVER-WETLAND CORRIDORS

Submitted by

Sarah Kathleen Hinshaw

Department of Geosciences

In partial fulfillment of the requirements

For the Degree of Doctor of Philosophy

Colorado State University

Fort Collins, Colorado

Summer 2022

Doctoral Committee:

Advisor: Ellen Wohl

Sara Rathburn
Ryan Morrison
Dan McGrath

ABSTRACT

MONITORING HETEROGENEITY AND CARBON SEQUESTRATION OF RESTORED RIVER-WETLAND CORRIDORS

Innovation of new stream restoration strategies over the past three decades has added much-needed geomorphic complexity and ecological consideration to the practice of stream restoration. With the modernization of stream restoration to include biologically driven feedbacks, methods in monitoring must be simultaneously created to match the current progress. In addition, modern stream restoration practices offer significant opportunity to store carbon in restored river-wetland corridors by increasing carbon sequestration potential of the affected landscapes via rewetting valley bottoms and enhancing fluvial deposition. To address the need for monitoring techniques that capture complex river corridor restoration and carbon sequestration, I present in this dissertation: 1) the development of a geomorphic monitoring strategy that is applied to a valley-scale floodplain enhancement project that involved regrading of the valley bottom and abundant large wood placement, 2) a conceptual framework and protocol for estimating carbon sequestration potential in restored river-wetland corridors, and 3) the application of the latter protocol across multiple restoration projects in the western USA. With the monitoring protocol, which is based on plots rather than river cross-sections, I found finer substrate grain sizes, reduced canopy cover, spatial patterns in particulate organic matter, and the initial signatures of expected changes in heterogeneity at the valley-scale floodplain enhancement project over two years after project implementation. In the context of carbon sequestration among eight sites combined, I found the majority of pre-restoration or degraded condition sites to have significantly fewer carbon stocks than restoration projects or reference conditions, and the highest carbon stocks in reference condition sites. The chapters of this dissertation

are not only intended to provide context and methods to measure stream restoration projects, but also to examine the state and trends of stream restoration in general and to contribute to the understanding of rivers in the global carbon cycle.

ACKNOWLEDGEMENTS

There are numerous people and organizations who have contributed to the success of this project. First and foremost, I would like to thank my advisor, Ellen Wohl, for simply being the best mentor of all time, and the most intelligent and insightful person I have met. I am truly lucky to have received your steady guidance and inspiration over the past 5 years through the completion of my Master's and Ph.D.—it is an absolute honor to work with you.

Although I use the term "I" in this dissertation due to formatting requirements, in reality there are multiple direct contributors to each chapter. Ellen Wohl is a coauthor for all content of the dissertation. My coauthors for the development of the geomorphic monitoring strategy (Chapter 2) are Jonathan Burnett and Steve Wondzell of the US Forest Service. Thank you, Jon, for your friendship, career advice, technical support, and for providing me the opportunity to do this work in the first place. Thank you Steve for your excellent writing and editing skills, thorough conceptual knowledge and leadership, and for serving as a great role model. The rather intense fieldwork for the monitoring strategy would not have happened without the help and field hardiness of Matthew Barker and Katie Nicolato. Thank you both for not only suffering with me, but also for maintaining positive attitudes and having the best sense of humor in the process. Another special thanks goes to my committee members: Sara Rathburn, Ryan Morrison, and Dan McGrath.

The third major component of this dissertation (Chapter 4) required a small army of people to help choose sites, obtain access, learn the background of each restoration project, and to collect field samples. I appreciate field support especially from Juli Scamardo, my close friend, who helped for two years, and the enormous support from Anna Marshall, Taylor Kenyon, John Kemper, Shea Slonkosky, Regi Johnson, Anders Eckert. I am grateful for the following people who helped immensely with project

selection: Paul Powers, Mark Beardsley, Jessica Doran, Johan Hogervorst, Kate Meyer, Lauren Mork, Janice Gardner, Lisa Kurian, all staff at Swaner EcoCenter, and many more.

Funding for this work was provided by Sageland Collaborative (formerly Wild Utah Project), Patagonia, Oregon State University, Colorado Open Lands, and Colorado State University scholarships. Anonymous reviewers provided feedback during the publication process for Chapters 2 and 3.

Finally, I thank the fluvial geomorphology group, or fluvial “flamily”, for the abundant friendship, academic stimulation, and positivity during my time at Colorado State University. I would also like to thank my family, the Hinshaws, for being the best nerds around, my partner, Sean Fancher, who has supported me during my entire PhD through all of the highs and lows, and our cat, Finn, who provided cute distraction throughout the research process. Thank you all for the love and support!

DEDICATION

I dedicate this dissertation to my parents, Jeffrey and Barbara Hinshaw, who have always supported my never-ending natural curiosity. Coincidentally, my father Jeff, a professor at NC State University, plans to retire this year. Thank you, Dad, for encouraging me to get a doctorate degree and inspiring me to continue your legacy as a scholar.

TABLE OF CONTENTS

LIST OF TABLES

LIST OF FIGURES

Chapter 1 Introduction

1.1 Introduction

Process, form, and function of rivers and their floodplains are inextricably linked. Widespread alteration of river process and form occurs as a result of channelization, flow regulation, and changes in land cover (Graf, 1999; James and Marcus, 2006; Grill et al., 2019; Knox et al., 2022). During the past 30 years, river restoration has become a multi-billion-dollar industry within industrialized nations of Eurasia, North America, and elsewhere (Bernhardt et al., 2007), but the ability of restoration to enhance the functions of altered rivers remains limited and controversial (Lave, 2008; Lave and Doyle, 2021). In response to frustrations over the limited effectiveness of past restoration efforts, focus has shifted toward the consideration of rivers and floodplains as ecosystems that rely on interacting physical and biologic drivers (Castro and Thorne, 2019), rather than neutral pipes that convey water and sediment. At the core of these ecosystems are the processes that influence river planform, connectivity, diversity, persistence, resilience, and retention. In recognition of these processes upstream, downstream, and at the watershed or larger scale, process-based restoration was developed as a paradigm shift in the restoration industry that more effectively captures the complex nature of river corridors (Beechie et al., 2010).

1.2 Process-based river restoration

Process-based river restoration is an umbrella term well described by Beechie et al. (2010). This type of restoration differs from form-based restoration due to the consideration of stressors and site-specific floodplain processes that influence the needs of each project. The counterpart to process-based restoration is form-based restoration, where a prescriptive form can be engineered and applied ubiquitously according to the physical form of the existing channel (Rosgen, 2011). To conduct process-

based restoration in rivers, the first task is to identify processes causing degradation, then match natural processes that can be enhanced to improve floodplain function and address the cause of degradation. Examples of geomorphic processes considered are hydrologic connection, sediment and organic matter deposition, lateral channel migration, and groundwater recharge. Biological processes such as vegetation succession and ecosystem engineering by beaver (*Castor* spp.) are equally important in their influence on floodplain function (Castro and Thorne, 2019; Johnson et al., 2020). To restore river corridors with processes, floodplains are supplemented with materials to "restore themselves" to dynamically stable and resilient forms, utilizing natural processes to enhance desired functions.

Fully functional floodplains, sometimes considered reference floodplains or successful projects if they underwent restoration treatment, typically reach self-sustaining conditions and show expressions of a combination of processes that facilitate diversity and resilience. Two of these conditions are the Stage 0 anastomosing wooded wetland and anastomosing grassed wetland in the stream evolution model described by Cluer and Thorne (2014). This stage in the stream evolution model (Cluer and Thorne, 2014) and henceforth the term "Stage 0" represents a pre-anthropogenic disturbance, anastomosing planform in a hydrologically connected floodplain wetland corridor. It is important to note that Stage 0 is a river condition rather than a restoration technique, and that the increasingly popular phrase "Stage 0 Restoration" does not imply the use of heavy machinery or any other technique to achieve the Stage 0 condition. Recognizing the examples of the two mentioned floodplain forms, it is also important not to repeat mistakes associated with practices such as natural channel design (NCD; Rosgen 2011) by subscribing as a river restoration community to a trend or universal style of restoration based on a river's appearance (Lautz et al., 2019). Instead, river restoration designers should think critically about what processes are specifically relevant to a floodplain on a case-by-case basis.

Actions to implement process-based restoration (PBR) follow a continuum from simple intervention to total valley reset (Figure 1.1, e.g., Powers et al., 2019) in which the entire river corridor is regraded to enhance channel-floodplain connectivity. Examples of restoration actions along the PBR continuum, in order of ascending magnitude of intervention in river process and form, are low tech process-based restoration (LTPBR; Wheaton et al., 2019) and installation of a few smaller scale obstructions in the channel that are designed to mimic beaver dams (e.g., beaver dam analogues, BDAs, or post-assisted log structures, PALs) ; abundant LTPBR involving numerous structures within a small area; regrading of the valley bottom to a geomorphic grade line that reflects the pre-disturbance valley surface (Powers et al., 2019), and legacy sediment removal (Walter and Merritts, 2008). The action chosen for treatment of a floodplain depends on local constraints including the scale of the problem, local infrastructure, property ownership, permits, funds, staffing, and regulations.

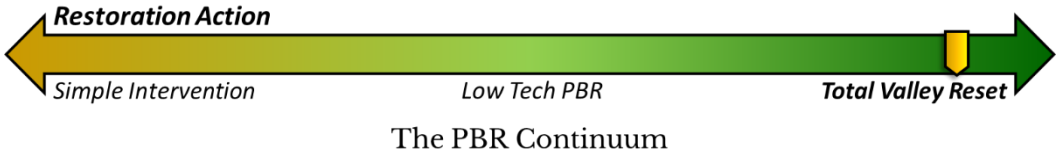

Figure 1.1. Conceptual diagram of the "PBR Continuum" which illustrates that process based restoration (PBR) can take place with a variety of methods that vary in magnitude of restoration action depending on the site in question. The yellow slider is intended to appear mobile and is currently positioned over “Total Valley Reset” because the example project described in the first chapter of this dissertation can be considered a total valley reset.

Process-based restoration continuously enhances ecosystem services provided by floodplains including habitat, fire and drought mitigation, flood attenuation, climate change resilience, recreation, and potential for carbon sequestration (Daily 1997; Hanna et al., 2018; Kaiser et al., 2020). The use of the term ecosystem services can be interpreted to imply that the value of ecosystems is solely related to how humans can benefit from floodplains (Daily, 1997; Chan et al., 2012, Norton 2012), but in this dissertation the term is used due to its widespread familiarity with readers and is intended to include the intrinsic value of floodplain ecosystems and the benefits to other species. Ecosystem services such

as habitat provision and attenuation of peak flow magnitude and energy are often prioritized over carbon sequestration due to perceived immediate stakeholder needs, and because there is limited scientific evidence within existing literature of carbon sequestration within restored floodplains.

With this dissertation, I discuss two needs that occur simultaneously with new and innovative styles of river restoration and the rapid growth of the river restoration industry. The first need is a monitoring strategy that captures variability within restoration projects that include entire floodplains with multiple channels, and in projects that strive to increase floodplain heterogeneity. Traditional transect-based geomorphic monitoring techniques that were developed for single thread channels are less relevant to multithreaded channel planforms and projects that include the entire valley bottom. The first chapter of my dissertation addresses this need and provides an alternative to transect-based monitoring with the development of an unbiased and spatially comprehensive monitoring strategy that can be paired with remote sensing data in the future. This chapter is published in *Earth Surface Processes and Landforms* (Hinshaw et al., 2022).

The second need includes a method to determine capacity for carbon sequestration in process-based stream restoration, particularly in the forms of soil carbon and large wood. It is not yet known how restoration can impact organic carbon stocks, and a better understanding of this concept can first be addressed through determination of potential controls on carbon storage in floodplains in general. This need is addressed in the second and third chapters of the dissertation. In the second chapter, I introduce and review a conceptual model for drivers of carbon sequestration in the context of river restoration and provide a protocol for measurement of carbon stocks of restoration projects in comparison to surrogates for pre and post restoration conditions. This chapter is published in *Frontiers in Earth Science* (Hinshaw and Wohl, 2021). In the third and final chapter of the dissertation, I present a test of this protocol across more than 30 floodplains and eight restoration projects in the western United States.

Chapter 2: Development of a geomorphic monitoring strategy for Stage 0 Restoration in the South Fork McKenzie River, Oregon, USA[1]

Summary

The South Fork McKenzie River (SFMR) in western Oregon, USA hosts one of the largest Stage 0 stream restoration projects implemented to date. Stage 0 refers to a multichannel planform with strong hydrologic connectivity to the adjacent floodplain and surface-subsurface connectivity. Stage 0 restoration was implemented on a 900-m-long reach of the SFMR by re-grading the channel and floodplain using 65,000 m^3 of sediment to raise the channel bed. Thousands of large logs were added and the ends of some logs were buried in the sediment to provide foundations for future log jams. My primary objective is to present a monitoring protocol based on randomly located sampling plots. I also analyze results from two years of data collection since project implementation. Within each plot, I measured canopy cover, wood volume, flow depth and velocity, organic cover (area covered by coarse and fine organic material), and substrate grain size. I used intracluster correlation coefficients and variance of measured variables to assess heterogeneity at three spatial scales: within plots, between adjacent plots, and across the entire site. Here, I evaluate changes in the first two years after restoration (i.e., not pre- vs post-restoration). I hypothesized that heterogeneity within a plot would decrease as the plot adjusted to local-scale hydraulics and sediment and particulate material transport. I hypothesized that heterogeneity would increase between adjacent plots and across the entire site. I found that spatial heterogeneity of geomorphic variables decreased within plots. Heterogeneity of organic cover, sediment size, and flow depth increased between adjacent plots, although other variables did not change. Site-

---

[1]Chapter published as Hinshaw, S., Wohl, E., Burnett, J.D. and Wondzell, S., 2022. Development of a geomorphic monitoring strategy for stage 0 restoration in the South Fork McKenzie River, Oregon, USA. Earth Surface Processes and Landforms. **https://doi.org/10.1002/esp.5356**

scale heterogeneity decreased for all variables except organic cover and substrate. I interpret the observed geomorphic responses to reflect decreased longitudinal connectivity and increased lateral and vertical connectivity at the restoration site.

2.1 Introduction

2.1.1 Stage 0 restoration

Process-oriented stream restoration has gained traction as an alternative to form-based restoration in recent decades (e.g., Palmer et al., 2014; Wohl et al., 2015). Process-based restoration accounts for the trajectories of channel form and function through time, beginning from pre-restoration conditions and extending decades or more beyond treatment. This type of stream restoration incorporates drivers of channel change such as water and sediment supply, anthropogenic influence, and natural trends in channel evolution (Brierley and Fryirs, 2016). Conceptual cycles of channel evolution such as the channel evolution model (Schumm et al., 1984), stream evolution model (Cluer and Thorne, 2014), and stream evolution triangle (Castro and Thorne, 2019) have guided our understanding of how rivers evolve and respond to disturbance.

There will likely be more iterations of how geomorphologists describe the nuanced progression of fluvial landscapes, but several key components of "healthy" river corridors have already emerged. These include increased planform complexity (Martens and Connolly, 2014), more abundant large wood where applicable (Wohl 2017a; Wohl et al., 2019), biota as an important driver of channel form (Gurnell et al., 2016; Castro and Thorne, 2019; Polvi et al., 2020), and re-establishment of three-dimensional connectivity for water, sediment, nutrients, particulate organic matter, and large wood to a degree that would be expected under natural conditions in a particular river corridor (e.g., Stanford and Ward, 1993; Pringle, 2001; Wohl, 2017b). (Here, large wood refers to pieces > 10 cm diameter and 1 m long.) The emphases on planform complexity and greater abundance of large wood in the channel(s) and

floodplain reflect the realization that channel and floodplain spatial heterogeneity were much greater in many rivers prior to anthropogenic modifications (e.g., Triska, 1984; Collins et al., 2012; Brown et al., 2018) and that large wood was much more common and widespread in forested river corridors (e.g., Montgomery et al., 2003; Wohl, 2014). Changes in spatial heterogeneity and large wood have in turn strongly influenced connectivity, typically by increasing longitudinal connectivity but decreasing lateral and vertical connectivity within the river corridor (Collins et al., 2012; Wohl and Beckman, 2014; Doughty et al., 2020).

In practice, stream restoration project designers may choose ideal conditions to restore to, such as Stage 0 or Stage 8 of the stream evolution model (Cluer and Thorne, 2014). Both of these stages represent anastomosing wet woodland or grassed wetland river corridors, but Stage 0 is assumed to reflect conditions prior to anthropogenic modification and Stage 8 represents a stable endpoint after multiple adjustments following anthropogenic modification. There are many interventions that can nudge a channel-floodplain complex toward Stage 0 conditions, including low-tech process-based restoration (Wheaton et al., 2019), valley-scale matching to a geomorphic grade line (Powers et al. 2019), and removal of legacy sediment (Walter and Merritts, 2008; Booth et al., 2009; Hartranft et al., 2011). Restoration toward the Stage 0 condition at the South Fork McKenzie River (SFMR) in Oregon, USA utilized the entire valley bottom to reconnect an incised channel to its floodplain, disperse surface flow into multiple complex channels via an anastomosing planform, and enhance lateral and surface-subsurface hydrologic connectivity. The primary goal of this restoration was to enhance habitat for fish by providing more in-channel complexity with large wood and side channels, which can enhance biological productivity (Bellmore et al., 2013; Ogston et al., 2014), and by retaining sediment finer than cobble- to boulder-size in order to provide salmonid spawning habitat.

2.1.2 Monitoring, spatial heterogeneity, and connectivity

It is important to quantify changes and track channel evolution in response to restoration treatment. Because restoration toward Stage 0 conditions is both relatively new and becoming increasingly popular (Hartranft et al., 2011; Powers et al. 2019), monitoring can help quantify outcomes and keep track of lessons learned from early Stage 0 projects, addressing such questions as: Are the restoration projects sustainable on decadal scales? How do channels evolve through human-made anastomosing conditions? How much added wood is appropriate to transform the full valley bottom into well-connected floodplain, and how is the wood retained and reorganized over time? These questions can be answered by long term monitoring efforts that track restoration projects from initial construction through continuing channel adjustment over a period of years. Monitoring is critical for any restoration (e.g., Bernhardt et al., 2005; England et al., 2008), but especially in innovative styles of restoration that may become more widely adopted and repeated within a short time span. Typically, funding for monitoring is much less available than is funding for project construction and is not allocated to support long term monitoring efforts (Lautz et al., 2019). Thus, to utilize monitoring data to improve restoration designs, monitoring techniques must balance thorough, accurate, and frequent data collection with budget constraints.

The SFMR Floodplain Enhancement Project is a spatially extensive Stage 0 restoration project in the western Cascade Mountains of Oregon. The large scale and strenuous nature of ground-based access at the project led to potential difficulties with traditional, transect-based geomorphic monitoring efforts on the SFMR, especially during high flows. Hence, the need for new geomorphic monitoring techniques that can apply to this project and can also be extended to other large, valley-scale restoration projects. To address this challenge, I designed a sampling strategy utilizing geomorphic field plots that can be paired with data collection by Unmanned Aerial Vehicles (UAV; i.e., drones). My primary objective in this chapter is to present the field component of this monitoring strategy. I also explore the results of the first two years of field data following implementation of the new field-based

monitoring strategy by examining adjustment and analyzing geomorphic spatial heterogeneity at multiple spatial scales. Addressing the questions listed earlier requires monitoring over much longer periods of years to decades. However, it is useful to provide a preliminary test of that strategy in the first years after restoration so as to determine the efficacy of the proposed strategy and identify potential modifications. In this chapter, I also explicitly apply the metrics measured as part of monitoring to understanding spatial heterogeneity and connectivity within the treated river corridor.

My primary goal is to develop a field geomorphic monitoring strategy that is easily accessible, statistically viable, and pairs well with remote sensing data. I chose to measure geomorphic field plots, rather than traditional transects, because plots are more likely to capture diverse scales of spatial heterogeneity that are an emphasis of restoration at the site. Transect-based stream monitoring was developed for single-threaded systems as a means of quantifying variables used in hydraulic equations (e.g., Leopold, 1962; Osterkamp et al., 1991). Although concepts addressed by transects remain relevant, valley-scale floodplain reconnection is more complex than a single channel and needs better representation than a single variable such as the hydraulic radius. In addition, the increasing availability of monitoring with drones allows most plan-view, and sometimes vertical, hydraulic geometry variables to be estimated remotely with aerial imagery.

I align my monitoring efforts with the original goals of restoration. Geomorphic field plots can capture changes in geomorphic variables and spatial heterogeneity, which I assess using the variables of substrate (sediment size), hydraulics (surface water depth and flow velocity), wood volume, organic cover (proportion of area covered by organic material), and canopy cover. Changes in these site characteristics impact habitat conditions for spring Chinook salmon (*Oncorhynchus tshawytscha*), bull trout (*Salvelinus confluentus*), Pacific lamprey (*Entosphenus tridentatus*), and many other species.

I do not have pre-restoration plot data from the site because my plots were established after the site was treated. Consequently, I cannot directly compare pre- and post-restoration site characteristics and I focus my analyses on changes occurring the first two years following restoration. I evaluate changes in each of the variables listed above (Table 2.1 lists expected changes during the 2 years). Initial conditions immediately after restoration largely reflect the placement of large wood and anthropogenic disruption of topography and sediment distribution. With time, geomorphic processes will presumably redistribute sediment, as well as large wood and particulate organic matter, creating associated changes in substrate, hydraulics (flow depth and velocity), wood volume, and organic cover.

I define three spatial scales at which I evaluate changes in heterogeneity during the first two years following restoration: intra-plot, intermediate-scale inter-plot, and site-scale inter-plot. Intra-plot represents heterogeneity at length scales of a few meters within sampling plots. Intermediate-scale inter-plot represents heterogeneity among adjacent plots at 10^1–10^2 meters, which average 68 m apart, with a range of 29 to 204 m. Site-scale inter-plot represents heterogeneity across the entire restoration site covering 45 ha, extending along a 900-m long reach of valley floor that averages 500 m in width. I hypothesize that intra-plot heterogeneity will decrease with time since restoration as plot characteristics increasingly reflect local hydraulics and sources of sediment, wood, and particulate organic matter. I hypothesize that intermediate-scale heterogeneity will increase, such that heterogeneity between adjacent plots will be greater than heterogeneity within a single plot. I expect that abundant, newly placed large wood provides the context for diversity of depositional rates and revegetation at this intermediate scale, leading to the formation of patches. Finally, I hypothesize that site-scale inter-plot heterogeneity will increase as local controls exert progressively more influence after the initial disturbance of restoration that tended to homogenize conditions throughout the floodplain. The data collected during these first two years after restoration will provide a baseline for evaluating ongoing, longer-term river adjustments.

The objective of this chapter is to utilize and evaluate a new method for monitoring stream restoration projects where traditional monitoring is less appropriate. I compute simple statistics to assess geomorphic change over two years of monitoring, use field data to examine potential changes in heterogeneity at the three spatial scales, relate changes in heterogeneity to inferred connectivity, and evaluate the benefits and shortcomings of the new monitoring strategy.

Table 2.1. Expected changes for the South Fork McKenzie River

Variable	**Expected change**	**Influences: short term**	**Long term**
Canopy cover	Decrease	Trees falling due to raised water table	Decrease until stable vegetated islands form, then increase with growth of riparian trees
Organic cover	Increase	Accumulation of OM due to lower slope and trapping potential by LW, depositional setting	Increase to stable level
Wood volume	Dependent on flows	1) Insufficient peak flows to move large wood or 2) With sufficient flow, LW pieces will condense into jams, reducing the average encountered LW volume per plot	Decrease as wood forms jams, jams initiate island formation, and islands become vegetated
Grain size	Decrease	Construction upstream (Phase 2) loosened fine materials that are deposited in Phase 1	Depending on peak flows, fines from construction may be flushed. Main channels: gravel and cobble expected, Side channels: Sand and silt expected until incision to a former channel surface, then gravel
Water velocity	Stay the same	Water is spread out across the floodplain; 2 years not adequate to form channels	Eventual formation of more established multithreaded channels with many pockets of slow areas
Water depth	Stay the same	2 years not enough time for more defined channels to form below a dam.	Increase until a threshold is reached as stable multithreaded channels form
Heterogeneity	Increase	Stay the same over 2 years, but has increased compared to pre-restoration	Islands form, vegetation establishes, flow is diverted to secondary channels and forms patches of different substrate size; wetlands form in forested floodplain

2.2 Study Area

The SFMR (44.16°N 122.29°W; Elev. 340 m) is located near Rainbow, Oregon, USA in the western Cascade Mountains. Annual precipitation exceeds 1778 mm in the Western Cascades Lowlands and Valleys Ecoregion, supporting lush western hemlock (*Tsuga heterophylla*)-Douglas-fir (Pseudotsuga menziesii)- western redcedar forests (Thuja plicata) with red alder (Alnus rubra) and cottonwood (Populus trichocarpa) adjacent to stream channels. The river drains approximately 560 km^2. Streams provide habitat for spring Chinook salmon and bull trout among other species (Thorson et al 2003).

Potential flood hazards to the city of Eugene and surrounding areas led to the construction of dams and reservoirs throughout the western Cascade mountains in the mid-20th century, including Cougar Dam on the SFMR. These reservoirs generate hydroelectricity, store snow melt for irrigation, and augment summer low flows and thus improve water quality in the downstream Willamette Valley. The construction of Cougar Dam in 1963 reduced sediment supply to the lower river and led to channel degradation in the lower South Fork McKenzie River. Peak flows were drastically reduced from 280 to 120 m^3/s, with base flows around 9 m^3/s (Figure 2.1). Based on valley-floor morphology and nearby reference sites that have not been affected by flow regulation, the portion of the SFMR below the dam likely transformed after dam construction from a multithreaded system into a single thread, high energy, transport-dominated system. Despite the reduction in peak flows, simplification to a single channel and lack of sediment connectivity with upstream reaches caused streambed incision of up to 4.3 m (Meyer 2019). The channel bed became armored with boulders, with little to no gravel-sized sediment to provide spawning habitat for Chinook salmon. Streambed substrate suitable for spawning is critical for sustaining salmonids. Fish of a given species or length can spawn in a range of substrate sizes. In general, however, individual fish can spawn in sediment with a median diameter up to about 10% of their body length (Kondolf and Wolman, 1993). For Chinook salmon, this equates to a range of about 25–150 mm median diameter (Merz and Setka, 2004).

In an effort to improve habitat and reconnect the SFMR to its floodplain, the US Forest Service and McKenzie Watershed Council partnered to reset the valley bottom in the 6 km stretch between Cougar Dam and the confluence with the McKenzie River.

The project is divided into phases that progress from downstream to upstream. Phases I and II were completed in 2018 and 2019, respectively. Project construction followed the Geomorphic Grade Line approach of Powers et al. (2019), where the channel and floodplain are graded to match the average slope of the valley. Nearly 4,000 large wood pieces were placed throughout the valley bottom and 65,000 m3 of sediment were redistributed from leveed banks and other high portions of the floodplain in Phase I (Figure 2.2, Meyer et al., 2018). Monitoring efforts in 2019 and 2020 included teams of geomorphic, ecologic, remote sensing, aquatic invertebrate, and fisheries scientists. The monitoring strategy described in this chapter was piloted in Phase I for the geomorphic characteristics of the restoration area. Phase I lies downstream from Phase II and was implemented before restoration activities immediately upstream in Phase II. Due to construction during 2019 in Phase II upstream, the portion of floodplain restored during Phase I may have been affected by mobilization of sediment during restoration-related disturbances in Phase II. However, flow is diverted during in-channel work and because the wetted channel is widened and large wood pieces increase hydraulic roughness, it is not clear how much the upstream restoration work would influence my results from the second year of monitoring.

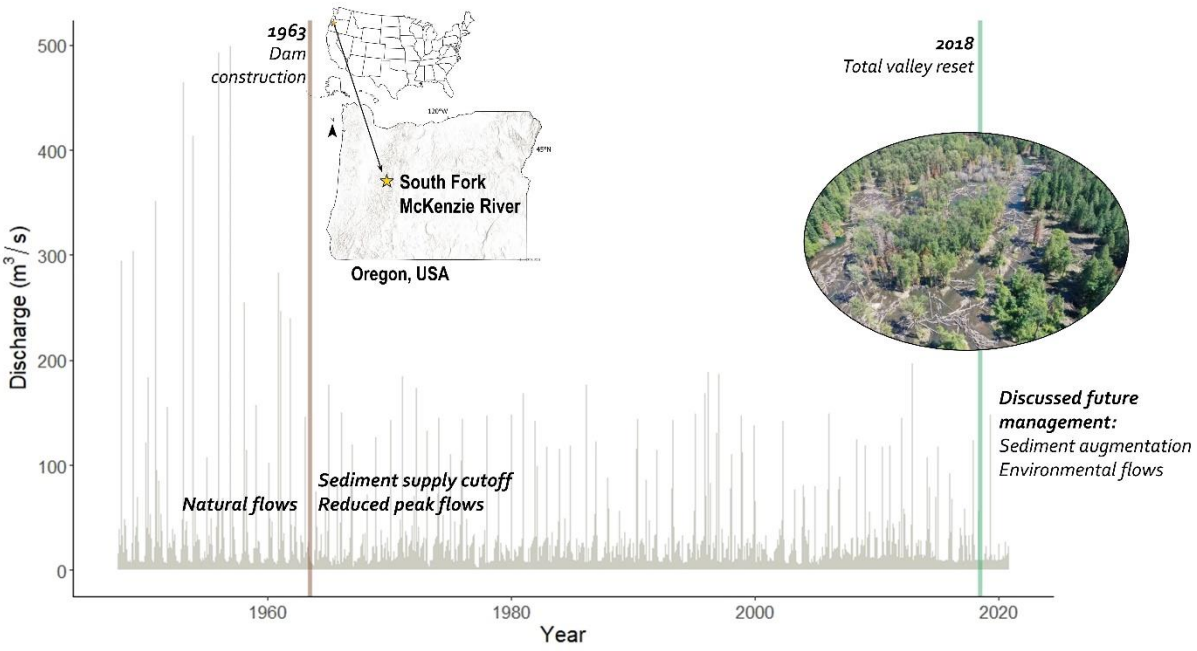

Figure 2.1. Flows at the South Fork McKenzie River (44.1596°N, 122.2864°W) before and after Cougar Dam construction in 1963. Phase I of the South Fork McKenzie River Floodplain Enhancement Project was implemented in 2018. The photo of the SFMR in this figure was obtained from an October 2019 NBC16 Eugene news article by Kelsey Christensen.

2.3 Methods

My geomorphic sampling design includes 40 hexagonal plots selected at random from a 4000-plot tessellation overlaid on the 0.45 km^2 Phase I treatment area. Each plot has an area of 42 m^2 and contains four 1-m-radius circular subplots. Plots are distinguished as either interfluve forested land (not flooded at typical high flows) or surface inundated at high flow (which includes the active channel). I chose 40 plots to pilot the monitoring strategy as a means of balancing time constraints and the need for a sufficiently large dataset for statistical analyses.

The highest flow released from Cougar Dam over the duration of my study was 141.6 m^3/s. This discharge has a recurrence interval of 3.1 years, calculated using the period of record after dam construction (Moore, 2002). The geographic extent of the floodplain was mapped and divided into high

flow wetted area, forest, and barren ground. In this study, I discuss only the area inundated during high flow. Regions of flow were not further stratified into back channels, main channels, flooded forest, etc. because the distribution of those potential strata is expected to change dramatically as the newly restored channel reaches a dynamic equilibrium over time. In total, 36 geomorphic instream plots were surveyed during the summer of 2019. The instream plots that were not surveyed in 2019 were either deemed unsafe for field measurements or unintentionally missed during my field work. Due to limitations imposed in response to the COVID-19 pandemic, I was only able to resurvey 23 of the 36 plots during the summer of 2020 (Figure 2.2). The paired data from these 23 plots were used for statistical tests.

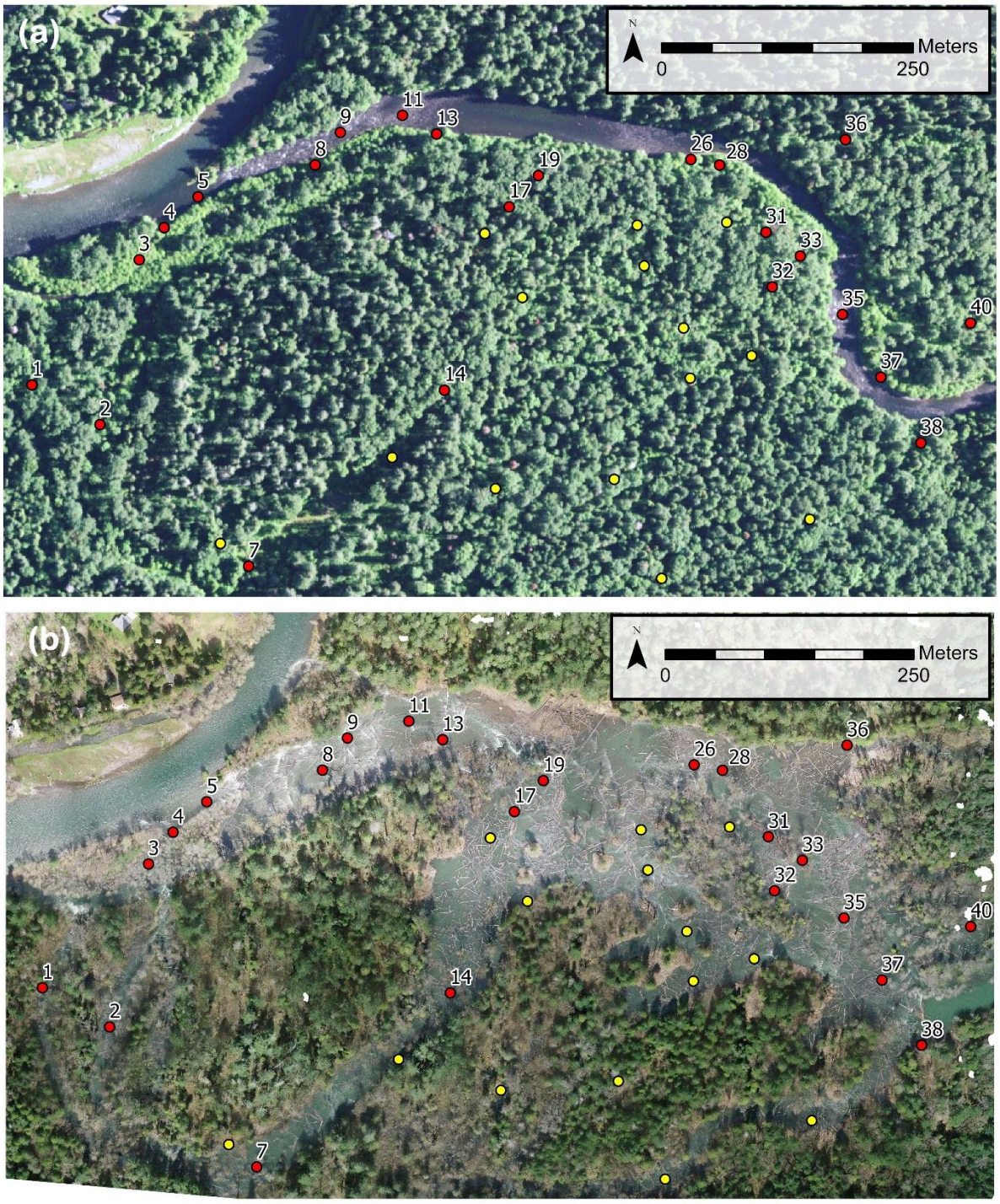

Figure 2.2. (a) Pre-restoration 2016 NAIP imagery with geomorphic plot locations. (b) Drone imagery captured during a high flow event in April 2019 of Phase 1 of the South Fork McKenzie River (Scott, 2019) . Geomorphic field plots measured in both 2019 and 2020 are red and labeled with plot numbers. Yellow plots were measured only in 2019 but may be surveyed in future monitoring strategy iterations.

The design of the geomorphic monitoring plots was based on US Forest Service Forest Inventory and Analysis protocols (Bechtold and Patterson, 2005). I used a two-stage cluster sampling design in which geomorphic field plots are the primary sampling units and subplots within geomorphic field plots are secondary sampling units. Thus, each 42 m^2 hexagon was divided into four subplots: one center subplot, and three outer subplots, the centers of which are located 3 m from the center at azimuths 30°, 150°, and 270° (Figure 2.3). In the field, the survey team navigated to the center plot location using a 0.3 m horizontal accuracy EOS Arrow 100 GNSS receiver and used a tape and compass to determine the outer subplot locations. The design of four closely spaced subplots allows for analysis of spatial heterogeneity at multiple levels of proximity.

At each subplot, I measured large wood volume, percent organic cover, water depth and velocity, canopy cover, and substrate (Table 2). Velocity was measured at both the surface and 60% depth to identify differences between surface and deeper water. Water depth, velocity, and canopy cover were measured at the center of the subplot, and were expected to represent the average of the 3.14 m^2 area. Organic cover, large wood, and substrate measurements covered the entire subplot, and were measured via trained visual estimation, diameter and length measurements, and a random 10-clast sample, respectively. I chose these variables because they represent easily measured components of aquatic ecosystems (Baron et al., 2002). For example, canopy cover can provide shade which is often important in maintaining thermal refugia, may limit algal growth (Mosisch et al., 2008), and influences litterfall and particulate organic matter in the stream (Maguire, 1994). Substrate size determines physical habitat available for spawning (Tappel and Bjornn, 1983); large wood provides habitat structures and food resources (e.g., Fausch and Northcote, 1992; Wipfli and Baxter, 2010); organic cover provides energy sources to stream organisms (Tank et al., 2010); and water flow and its variability provide dissolved oxygen, habitat diversity, and connectivity (e.g., Pringle, 2001).

An identical set of measurements was collected at each of the four subplots. However, I slightly modified the field sampling protocol in 2020, adding the large wood measurements in all three of the outer subplots. Previously, these data were only collected in the central subplot (Figure 2.3, Table 2.2). At each 1 m-radius subplot, I measured canopy cover with a modified 17-point spherical densiometer in each cardinal direction; water depth with an engineer's rule; velocity at the surface and 60% flow depth using a Marsh-McBirney 1D velocimeter; the size of each piece of large wood that intersected the plot, using a metric tape for piece diameter and TruPulse 360° laser range finder for piece length; and sediment size via gravelometer with 10 randomly selected clasts per subplot (Table 2). Because field surveys took place in July-August 2019 and 31 August-4 September in 2020, I expect there to be no change in canopy due to seasonal differences.

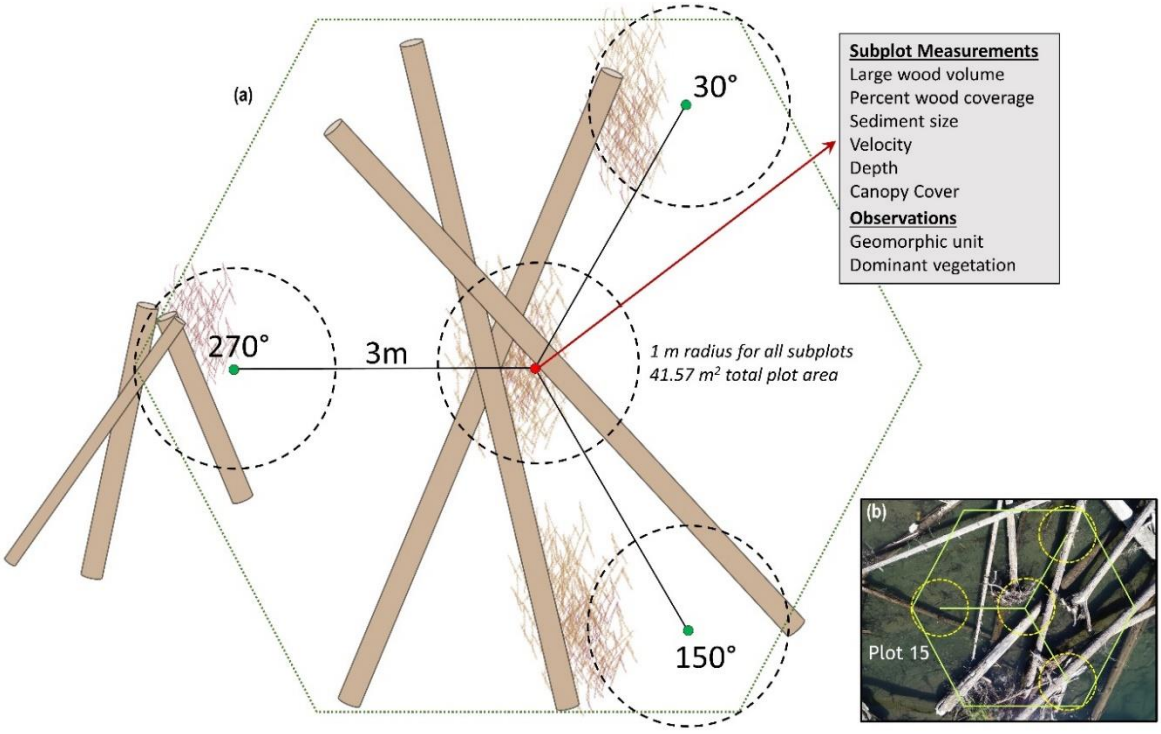

Figure 2.3. (a) Layout of geomorphic field plot. Outer subplots are distributed around the center subplot at 30°, 150°, and 270° azimuths. (b) A photo example of a geomorphic field plot with overlay of plot design.

Table 2.2. Measurement methods for on-the-ground plots at South Fork McKenzie River

Category	Location	Measurement technique
Large wood (>10 cm diameter, > 1 m length)	Center subplot, 2019 All subplots (2020)	• Measure diameter within subplot area of each piece with diameter tape • Measure length with tape or laser range finder
Organic cover: percentage area covered by large wood, fine wood, and particulate organic matter	All 4 subplots	• Estimate visually *Note: Field technicians must train their eyes on a control area beforehand*
Water depth	All 4 subplots	• Measure with tape at each subplot center. Note if dry.
Water velocity	All 4 subplots at surface and 60% depth	• Measure velocity in maximum flow direction with Marsh McBirney velocimeter
Water temperature	One sensor per plot	• Tie HOBO temperature sensor to log or other stable object at plot center. Take photo, GPS point, and location description
Canopy cover	All 4 subplots	• Average 4 densiometer readings, one for each cardinal direction
GPS location	All 4 subplots at center	• Record GPS points within 0.3 m accuracy (used Arrow GNSS receiver)
Sediment	All 4 subplots	• Measure b-axis of 10 randomly selected clasts per subplot with a gravelometer.

2.3.1. Data analysis

2.3.1.1 Quantifying geomorphic change

I used the survey package in R to estimate site-scale means and variances for canopy cover, organic cover, median grain size, water velocity, and water depth that account for my two-stage (plot and subplot) cluster sampling design (Lumley, 2020; Lohr, 1999). Cluster sampling design-based t-tests were used to assess significant differences in site-scale summary statistics. For wood volume, only the center subplots were compared because the outer subplots were not measured in 2019; thus, a paired Welch Two Sample t-test was used to estimate change in mean wood volume per plot.

Water depth and velocity were scaled according to the discharge on the day they were measured using the equation in Table 3 to account for potential differences due to discharge (discharges averaged 9.3 m^3s^{-1} during measurements in 2019 and 14.2 m^3s^{-1} during 2020, SI Tables 2-4). I used the Pearson correlation coefficient to evaluate whether wood volume and organic cover were changing as a function of location of plot within the study reach, and an F test to compare variance in velocity.

I used the nonparametric, matched-pairs Wilcoxon Signed Rank Test, adapted for clustered data, to determine significant differences in grain size between the two years of measurement. This test was conducted using all the measured sediment clast sizes, with 10 clasts per subplot and totaling 40 clasts per plot and run with the clusrank package in R (Jiang et al., 2017).

I used Gaussian Mixture Modeling with the mclust package in R to separate the sediment distribution for each year into separate fine and coarse distributions (Scrucca et al., 2016). Welch two sample t-tests were performed on the coarse and fine distributions separately to determine significant differences between years. Substrate was also separated into categorical classes of silt, sand, gravel, cobble, and boulder, and frequencies of each class were calculated for each of the 23 plots measured in both years.

2.3.1.2 Heterogeneity

Floodplain spatial heterogeneity is well established as an important component of biologically and geomorphically functioning river corridors (e.g., Zeug and Winemiller, 2008; Bellmore et al., 2015; Wohl, 2016; Camara dos Reis et al., 2019). However, methods of measuring floodplain heterogeneity are inconsistent in the literature (Wohl, 2016). I used the intra class correlation coefficient, also called the intracluster correlation coefficient (ICC), to assess the correlation among subplots within a plot compared to the correlation between plots throughout the entire site. I expect subplots within a plot to be highly correlated and I am interested in the magnitude of change in similarity after a year of adjustment. The equation for ICC is from Lohr (1999) and was implemented using the fishmethods package in R (Nelson, 2014, 2019):

$$ICC = 1 - \frac{M}{M-1}\ \frac{SSW}{SSTO} \qquad (1)$$

where M is the number of secondary sampling units in each primary sampling unit, SSW is the sum of squares within a cluster and SSTO is the sum of squares total. As ICC approaches 1, elements within a cluster are more homogenous and contribute little to the efficiency of the clustered sampling design compared to a simple random sample. Changes in ICC over two years are used to assess whether plots are becoming more homogenous with site adjustment. Wood volume is not included in this comparison because wood volume was only measured in the center subplots in 2019 and therefore has only one measurement per plot. I use the cluster-sampling adjusted variance calculated with the survey package in R (Lumley, 2020) to examine differences in entire site scale heterogeneity for each measured variable.

I also used the ICC to assess heterogeneity at the intermediate inter-plot scale. Plots were combined with their nearest neighbor and evaluated as grouped clusters, with a total number of 8 combined subplots. From all possible pairs of plots, potential combinations were identified based on minimum distances between plots, and pairs for analysis were chosen based on judgement of similar geomorphic conditions. Five of the 23 plots were left out due to distance of >100 m away from their nearest neighbor, or due to their nearest neighbors having already been accounted for within a pair of plots, leading to nine pairs input into the ICC calculation.

I recorded the geomorphic unit at each subplot based on my observed surroundings. I then input these field-determined geomorphic units to the Gini-Simpson diversity index to quantify an integral representation of overall site diversity (Simpson, 1949):

$$SIDI = 1 - \sum_{i=1}^{m} P_i^2 \qquad (2)$$

Pi is the proportion of the landscape occupied by each patch type. Simpson's diversity index represents the probability that any two plots measured would be different patch types. I intend this to show a simple example of how to use a biological heterogeneity metric in a geomorphic context.

In summary, I used ICC to assess spatial heterogeneity at the intra-plot and intermediate inter-plot scales, variance to assess site inter-plot spatial scales, and Simpson's diversity index to assess integrated spatial heterogeneity at the site inter-plot scale.

2.3.1.3 Evaluation of the monitoring strategy

I used categorical sediment data in a non-parametric difference test, and power analysis to evaluate the number of geomorphic field plots needed to optimize the field monitoring strategy presented here. Due to the size-based categorical nature of the sediment size classes measured in subplots, ordinal logistic regression with a random effect for plot was conducted using the mgcv package in R (Wood, 2011). The random effect accounts for correlation among observations in the same plot. Difference detection for sediment classes relies on a contrast of likelihoods of whether an observation falls within the same category in 2019 versus 2020 and is approximated by a modified Friedman's test. A non-parametric power analysis was conducted by simulating sediment data for an experimental number of plots (n) and repeating an ordered logistic regression model fit 100 times for each non-parametric modified Friedman's Test of n plots for each year. The statistical power (%) at the $p \leq .05$ level is the proportion of iterations that detected a significant contrast between 2019 and 2020 data. Data were simulated by random draws of 2019 and 2020 observations, where randomness was weighted by the distribution of the categories for each year. This analysis is expected to be a conservative representation of power because random sampling error was introduced by taking a random draw from the population of the original model's residuals and applying the residual to the simulated observation, thus moving the observation up or down i category levels as determined by the randomly drawn residual. Random draw was appropriate because residuals were normally distributed about 0.

2.4 Results

I first present results in the context of overall changes with time in individual variables at the restoration site and then evaluate changes in the three spatial scales of heterogeneity.

2.4.1. Geomorphic change

Canopy cover decreased significantly from 2019–2020 according to the clustered Welch two-sample t-tests (Figure 2.4a). Aside from the nonparametric test for sediment described later in this section, no other measured variables experienced statistically significant changes over the two measurement years. However, there was a significant negative correlation between organic cover and distance downstream in 2020 as well as a significant negative correlation between change in organic cover and distance downstream between 2019 and 2020 (Figure 2.4c and d). With increasing distance downstream, organic cover in 2020 decreased, and the change in organic cover between the two years transitioned from positive to negative, indicating that measured locations gained organic material upstream and lost material downstream. Of the 23 plots, 12 experienced a relative increase in organic cover, eight decreased, and three remained unchanged. The positive increases in organic cover occurred within plots upstream of plots 9, 11, 13, and 14, which cluster in longitudinal position near the linear model-estimated value of 0 change (728 m, Figure 2.4d). This location aligns with a downstream slope increase in the path of the historic main channel, observable in post-treatment high flow aerial imagery (Scott, 2019). Due to a limited number of plots in the higher gradient area, I did not observe a significant trend in velocity with downstream distance. This longitudinal position also coincides with the entrance to a previously dry channel that contains plots 7, 2, and 1, which experienced the largest decreases in organic cover. There is no correlation between canopy cover change and distance downstream, nor is there a correlation between canopy cover change and organic cover change.

Results for significant differences in sediment using the non-parametric test were obtained from tests of the total sediment dataset and from the compiled medians of each set of 10 clasts per subplot

(p < 0.001 for the entire dataset and the dataset of subplot medians). The nonparametric test does detect sufficient evidence to conclude that there is a significant difference in grain size between 2019 and 2020 (Table 3).

Table 2.3. Estimates for the mean values of measured variables 2019-2020 and their standard errors

Variable	2019	2020	Significant change?
Canopy cover (%)	40 ± 6	26 ± 6	**Y (p < 0.0001)**
Organic cover (%)	20 ± 3	23 ± 4	N (p = 0.33)
Wood volume, center subplot (m^3)	2.8 ± 0.4	2.4 ± 0.3	N (p = 0.40)
Median grain size (mm)	37 ± 8	33 ± 8	N (p = 0.37)
Wilcoxon Signed Rank Test			**Y (p < 0.0001)**
Water velocity at surface (m/s)*	0.16 ± 0.04	0.16 ± 0.04	N (p = 0.98)
Water velocity at 60% depth (m/s)*	0.15 ± 0.04	0.14 ± 0.03	N (p = 0.67)
Water depth (cm)*	26.4 ± 4.6	23.0 ± 3.8	N (p = 0.19)

**Water depth and velocity are scaled according to discharge at the time of measurement using* $\left(\frac{x}{Q_{survey}}\right) * \boldsymbol{Q_{avg}}$, *where* Q_{avg} *is the average discharge between the survey times for each measurement. Dry plots are included in parameter estimates for depth and velocity.*

Cumulative distribution function (CDF) plots for each year show lower proportions of substrate smaller than 32 mm (coarse gravel and finer) in 2019 compared to 2020 (Figure 2.4c). Fine sediment increased significantly (p=0.01) in 2020 compared to 2019 when bimodal distributions were split into coarse and fine distributions. When analyzed as categorical classes, a 3% increase of sand was measured in 2020, balanced by a relative decrease in cobbles and boulders (Table SI 1).

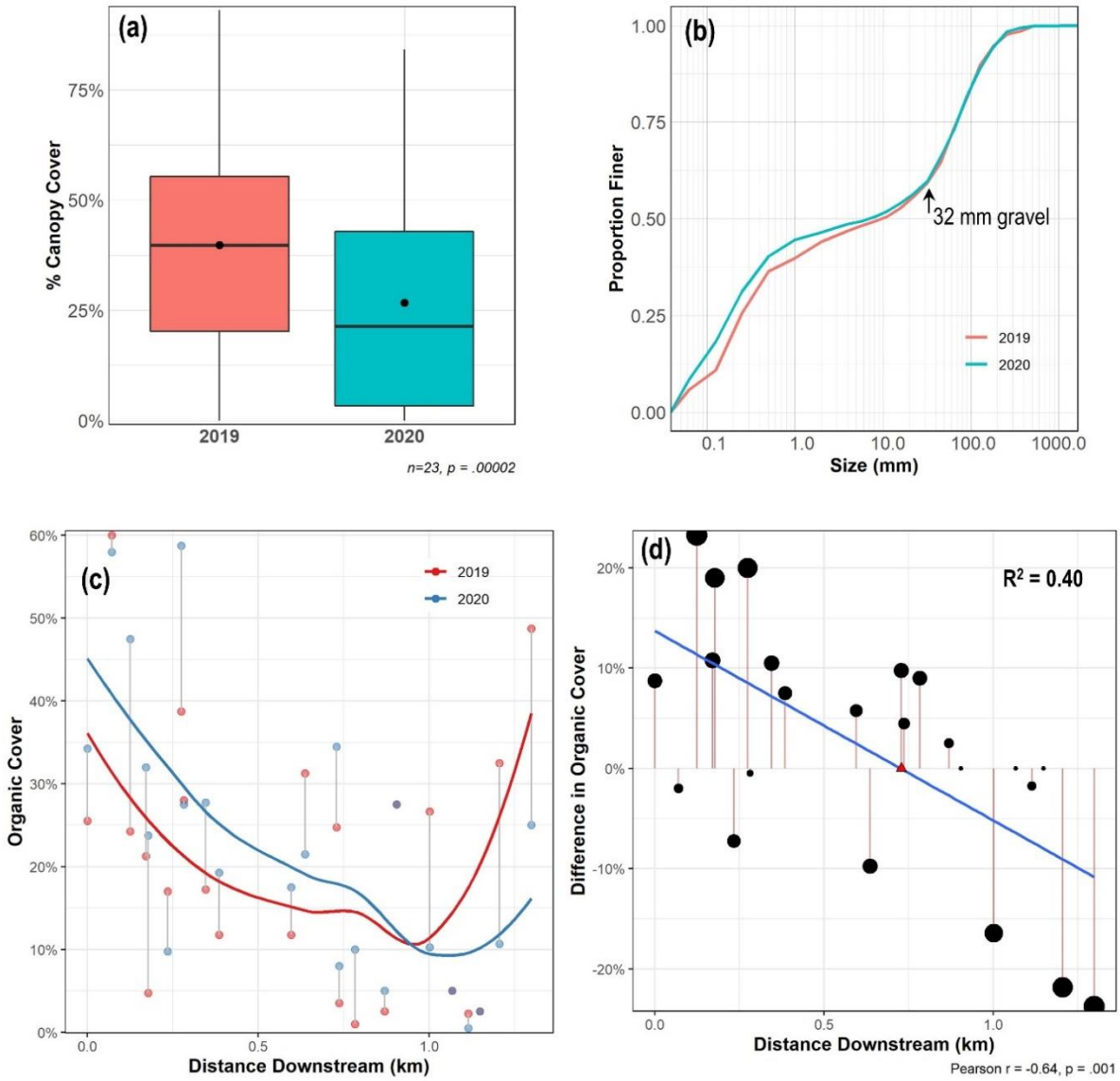

Figure 2.4. (a) Change in canopy cover from 2019-2020. Canopy cover was the only significant change with a parametric cluster-sampling adjusted two-sample t-test (p=1e-5) and thus is the only variable shown. Dots represent the mean for each year. (b) Empirical cumulative distribution showing grain size converging for two years for sizes above 32 mm. Nonparametric tests indicate fining between 2019 and 2020. (c) Organic cover, or percent plot area covered by organic matter, in 2019 and 2020. Colored dots represent 2019 (red) or 2020 (blue) organic cover at each plot, and colored lines show locally weighted smooth (loess) curves of best fit. Vertical lines connect the same plots for different years. (d) Trend in downstream organic cover change. With distance downstream, the change in organic cover decreases (R^2 = 0.40, p=0.001). Vertical line segments connect the magnitude of change for each plot to 0, and a red triangle shows the model-predicted value of 0 change in organic cover.

2.4.2 Heterogeneity

The ICC increased for all variables in the intra-plot analyses between 2019 and 2020, except for organic cover (Table 4), indicating that canopy cover, substrate, water velocity, and water depth became more spatially homogeneous at the intra-plot scale. This supports my first hypothesis.

My second hypothesis regarding intermediate-scale inter-plot heterogeneity is partially supported. The ICC for organic cover, sediment size, and water depth decreased from 2019 to 2020, suggesting that the spatial heterogeneity of these variables increased at distances up to 100 m between the paired plots (Table 4). The ICC of the paired plots was smaller than the intra-plot ICC, indicating that among-plot heterogeneity was greater than within-plot heterogeneity in both years for all variables except sediment size in 2019 and organic cover in 2020. For these, heterogeneity is higher when examined at the intra-plot scale.

Site-scale heterogeneity increased for organic cover and sediment size (Table 4). However, confidence intervals for variance estimates all overlapped and thus only show qualitative evidence for trends over the two years. Simpson's diversity index shows an overall decrease in diversity from 0.89 in 2019 to 0.74 in 2020. This number represents the probability that two randomly chosen plots will be different habitat types and depends on similarity of reported geomorphic units during the field surveys. The decrease in overall diversity suggests that the entire restoration reach has also become more spatially homogeneous with time, which contradicts my third hypothesis.

Table 2.4. Intraclass correlation coefficients showing similarity between subplots within a geomorphic plot for 2019 and 2020 at two scales, standard deviation of measured variables (units in Table 3), Gini-Simpson Diversity Index, and observed trends; plus signs indicate an increase in heterogeneity and minus signs show a decrease during the monitoring period.

	10 m intra plot scale			100 m inter plot scale			Site Scale		
Variable[1]	**ICC 2019**	**ICC 2020**	**Trend**	**ICC 2019**	**ICC 2020**	**Trend**	**Std. Dev. 2019**	**Std. Dev. 2020**	**Trend**
Canopy cover	0.67	0.89	-	0.49	0.59	-	0.30	0.28	-
Organic cover	0.45	0.28	+	0.40	0.34	+	0.20	0.24	+
Sediment size	0.15	0.32	-	0.27	0.21	+	46	51	+
Water velocity, surface	0.64	0.75	-	0.16	0.27	-	0.22	0.20	-
Water velocity, subsurface	0.63	0.69	-	0.16	0.29	-	0.21	0.18	-
Water depth	0.59	0.67	-	0.22	0.19	+	26	21	-
Gini Simpson Diversity Index							0.89	0.74	-

[1] *Wood volume is not included due to the single sample per plot in 2019.*

2.4.3 Evaluation of the monitoring strategy

I detected fining in categorical sediment classes between 2019 and 2020 ($p=0.01$). Using the same test over multiple iterations, I found that the non-parametric power analysis with categorical sediment data reaches 80% power at 60 plots (Figure 2.5). Based on sediment data alone, 60 plots each year are required to ensure >80% statistical power to detect a change in sediment size. With the current study design of 40 plots, I achieve 67% power to detect differences in substrate classes.

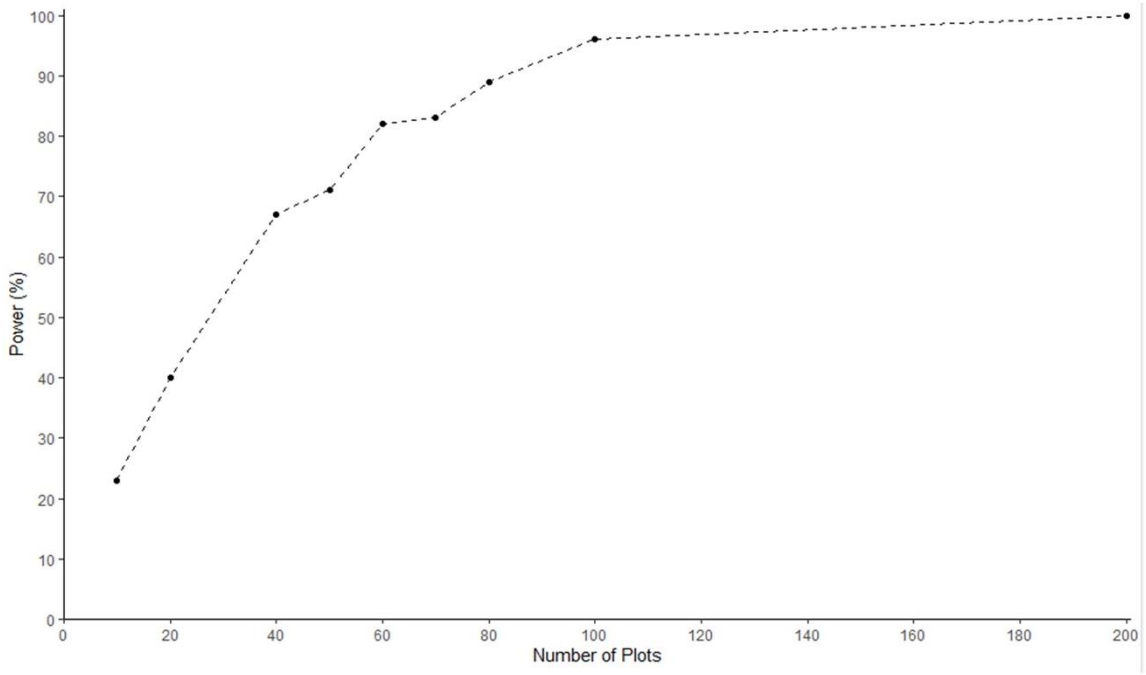

Figure 2.5. Results of non-parametric power analysis with 100 iterations of a model fit to categorical sediment data.

2.5 Discussion

Two years of data from the geomorphic plot monitoring design allowed us to assess site adjustments immediately after the restoration was completed and to evaluate the monitoring strategy and its efficiency.

2.5.1 Geomorphic change and connectivity

Between 2019 and 2020 I observed a 35% loss of tree canopy cover. Surveys were completed in July-August of 2019 and August 31-September 4, 2020, so canopy cover decrease due to seasonal change alone is unlikely. I did observe many dead trees as well as many newly toppled trees in 2020, which likely explained the loss of canopy cover. There are multiple potential causes. Channel filling raised water levels across the entire floodplain of the SFMR, including persistent rises in the water table

and flooding in many areas, killing many large trees. Also, large areas of the site were opened during the restoration, leaving remaining trees more exposed to the wind. Finally, flooding and high water tables might have softened the soils so that trees were less wind-firm after restoration. In most streams, newly recruited large wood can foster feedbacks, increasing sediment deposition and channel-floodplain connectivity (Sear et al., 2010; Collins et al., 2012), but the number of trees that fell between 2019 and 2020 was small relative to the thousands of large wood pieces added during the restoration, so I expect newly recruited wood had little impact. This is supported by my plot measurements which did not show a significant change in large wood volume or organic cover when averaged across the entire site. It is likely, however, that these losses in canopy cover led to less shade, which could increase primary production of algae, potentially enhancing food web richness and complexity (e.g., McNeely et al., 2007).

Coarse particulate organic matter (CPOM) can be a critical foundation to the food web, supporting primary consumers (Tank et al., 2010). The SFMR is a large, poorly shaded river, and the restoration greatly expanded the wetted area and perhaps changed the relative importance of allochthonous versus autochthonous CPOM. However, I see strong changes in organic cover with flow distance through the restoration site. My data suggest that CPOM is efficiently trapped in the upper portion of the study area but lost in the lower portion of the study area. Between construction in 2018, and consecutive years of measurement in 2019 and 2020, organic material deposited before restoration on dry forest floor was inundated, reworked, and transported, especially in the reactivated secondary channel in the southern portion of the restoration site. Longitudinal connectivity of CPOM has thus decreased within the upstream portion of the study area and increased in the downstream portion. The explanation for this difference in CPOM retention between the upstream and downstream portions of the study area is not known but could involve the steeper gradient of the downstream portion or the more efficient transport of CPOM within the reactivated secondary channel in the downstream portion.

I do not see a pattern of fining substrate similar to that of accumulating organic cover at upstream plots. Organic material transported from upstream, especially material mobilized by upstream restoration, was likely trapped at the surface by placed large wood pieces and constructed log jams, while fine sediment carried in suspension downstream is distributed throughout the site. Substrate fining over two years since construction aligns with the goal of providing more suitable habitat for fish. Salmonids require gravel for rearing and spawning (Keeley and Slaney, 1996). Although the proportion of gravels did not significantly increase, the proportion of gravel in both years is higher than the proportion of cobbles and boulders, providing more spawning opportunity than the primarily boulder-bedded condition prior to restoration. I assume that the increase in sand is temporary and associated with disturbance from restoration activities upstream, based on the increased sand proportion, my field observations of Phase I during upstream construction, and direct observation of construction activity in Phase II. In a connectivity context, longitudinal connectivity of fine sediment has decreased, allowing local deposition of fine sediment and creating spawning habitat.

2.5.2 Heterogeneity and connectivity

Intraclass correlation coefficients (ICCs) with intraplot and intermediate-scale inter-plot data reveal changes in spatial heterogeneity and provide evidence that, at a scale of tens of meters, habitat is stabilizing in a pattern that reflects local-scale controls. The channel restoration and regrading of the valley floor by heavy equipment destroyed the previous armor layer and fill materials mixed deeper sediment layers and floodplain surface sediment so that the as-built restored surface was much finer textured. The restoration was completed in late summer of 2018 and my first post-restoration measurements were collected in 2019, after winter high flows had already started reworking the sediment. Local processes have continued to rework this sediment and my plot data reflect the changes that occurred between 2019 and 2020.

Initial disturbance via construction and rewatering of the floodplain also altered the boundaries of dry forest and fluvial process domains. Heterogeneity decreased at the intraplot scale for all the metrics I measured except organic cover. At the intermediate-scale, heterogeneity increased for organic cover, substrate, and water depth. Organic cover and substrate also had increased variance when calculated for the entire site. These increases in diversity reflect promising trends in local-scale habitat availability for organisms throughout multiple life cycle stages. At the site-scale, measured by Simpson's diversity index, I recorded an overall decrease in heterogeneity. Some geomorphic units, such as flooded forest and flooded meadow, may change to different geomorphic units as inundated vegetation dies, sediment is deposited, and wood aggregates into log jams, forming islands and more secondary channels. In contrast, I expect dry areas outside of the wetted channel study area to become more diverse as the elevated water table, and therefore increased subsurface hydrologic connectivity, interact with topographic lows in the forested floodplain and form wetlands.

Qualitative observations suggest that restoration activities at the study site have altered connectivity. The direct addition of substantial large wood and the resulting formation of an anastomosing channel planform have reduced longitudinal connectivity within the channel. Removal of artificial levees and regrading of channel and floodplain surfaces have increased lateral connectivity. The combined effects of more in-channel obstructions from large wood and the greater inundated surface area have likely increased vertical connectivity. These changes to 3D connectivity better represent natural conditions in river corridors of this region prior to intensive human alteration starting in the 19th century (Sedell and Froggatt, 1984; Collins and Montgomery, 2002).

2.5.3 Evaluation of the monitoring strategy

The monitoring protocols I developed for the SFMR were intended to serve as a pilot that could be modified to better capture geomorphic change and complexity and to allow monitoring of other

ecological and remotely sensed metrics. Having evaluated the first set of monitoring results using these protocols, I consider it useful to present the results of the initial monitoring protocol and my recommended changes because stage 0 restoration is becoming increasingly common and other investigators may face the same uncertainties and period of 'experimentation' in designing monitoring protocols.

The described monitoring approach is necessary to inform adaptive management that may influence future intervention on the site and future implementation of the stage 0 restoration approach in other locations. Additionally, monitoring of this nature facilitates an assessment of post restoration site evolution, and potentially pre-to post restoration change if timed appropriately. Cost and time-feasible monitoring allows documentation of short and long-term temporal change of multiple aspects (e.g. wood retention, sediment size, channel planform, etc.) of the post-restoration site. Stage 0 restoration produces a spatially extensive post-restoration site that is much more complex than pre-restoration conditions and can be more complex than applications of previous restoration styles (e.g. Rosgen Natural Channel Design; Rosgen 2011), and so requires a monitoring approach that is more capable of capturing the spatio-temporal heterogeneity of these different aspects than more conventional approaches designed around single threaded stream systems. I recognize that the monitoring approach presented here has room for improvement, but think it is important to share with the broader scientific community in effort to begin the process of establishing best practices for Stage 0 restoration monitoring through replication, repetition, expansion to new sites and regions, and inspiration of new methods.

This protocol in particular is designed to complement a suite of remote sensing methods where similar measurements can be obtained from unmanned aircraft systems (UAS; i.e. drones) and subsequently calibrated using field measurements. Once calibrated, future iterations of remote monitoring can be implemented in a low-cost, time-efficient manner with seasonal or annual frequency

adapted to local needs. In the meantime, field-based monitoring methods that aim to eliminate bias and capture spatial heterogeneity are useful in the initial evaluation of large-scale projects such as the one described at SFMR.

Based on my power analysis and the results from the ICC analysis, I suggest that simple random sampling might provide a better alternative than the two-stage cluster sampling design I employed here. Having a single plot (or a single subplot within a plot) is reasonable because of the relative homogeneity I observed within clusters when compared to heterogeneity throughout the site. This modification would also increase statistical power for determining changes through time, because, for the same effort, field crews could substantially increase the number of plots sampled. For example, a sample size of n=60 plots with only one subplot per plot would provide a balance of statistical viability and field feasibility. However, the tradeoff for replacing clustered plots with single subplots is a limited ability to capture small-scale heterogeneity.

Future iterations of field plots at the SFMR could incorporate the following changes to address potential shortcomings in the design: 1) a larger subset, or the entire sample size, of the original 40 plots can be measured in order to increase statistical power, and if possible more plots will be added; 2) flow direction can be added to the hydraulic measurements to gain insight about primary flow paths and potential for incision and island formation; and 3) geomorphic units can be selected from a preexisting list to better estimate large scale heterogeneity. I also find it appropriate to move forward with measurements of only surface velocity due to the large sample size (n=184) used to establish the linear regression of surface velocity and velocity at 60% depth. Use of surface velocity measurements can be used directly to calibrate estimated velocity from video footage, and the linear regression can be used to predict velocity deeper in the water column.

2.5.4 Long-term channel adjustment

In designing this study, I were less motivated by pre- and post-restoration assessment, and more motivated to establish a method to capture post-restoration baseline conditions in the earliest stages of adjustment toward a retentive and complex floodplain. Acquisition of pre-restoration and reference site plot data of the type described here would greatly strengthen the ability to assess the effects of restoration. I anticipate subsequent uses of this strategy at the South Fork McKenzie River to assess resilience to current and future disturbances, such as forest fire. Within one week after 2020 field measurements, the Holiday Farm Fire initiated and eventually burned over 700 km^2 in the McKenzie River watershed, including the South Fork McKenzie River Floodplain Restoration Project outlined in this study.

I have described the short-term, small-scale river adjustments that occur immediately after construction associated with restoration (Erwin et al., 2016). Larger-scale progressive adjustments over many years could maintain a dynamically stable channel or could result in changes indicating that a channel was not properly designed for the flow regime and sediment supply (Brierley and Fryirs, 2016; Erwin et al., 2016). At the SFMR site, I assume that spatial heterogeneity will continue to decrease within plots but increase between plots and at the scale of the entire site as a result of gradual redistribution of large wood by higher flows and associated spatial organization of hydraulics and sediment transport. The timespan over which these adjustments will occur largely depends on external disturbances including (i) high flows that influence wood transport and deposition and (ii) wildfires that influence wood recruitment and retention. Because the site is below a dam and has regulated flows, redistribution of wood will likely occur more slowly than under a natural flow regime. The frequency and severity of wildfires, however, seem to be increasing with climate warming, suggesting an acceleration of wildfire-induced wood dynamics. In the best-case scenario, the river corridor will continue to adjust to a multithread channel with high lateral and vertical hydrologic connectivity, limited longitudinal sediment connectivity, and high habitat diversity. In the worst-case scenario(s), (i) the introduced large

wood would all be transported downstream and the restoration-induced heterogeneity would be lost, (ii) insufficient flow would result in gradual filling and terrestrialization of newly created secondary channels, or (iii) insufficient sediment supply would limit retention of substrate grain sizes suitable for salmon spawning. I consider these scenarios unlikely because of (i) limited peak flows downstream from the dam, (ii) sufficient flow to maintain some sediment transport and a multithread channel planform, and (iii) continuing introduction of finer sediments through lateral channel movement.

Process-based restoration is most likely to prove successful if matched with process-based management that is informed through spatially representative monitoring for at least several years post-restoration. Opportunities for process-based management at the South Fork McKenzie River may be relatively limited by the large dam and flood-control reservoir located only a few kilometers upstream. Thus, the degree to which historic natural processes can be restored will depend on the degree to which sediment augmentation and environmental flows can also be restored (Poff et al., 1997; Beechie et al., 2010). However, within the human-generated constraints, the project implementation at the SFMR utilizes maximum valley space and available sediment, wood, and water resources to create a more heterogeneous and laterally connected river corridor. The restored configuration of the river corridor is likely to be persistent and resilient to diverse disturbances because of the higher floodplain water table and surface inundation (resilient to wildfire and drought) and the much greater cross-sectional area and hydraulic roughness of channels (resilient to floods). Analogous to dam removal projects and associated studies, restoration efforts of this type and scale should be targets for scientific research (Bellmore et al., 2017). Restoration toward Stage 0 conditions offers a unique opportunity to adapt post-project management efforts with modern monitoring techniques.

2.6 Conclusion

The monitoring strategy described here used a randomized two-stage cluster sampling design to ensure unbiased location of study plots while also maximizing observation of habitat types across the site. Habitat complexity increases potential for biotic diversity and resilience (Uno and Pneh, 2020; Bellmore et al., 2015), so geomorphic monitoring should be paired with biotic sampling and water quality monitoring to assess holistic success of stream restoration project designs. The geomorphic plot design is matched with a suite of additional monitoring efforts at the study site that are not discussed in this chapter but include biotic counts, a food web analysis, and seasonal remote sensing data collection.

My conclusions that spatial heterogeneity is increasing at intermediate spatial scales, but not within individual plots or across the entire restoration site, are limited by the lack of pre-restoration data and by the short timeframe (2 years) of monitoring. Qualitative assessments of site condition suggest an increase in intermediate- and site-scale spatial heterogeneity relative to conditions prior to restoration and I expect these trends to continue with time. Decreased longitudinal connectivity and increased lateral and vertical connectivity have likely improved floodplain function and habitat conditions since restoration and I expect these trends to continue.

Chapter 3 Quantitatively estimating carbon sequestration potential in soil and large wood in the context of river restoration[2]

Summary

Restoration aimed at rewetting the valley floor has the potential to increase organic carbon stock in the form of floodplain soil carbon, downed wood, and riparian vegetation. The primary goal of stream restoration is typically to restore habitat or maintain balance between natural ecosystem function and human land use. Although many benefits result from stream restoration, the carbon sequestration potential of different restoration approaches in diverse geographic settings has not yet been quantified. I investigate the carbon storage potential of restored stream segments (known as treatment segments) relative to otherwise analogous degraded and reference segments. I develop a conceptual framework to identify the conditions that maximize carbon storage in relation to characteristics of the river corridor and specific restoration practices. I illustrate application and quantification of the conceptual framework using data from a pilot study of treatment, degraded, and reference stream segments along two streams in Oregon, USA. The conceptual model is designed to help managers identify levels of hydrologic connectivity, channel and floodplain dynamics, floodplain vegetation, and other variables that may optimize carbon storage at a treatment site.

3.1 Introduction

Increasing concern about warming climate is driving increased interest in diverse forms of carbon sequestration (e.g., Lal, 2008; Villa and Bernal, 2018; Gifford, 2020). The saturated, reducing

---

[2]Chapter published as Hinshaw, S. and Wohl, E., 2021. Quantitatively Estimating Carbon Sequestration Potential in Soil and Large Wood in the Context of River Restoration. Frontiers in Earth Science 9: 975.

environment of wetlands limits microbial decay of organic material, and wetland soils therefore typically have much higher concentrations of organic carbon than nearby soils with lower soil moisture (e.g., Nahlik and Fennessy, 2016; Carnell et al., 2018). Wetlands can also sequester carbon at rates 30 to 50 times higher than forests (e.g., Tangan and Bansal, 2020). River floodplains that are hydrologically connected to the active channel can include substantial areas with ponds, lakes, and diverse types of wetlands (e.g., marshes, swamps, carrs, wet meadows). River floodplains can also be seasonally or perennially wet because of regional groundwater inputs associated with geologic structures (e.g., Tooth and McCarthy, 2007; Assine et al., 2015; Koltzer et al., 2019). Consequently, river floodplains can contain disproportionately large soil carbon stocks relative to adjacent uplands (Wohl et al., 2012).

Organic carbon stock in river corridors (active channel(s), floodplain, hyporheic zone) occurs primarily in the form of floodplain soil (here, soil refers to all floodplain sediment and includes litter and duff created by particulate organic matter smaller than large wood), downed dead wood pieces > 10 cm in diameter and 1 m in length (hereafter, large wood), and living riparian vegetation (Sutfin et al., 2016). Active channels can contain substantial quantities of large wood (Triska, 1984; Wohl, 2014; Boivin et al., 2015), but the majority of carbon in most river corridors is found in the floodplain (e.g., Sutfin et al., 2016; Scott and Wohl, 2020). River restoration has traditionally been focused on the active channel but is gradually broadening to include an explicit focus on hydrologic connectivity within the river corridor. River restoration has also expanded to include processes that create and maintain desirable floodplain characteristics (Wohl et al., 2015), such as lateral channel migration that results in secondary or abandoned channels and associated habitat diversity (Hall et al., 2007). In the context of this broadening focus, river restoration strategies that have the potential to increase diverse forms of floodplain carbon stock may be justified as a mechanism of carbon sequestration.

The cumulative historic, contemporary, and potential future carbon stocks in river corridors worldwide have not been quantitatively estimated, but evidence suggests that this cumulative stock

could be significant for the global carbon budget. The most recent estimates of this budget suggest fluxes of 9.6 Gt C /y from fossil-fuel emissions, 1.6 Gt C/y from land-use emissions, 2.5 Gt C/y into the oceans, and 3.4 Gt C/y into terrestrial C sequestration (Friedlingstein et al., 2020). Floodplains constitute about 9% of total land area (Nardi et al., 2019). Although the range of soil organic carbon stock (Mg C/ha) reported for floodplains is too large to justify assuming a single median value (e.g., Sutfin et al., 2016), soils are the largest terrestrial carbon reservoir (e.g., Scharlemann et al., 2014) and wetland soils have higher carbon concentrations than other soils (e.g., Nahlik and Fennessy, 2016). Wetlands store 20-30% of the estimated 1500 Gt of global soil carbon, for example, but occupy 5-8% of land area (Nahlik and Fennessy, 2016). These numbers suggest that wetland floodplain soils can cumulatively create globally significant carbon sequestration.

Here, I propose a framework for using multiple lines of evidence to assess the carbon sequestration potential for a river corridor at the reach scale. I define a reach as a continuous length of river corridor that is at least several times the average bankfull channel width and has consistent channel and valley morphology as delineated based on valley floor width and gradient, channel planform, and flow regime. I also provide two case studies using recently completed stage 0 restoration sites in Oregon, USA. Stage 0 restoration refers to returning a river corridor to the stage 0 condition in the Cluer and Thorne (2014) stream evolution model. Stage 0 in this model is an anastomosing wet woodland or grassed wetland with a high floodplain water table that intersects the ground surface at least seasonally. Stream restoration to stage 0 conditions involves some combination of introducing in-channel obstacles such as large wood or beaver dam analogues to promote local aggradation and overbank flow (e.g., Pollock et al., 2014; Dixon et al., 2016) and regrading channel and floodplain topography to facilitate overbank flow and channel migration under an existing flow regime (Powers et al., 2019; Smith et al., 2020). My case studies come from the South Fork McKenzie River and Deep Creek in Oregon, USA. At both sites large wood has been added and material from high surfaces was graded

and used to fill previously straightened channel segments with the intent of facilitating more sinuous and multithread channel planforms. My primary objective in this chapter is to develop a methodology that can be used to identify river reaches with the greatest potential for carbon sequestration. I briefly illustrate the application of this methodology using preliminary data from the two case studies. I acknowledge that evaluating carbon stock at such recently restored sites does not effectively evaluate changes in carbon stock with time following river restoration. Rather, I use the case studies to illustrate the application and potential limitations of the method proposed here.

3.2 Materials and Methods

3.2.1 Conceptual Model of Factors Controlling Floodplain Carbon Stock

I start with a conceptual model of the factors that influence carbon stock (mass per unit area; e.g., Mg C/ha) in floodplain soil and large wood. I do not address carbon stock in living floodplain vegetation, which typically forms a smaller proportion of total floodplain carbon stock than does soil carbon (Wohl et al., 2012; Hanberry et al., 2015; Sutfin et al., 2016). I also do not explicitly address human activities in the drainage basin or the river corridor, which can either increase or decrease carbon stock by modifying the variables included in the conceptual model (Wohl et al., 2017).

3.2.1.1 Floodplain Soil Carbon Stock

Biogeochemists conceptualize wetland carbon sequestration as a balance between carbon inputs and outputs, which can also be done for floodplain soil carbon as a whole (e.g., Wohl et al., 2017). Inputs are primarily carbon within organic matter from plants (autochthonous) and carbon dissolved and suspended in inflowing waters or deposited from hillslope sources during slope wash or mass movements (allochthonous; this can originate from rock weathering as petrogenic carbon or from biotic processes as biospheric carbon; Blattmann et al., 2018). Outputs consist of dissolved and suspended organic carbon in outflowing waters, and CO_2 and CH_4 emissions from microbial decomposition of

organic matter (Villa and Bernal, 2018). Organic matter decomposition by microbes can be slowed by (i) scarcity of nutrients that limit microbial growth, (ii) physical protection of organic matter contained within soil aggregates, (iii) a high proportion of organic compounds that are recalcitrant and difficult for microbes to degrade, (iv) cold temperatures that limit plant productivity but also microbial activity, and (v) anaerobic conditions that force microbes to use less efficient metabolic pathways than exist under aerobic conditions (Villa and Bernal, 2018). Although carbon dioxide and methane emissions from wetlands can form a significant source of wetland carbon loss, particularly as climate warms, the large carbon stocks in wetland soils suggest that naturally functioning (rather than degraded) wetlands in temperate and boreal latitudes typically have a positive carbon balance and sequester carbon over periods of decades to millennia (e.g., Whiting and Chanton, 2001). Consequently, the remainder of this chapter focuses on influences on carbon sequestration. When referring to organic carbon present in soil, I am including carbon derived from autochthonous and allochthonous processes. I am using soil to refer to all floodplain sediments.

The carbon concentration of soil (% carbon) depends on multiple factors, including soil texture and the ability of carbon to sorb to soil particles; particulate and dissolved organic matter inputs; and temperature and moisture regimes, which influence microbial oxidation of soil carbon (Kaiser and Guggenberger, 2000; Rasmussen et al., 2018). In general, carbon concentration increases with clay content, organic matter inputs, and moisture, and correlates inversely with temperature (Jobbágy and Jackson, 2000; Falloon et al., 2011; Sutfin et al., 2016).

Starting with these immediate influences on soil carbon concentration, I can infer the reach-scale drivers of clay content, organic matter inputs, soil moisture, and temperature across various temporal and spatial scales.

At the largest scales of time and space, geology and climate interact to govern the physical configuration of the river corridor, the weathering of bedrock, the fluxes of material into and through the river corridor, and the biotic communities present (upper, central box in Figure 3.1). Geology and climate govern valley geometry and the space available for floodplain storage (physical configuration); as well as soil texture, floodplain water table, and soil organic matter (material fluxes). The influences of geology and climate on these properties are direct but are also mediated by geomorphic and biotic drivers as listed in the second tier of boxes in Figure 3.1. All of the factors mentioned thus far interact to determine the residence time of floodplain sediment. Residence time, along with soil texture, moisture, and organic matter content, determine soil organic carbon stock.

Human activities are not explicitly illustrated in the conceptual model but can alter the forms and processes of stream corridors in manners that influence floodplain carbon stock (e.g., floodplain drainage that lowers the water table and creates oxidizing conditions in floodplain soils).

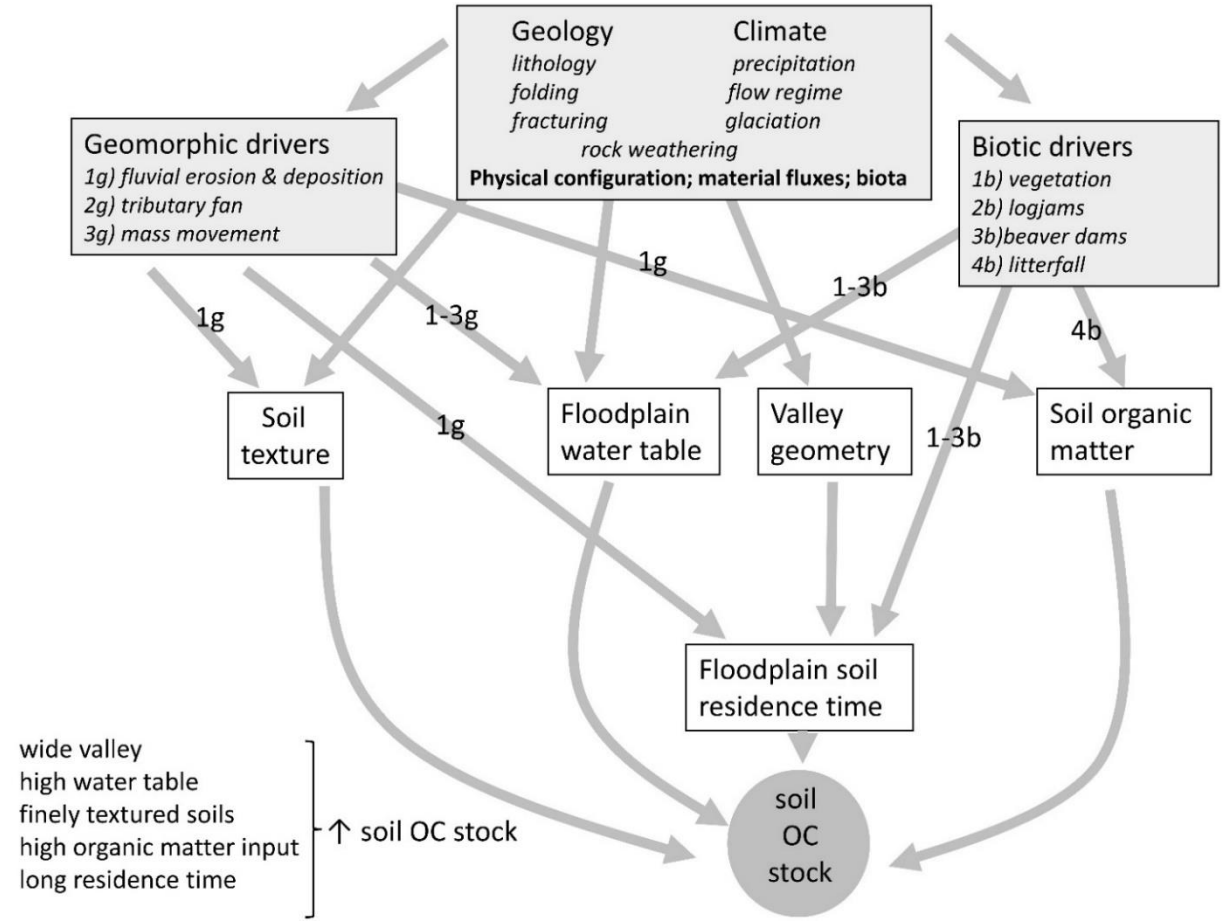

Figure 3.1. Conceptual model for influences on floodplain soil organic carbon stock. The numbers and letters superimposed on arrows represent the specific geomorphic ('g') and biotic ('b') drivers indicated by each arrow.

Geologic characteristics influence soil carbon via controls on valley geometry, floodplain water table, and soil texture. (1) Valley geometry. Bedrock structure, glacial history, and the spatial density of bedrock fracturing influence the width and downstream gradient of the valley floor and thus the space available for floodplain development. Structures such as grabens (Koltzer et al., 2019), glacially eroded troughs (Montgomery, 2002; Livers and Wohl, 2015), and dense fracturing that reduces bedrock resistance to weathering and erosion (Ehlen and Wohl, 2002) promote the presence of a wide, low gradient valley floor at the reach scale and this valley geometry facilitates sediment storage in the floodplain. (2) Floodplain water table. Geologic characteristics can also promote the presence of a high water table, even in dry climates. Examples of such characteristics include structures that retain

groundwater inputs from adjacent uplands (Koltzer et al., 2019); folded aquifer units (DesRoches et al, 2014); lithologic contacts between units with differing hydraulic conductivity (Muldoon et al., 2001); resistant lithologies that create a local base level and upstream alluvial depositional zone (Tooth and McCarthy, 2007); undulating bedrock topography that facilitates high water tables where bedrock is close to the surface (Hardie et al., 2012); and fractured bedrock that transmits groundwater readily to topographic lows (Briggs and Hare, 2018). (3) Soil texture. Lithology, in combination with climate and land cover, influences weathering regime and thus the soil texture of the floodplain.

Geomorphic processes influence soil carbon via controls on floodplain water table, soil texture, organic matter input, and sediment residence time in the floodplain. (1) Floodplain water table. Lateral and end moraines can influence groundwater fluxes and valley floor gradient in a manner that promotes a high water table (e.g., Christensen et al., 2020). Similarly, tributary alluvial fans and debris-flow fans, talus slopes, and landslide deposits can influence subsurface and surface water fluxes and create a high water table. Alluvial fans, for example, can serve as groundwater recharge zones, with a line of springs along the base of the fan (Miller et al., 2012). (2) Soil texture. The spatial pattern, rate, and frequency of fluvial erosion and deposition strongly influence the thickness, stratigraphy, and texture of floodplain alluvium (Bridge, 2003). (3) Organic matter input. Overbank deposition of particulate organic matter in transport within the channel reflects upstream sources of organic matter, but also the spatial details of deposition of upstream-sourced organic matter, as governed by hydrologic connectivity (Hupp et al., 2019). (4) Residence time. The balance between lateral and vertical accretion on the floodplain, as a function of active channel dynamics, exerts a fundamental control on the average residence time of sediment on the floodplain (Wittmann and von Blanckenburg, 2009; Wohl, 2015). A longer residence time can equate to higher soil carbon concentrations and stock if organic matter inputs continue through time (Lininger et al., 2018).

Biotic communities influence soil carbon via controls on floodplain water table, organic matter input via litterfall, and sediment residence time. (1) Floodplain water table. Living vegetation, beaver dams, and large wood can increase frictional resistance along channels and create obstructions to flow (Larsen and Harvey, 2010; Collins et al., 2012; Aberle and Järvelä, 2013). This can enhance hyporheic exchanges (Lautz et al., 2006; Sawyer and Cardenas, 2012; Doughty et al., 2020) and overbank flows (Westbrook et al., 2006; Oswald and Wohl, 2008) that result in a higher water table (Larsen et al., 2016). (2) Organic matter input. The primary productivity of floodplain vegetation and the rate of litterfall largely govern the organic matter added to floodplain soils along portions of a floodplain with dense vegetation and limited surface hydrologic connectivity with the active channel (Lininger et al., 2018; Hupp et al., 2019), although overbank deposition of fluvially transported organic matter can be important on some floodplains. (3) Sediment residence time. Sediment residence time is fundamentally a function of bank erosion and floodplain surface erosion, but these fluvial processes can be strongly mediated by floodplain vegetation, beaver dams, and large wood that increase streambank and floodplain erosional resistance and reduce the hydraulic forces of flow within the channel and across the floodplain (e.g., Micheli and Kirchner, 2002; Perignon et al., 2013).

3.2.1.2 Floodplain Large Wood Carbon Stock

The carbon concentration of large wood varies by tree species (Martin et al., 2018) but is typically on the order of 50%. The amount of large wood stored on the floodplain reflects a wood budget governed by inputs and outputs. Inputs occur as tree fall on the floodplain, mass movements that introduce large wood to the floodplain, and fluvial transport of large wood onto the floodplain (Wohl, 2020). Outputs occur as decay in situ and fluvial transport of large wood out of the floodplain. As for soil carbon, I can start with these immediate influences on floodplain large wood load (m^3 wood/ha) and infer the reach-scale drivers of large wood inputs and outputs at larger temporal and spatial scales.

Geology and climate are the primary influences on valley configuration, material fluxes, and biotic communities, as explained in reference to Figure 3.1. Geology and climate also influence the geomorphic and biotic drivers that are particularly relevant to floodplain large wood load (Figure 3.2). In particular, geomorphic and biotic drivers influence the supply of wood to the floodplain and the retention of wood on the floodplains. Again, the conceptual model does not explicitly include human activities, although many human activities (e.g., timber harvest, channelization, beaver trapping) strongly influence floodplain large wood load.

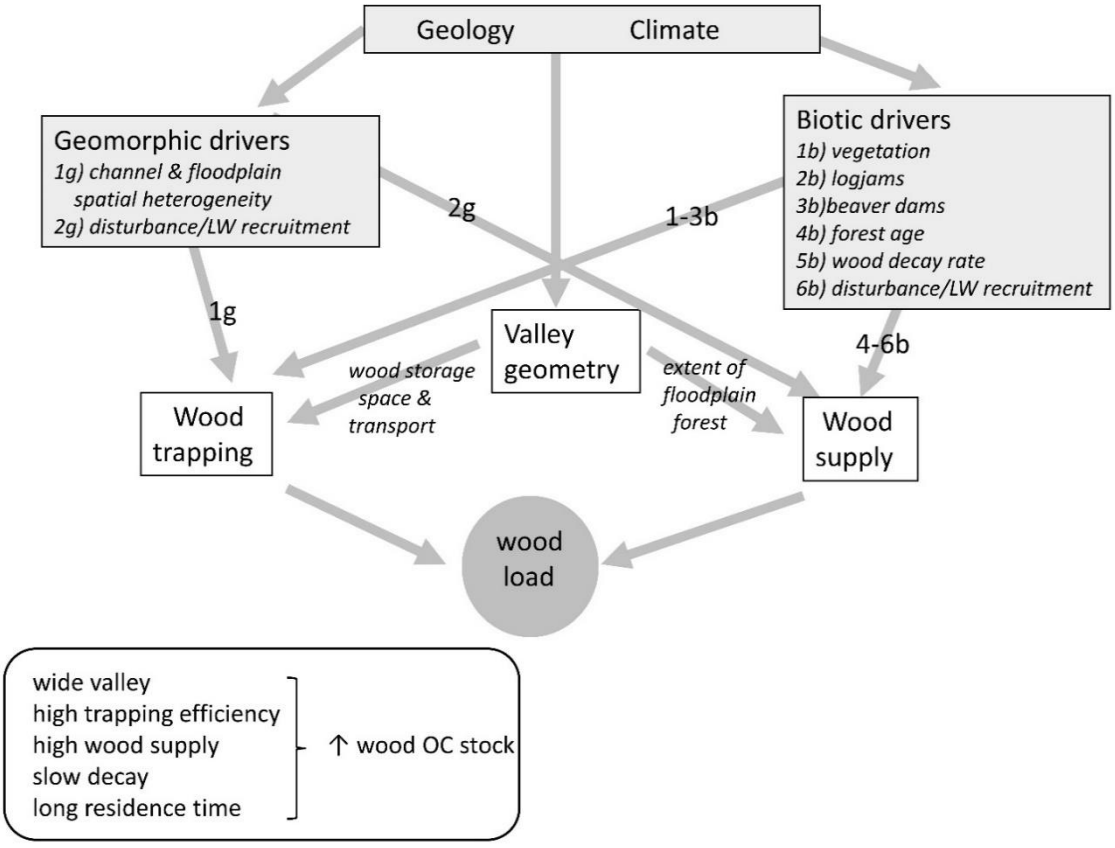

Figure 3.2. Conceptual model for influences on floodplain organic carbon stock in large wood. As in Figure 3.1, the numbers and letters superimposed on arrows represent the specific geomorphic ('g') and biotic ('b') drivers indicated by each arrow.

Geology and climate influence wood load via controls (weathering and erosion) on valley geometry, which then influences wood supply and wood trapping. The controls on valley geometry are as described for floodplain soil carbon. The width of the floodplain influences wood supply via the spatial extent of the floodplain forest and the potential for hillslope mass movements such as avalanches, landslides, or debris flows to directly introduce large wood to the floodplain (Wohl, 2020). The width of the floodplain and the channel planform also influence the retention of large wood moving down the river corridor. Wider reaches with anastomosing channel planform, bars and islands, and sinuous channels can be more effective at trapping and retaining large wood in transport than relatively straight, narrow channels (Gurnell et al., 2000; Wyzga and Jawiejska, 2005; Lassettre et al., 2008; Wohl and Cadol, 2011). Lateral channel migration and avulsion across broad floodplains can leave large wood that is buried and accreted to the floodplain (O'Connor et al., 2003; Guyette et al., 2008; Collins et al., 2012) and then sometimes exhumed and returned to the channel (Benda and Sias, 2003).

Geomorphic processes influence large wood load via controls on wood supply and wood trapping. (1) Wood supply. The supply of large wood to the floodplain partly reflects recruitment of living trees through bank erosion that topples the trees. Although many of these trees fall into the active channel and are carried downstream, others remain on the floodplain. Channel dynamics also indirectly influence wood supply by creating disturbances (erosion, deposition) that can limit the age of floodplain forests and create new germination sites for trees (e.g., Everitt, 1968). (2) Wood trapping. As noted in the description of interactions between valley geometry and wood trapping, the details of channel and floodplain spatial heterogeneity strongly influence how effectively wood being transported downstream in the active channel is trapped and retained on the floodplain (Scott and Wohl, 2018b). Numerous studies indicate that wood preferentially accumulates on geomorphic features such as bars, islands, meander bends, and secondary channels, as noted above, and these wood accumulations can be incorporated into the floodplain via lateral accretion.

Biotic communities influence floodplain large wood load through controls on wood supply and wood trapping. (1) Wood supply reflects the age of the forest and the processes of mortality and disturbance that change living trees to downed, dead wood. Individual tree mortality and mass mortality associated with wildfires, drought, insect infestations, and blowdowns can all recruit wood to the floodplain (Wohl, 2020). In regions with very rapid wood decay, however, such as the tropics (e.g., Clark et al., 2002), wood load may remain low despite substantial recruitment. (2) Wood trapping can reflect characteristics of floodplain vegetation, as well as geomorphically induced heterogeneity. Dense herbaceous or shrubby vegetation and closely spaced trees can limit and direct overbank transport of large wood (Wohl et al., 2018a,b) and significantly increase trapping and retention of large wood on floodplains.

3.2.2 Prediction of Floodplain Carbon Stock

Understanding the variables and interactions described in the preceding section can be used to identify reaches within a river network that have the potential for greater floodplain carbon stock in the form of soil carbon and/or large wood. Several sources of information can also be used to quantitatively constrain predictions of floodplain carbon stock. Among these are published values of carbon stock (Table 3.1) and rates (Table 3.2) of carbon inputs in diverse floodplains. This database is limited but steadily growing and at a minimum provides likely upper and lower bounds for floodplain carbon stock in a variety of field settings.

I used the data in Table 3.1 to create preliminary illustrations of the magnitude of floodplain carbon stocks in the form of large wood and soil in relation to mean annual precipitation and temperature (Figure 3.3). These are preliminary versions for several reasons. First, precipitation and temperature are not necessarily the most important controls on either form of floodplain carbon stock, but they do represent variables that are commonly reported or relatively easily accessible for published

field site locations. Both floodplain wood load and soil organic carbon concentration can increase with the age of the floodplain surface, for example, as a maturing floodplain forest provides a recruitment source for larger and more abundant downed wood and as litterfall from floodplain plants accumulates in reducing soils (Lininger et al., 2018; Scott and Wohl, 2018a). Similarly, within a spatially extensive floodplain on a large river, local differences in soil moisture can equate to significant differences in soil carbon stock, despite a consistent climate across the floodplain (e.g., Lininger et al., 2018). Consequently, differences in the ages or site-specific soil moisture of floodplain surfaces included in the dataset could produce trends in Figure 3.3 that might prove to be misleading as more quantifications of floodplain carbon stocks are published. Second, the number of published values is limited and these values do not fully represent the range of floodplain soil carbon or large wood carbon stocks likely to be present along rivers. Finally, I used median values to create a data point for each published case study. Most of the case studies included a range of values that reflect the local variation in floodplain carbon stock. Despite these caveats, I believe that in the absence of published floodplain carbon stocks for a particular geographic region, the data in Figure 3.3 provide a starting point for estimating potential floodplain carbon stocks (supplemental data tables).

Table 3.1. Review of published values of floodplain large wood and soil organic carbon stocks

Location	**Organic carbon stock (Mg C/ha)**	**Reference**
Large wood		
North St. Vrain Creek, Colorado, USA	166–2743	Wohl et al., 2012
Central Yukon River, Alaska, USA	2–11	Lininger et al., 2017
Congaree River, South Carolina, USA	26–44	Wohl et al., 2011
Quebec, Canada	57	Naiman et al., 1987
Central Chile	23–158	Comiti et al., 2008
SF Calawah River, Washington, USA	67–230	Scott & Wohl, 2020
Tierra del Fuego, Argentina	30	Comiti et al., 2008
Danube River, Austria	5–40	Cierjacks et al., 2010
Jalisco, Mexico	13-23	Jaramillo et al., 2003
Soil		
North St. Vrain Creek, Colorado, USA	60–1013	Wohl et al., 2012
Lower Mississippi alluvial valley, USA	167	Hanberry et al., 2015
Danube River, Austria	154–212	Cierjacks et al., 2010

Jalisco, Mexico	114	Jaramillo et al., 2003
Central Yukon River, Alaska, USA	152–402	Lininger et al., 2019
Congaree River, South Carolina, USA	248–1118	Ricker and Lockaby, 2015
MF Snoqualmie River, Washington, USA	123–263	Scott & Wohl, 2020
Big Sandy River, Wyoming, USA	57–131	Scott & Wohl, 2020
Headwaters in s New England, USA	117–400	Ricker et al., 2012
Rhine River, Germany	538–671	Hoffmann et al., 2007, 2009
Mid-Atlantic Piedmont streams, USA	250–1350	Walter & Merritts, 2008
MF Flathead River, Montana, USA	7735	Appling, 2012
Cosumnes River, California, USA	83–182	D'Elia et al., 2017
Midwestern US & Czech Republic	0.5	Craft et al., 2018
Tallgrass prairie streams, USA	166–610	Wohl & Pfeiffer, 2018
Shortgrass prairie streams, USA	4–326	Wohl & Pfeiffer, 2018
Queensland, Australia	57–430	Adame et al., 2020
Dee River, Scotland	323 (34–1469)	Swinnen et al., 2020
Mean of published values as of 2017	1.2	Craft et al., 2018

Table 3.2. Published values for soil organic carbon accumulation rates on floodplains (after Sutfin et al., 2016, Table 3)

Location	**Rate (Mg C ha^{-1} yr^{-1})**	**Reference**
Georgia, USA	0.18–1.07	Craft & Casey, 2000
Headwaters in s New England, USA	0.03–0.007	Ricker et al., 2012
Rhine River, Germany	0.034–0.254	Hoffmann et al., 2007, 2009
Virginia, USA	0.3–1.4	Noe & Hupp, 2009
Atchafalaya River, Louisiana, USA	8	Hupp et al., 2008
Tar River, North Carolina, USA	2.8	Brinson et al., 1980
Southwestern England	0.7–1.1	Walling, 2006
Danube River, Austria	2.9	Tockner et al., 1999
Ebro River, Spain	1.4–3	Cabezas et al., 2009
Kankakee River, Illinois, USA	0.6	Mitsch et al., 1979
Appalachicola River, Florida, USA	0.2	Mulholland, 1981
Amazon River, Brazil	1–2.5	Moreira-Turcq et al., 2004
Queensland, Australia	1.7–12.2	Adame et al., 2020
Amazon floodplain lake	2.7	Sanders et al., 2017

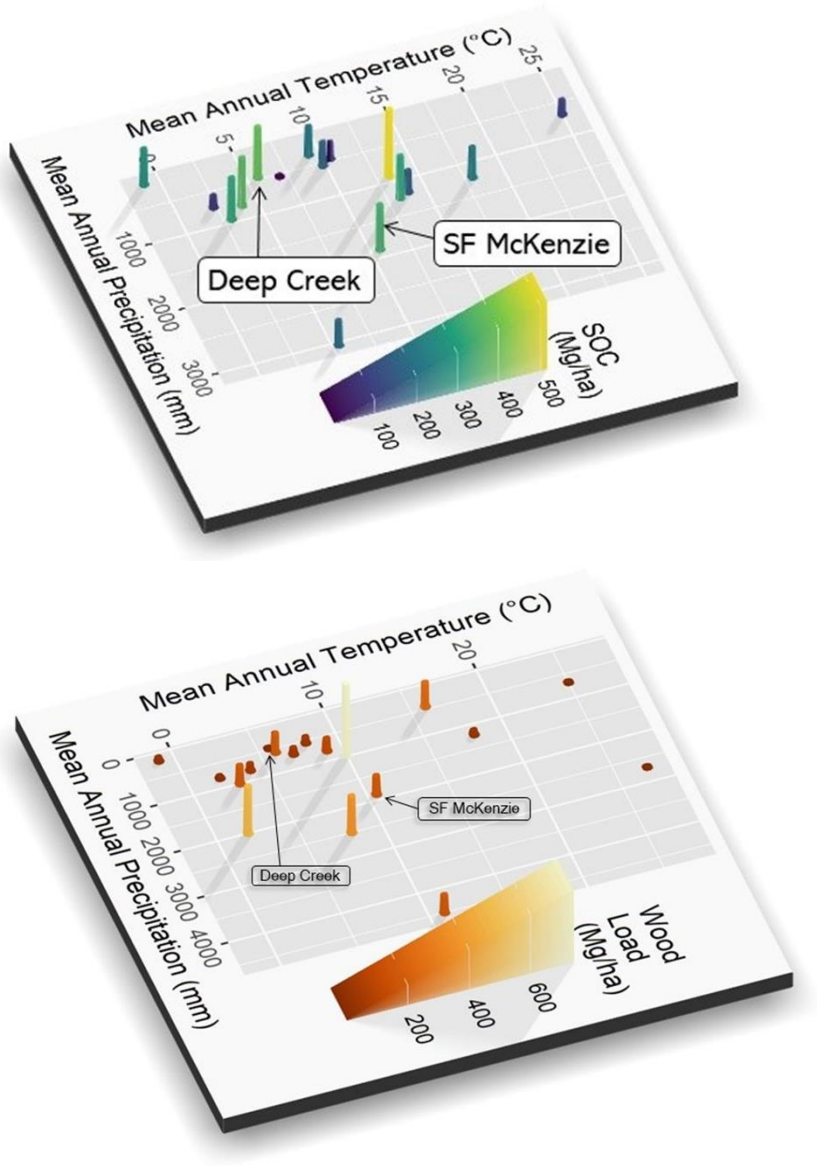

Figure 3.3. Magnitude of organic carbon stock in floodplain soil (top) and floodplain wood load (bottom). These distributions are based on limited data and thus likely to change as more field sites are characterized. Labels indicate the location of the reference-site values for the case studies in this chapter. Data used to generate these plots are in supplementary tables.

Existing quantifications of floodplain carbon stocks indicate enormous variation based on site-specific geology, climate, biome, flow regime, and channel and valley morphology, even within a single river network (Sutfin et al., 2016; Scott and Wohl, 2018a; Sutfin and Wohl, 2019). In the context of river restoration, regional reference sites based on the least human-altered portions of a river can help to

constrain estimates of the potential for enhanced carbon sequestration at a restoration site. This is the approach that I use in the case studies presented in this chapter. The quantification of carbon stock at reference sites can be based on field sampling or existing databases.

Field sampling for soil organic carbon requires (i) collecting sediment samples that represent the lateral heterogeneity of the site and variation with depth, and analyzing the percent of organic carbon and (ii) measuring or estimating soil bulk density (Structx, 2021). These measurements can then be used to calculate Mg C/ha of floodplain, commonly expressed as a volume based on 1 m depth of soil. The 1 m depth is based on the well-documented pattern of declines in organic carbon concentration with increasing depth in soils (e.g., Malone et al., 2009). Previous studies indicate that this depth decline is also common in floodplains (e.g., Lininger et al., 2018), in which most organic carbon comes from autochthonous sources such as litterfall from floodplain vegetation in portions of the floodplain that are farther from the active channel and have limited hydrologic connectivity (Hupp et al., 2019). In the floodplains of smaller rivers or on floodplains that have or are undergoing rapid deposition as a result of human activities such as altering land cover in the drainage basin, carbon-rich soil layers may be buried more deeply (Ricker and Lockaby, 2015; D'Elia et al., 2017). The potential for buried carbon-rich layers to exist in a floodplain should be assessed based on knowledge of site geomorphic and human history, and sampling depth for soil carbon should be modified if needed.

Previous work suggests that stratifying the floodplain into geomorphic units and then obtaining a minimum number of samples to adequately characterize the carbon concentration with depth in each unit (e.g., Lininger et al., 2018) can provide a basis for extrapolating carbon stock across an entire reach based on the spatial extent of each geomorphic unit (Sutfin and Wohl, 2017; Lininger et al., 2019; Scott and Wohl, 2020).

Field sampling for carbon in the form of large wood requires measuring the volume of individual wood pieces or logjams. This can be done for all pieces in the entire reach if the surface area is relatively small or wood loads are low. For larger areas or sites with substantial wood loads, stratified random sampling using floodplain transects (Wohl et al., 2018b) stratified on the basis of valley geometry, floodplain forest age or extent, or other relevant variables can provide sufficient data for extrapolation to the entire floodplain.

Existing databases can also be used to estimate floodplain carbon stock semi-quantitatively. Soil maps, including those available for much of the United States through the SSURGO online database (Soil Survey Staff, 2021), provide representative values for soil texture with depth, total organic carbon, bulk density, and soil thickness for a soil series, and these parameters can be used to calculate soil organic carbon stock (e.g., Wohl and Pfeiffer, 2018). Existing databases for large wood are largely nonexistent, although regional case studies that quantify expected wood loads based on position in the river network or channel width are available for a few locations, such as Washington State in the USA (Fox and Bolton, 2007). Remote imagery obtained via a drone, lidar data (Atha and Dietrich, 2016), Google Earth (Atha, 2014), aerial photographs, or other satellite imagery can be used to obtain at least a minimum count of large wood visible from the air. Ideally, ground measurements of piece diameters can be used to calibrate estimates of wood volume based on piece length, which is most easily measured in remote imagery. Where floodplain wood load is strongly influenced by fluvial transport, rather than just tree fall from the floodplain forest, the spatial distribution of large wood can be highly non-uniform (e.g., Piégay, 1993; Piégay and Gurnell, 1997; Wohl et al., 2018b), suggesting the need to obtain sufficiently large samples to include spatial heterogeneity of wood distribution.

3.2.3 Case Studies

3.2.3.1 Deep Creek

Deep Creek is located in Ochoco National Forest in the Ochoco Mountain range in central Oregon, USA (elevation 1325 m) (Figure 3.4). The creek drains 224 km^2 and flows southwest into the North Fork Crooked River immediately downstream of the study area. The catchment is dominated by old-growth ponderosa pine (*Pinus ponderosa*) forest. Average temperature and precipitation in Deep Creek are 5.7°C and 468 mm, respectively. Deep Creek represents a case study for potential carbon sequestration in a river corridor with mixed forest and beaver-modified willow carrs. Past grazing activities and artificial berms caused Deep Creek to incise up to 1 m below the floodplain and led to water table lowering and channel-floodplain disconnectivity. In an effort to restore habitat for Columbia River redband trout (*Oncorhynchus mykiss gairdneri*), Columbia spotted frog (*Rana luteiventris*), and other aquatic species, the U.S. Forest Service regraded the floodplain, added large wood, and reconnected relict secondary channels in 2018 and 2019 (Paul Powers, USDA Forest Service, June 2020, pers. comm.).The regional reference site used as a measure of carbon sequestration potential for Deep Creek is Gray's Creek, located approximately 15 km from Deep Creek and also in the larger North Fork Crooked River watershed. The Gray's Creek floodplain houses an active beaver complex that has been established for approximately 20 years (Jason Gritzner and Paul Powers, USDA Forest Service, June 2020, pers. comm.). I chose a degraded analog for Deep Creek just upstream of the restoration site, where the channel remains relatively incised with rows of alder (*Alnus* spp.) topping elevated surfaces surrounding the single active channel (Figure 3.5). Additional descriptive data for Deep Creek are in Supplemental Table 1 for this chapter.

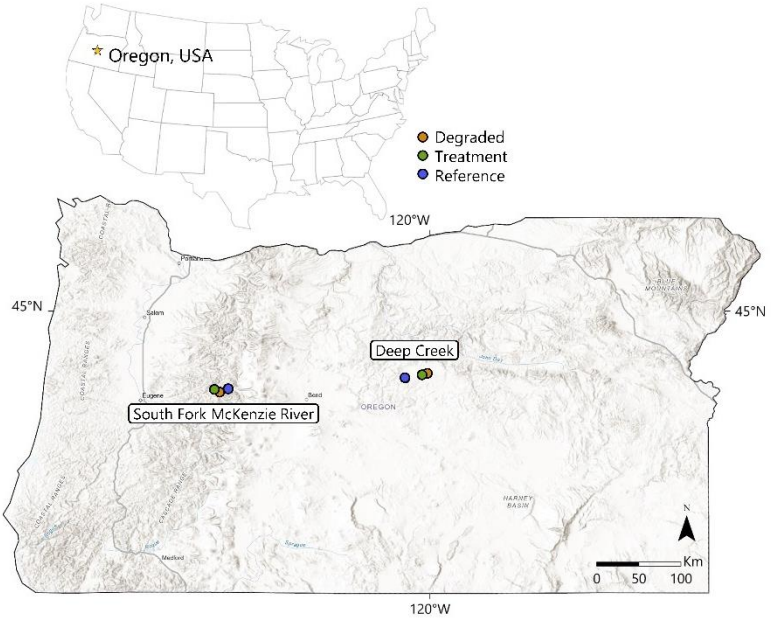

Figure 3.4. Location map of the sites in Oregon, USA used as case studies in this chapter.

3.2.3.2 South Fork McKenzie River

The South Fork McKenzie River (drainage area 560 km^2) is located near Rainbow, Oregon in the Willamette National Forest in the western Cascade Mountains (elevation 340 m) (Figure 3.4). With average annual temperature and precipitation of 10.6°C and 1882 mm, respectively, this site represents a case study for carbon sequestration potential in a densely forested river corridor and a Mediterranean climate with significant hydrologic influence from an upstream dam. Common forest species here include western hemlock (*Tsuga heterophylla*), Douglas-fir (*Pseudotsuga menziesii*), and western redcedar (*Thuja plicata*), with red alder (*Alnus rubra*) and cottonwood (*Populus trichocarpa*) adjacent to streams. Following construction of Cougar Dam in 1963, the channel incised to a single thread with primarily boulder substrate. Restoration was initiated in 2018 and involved dense placement of large wood across the entire floodplain, lowering of high alluvial surfaces, and filling of the incised channel to reconnect the channel and floodplain and improve habitat conditions for Chinook salmon

(*Oncorhynchus tshawytscha)*, bull trout (*Salvelinus confluentus*), Pacific lamprey (*Entosphenus tridentatus*), and other species. Horse Creek, approximately 10 km away, provides the reference condition for this site. Horse Creek has an anastomosing planform with one primary and several secondary channels, each with high wood load, frequent channel avulsions, and abundant forested wetlands in the river corridor. I selected a reach of the South Fork McKenzie upstream of the restoration activities for a degraded site. This degraded site is planned to be included in future restoration actions. The degraded reach is single threaded with a pine-dominated forested floodplain and history of channel manipulation and levee construction (Figure 3.5). Additional descriptive data for the South Fork McKenzie are in Supplemental Table 1 for this chapter.

Figure 3.5. Field photos of the South Fork McKenzie River in Willamette National Forest (left panel) and Deep Creek in Ochoco National Forest (right panel), Oregon, USA. Each photo is labeled with its assigned class as degraded, treatment, and design reference ("Reference"), and arrows in the bottom right of each photo indicate flow direction. The person in the left panel is 1.86 m tall and the person in the right panel is 1.58 m tall.

3.2.3.3 Methods

My sampling design to estimate carbon sequestration potential includes three classes per study area. The three classes, characterized by floodplain condition and inferred history, are referred to as degraded, treatment, and design reference. I assume that degraded sites represent typical pre-restoration conditions where human activities have moved the site beyond the natural range of

variability present prior to European settlement of the region (Rathburn et al., 2011; Wohl, 2011). Treatment sites represent conditions of recently implemented stream restoration treatments. Design reference sites represent relatively natural environments with minimal human alteration and carbon stocks that reflect the natural range of variability for a particular type of river corridor. Choice of degraded and design reference sites is subjective. The Deep Creek and South Fork McKenzie River sites are both on U.S. National Forest lands and I worked with local Forest Service hydrologists and fish biologists to identify degraded and design reference sites. I also used my knowledge of analogous sites from other portions of the western US.

A beaver-modified willow carr in which beaver are still present is characterized by numerous dams, ponds, and beaver canals in various stages of activity (i.e., active, or abandoned for progressively longer times) (Laurel and Wohl, 2019). The channel and floodplain are hydrologically connected. Abundant surface water storage in ponds (Hood and Bayley, 2008) and a high floodplain water table (Westbrook et al., 2006) create reducing conditions throughout much of the floodplain, even in regions with a dry climate. Spatially dense woody vegetation attenuates downstream fluxes of water and sediment, and beaver dams promote hyporheic exchange flows (Lautz et al., 2006). This configuration, known as a beaver-meadow complex (Polvi and Wohl, 2012), represents design reference conditions for Deep Creek treatment site. In contrast, when beaver abandon a site and their dams fall into disrepair, river flow is more likely to concentrate into a single channel. Consequently, the channel incises and helps to lower the floodplain water table, hydrologically disconnecting the channel and floodplain and creating an alternative state known as an elk grassland (Wolf et al., 2007). This configuration represents degraded conditions for the Deep Creek treatment site.

A densely forested river corridor, such as that in the South Fork McKenzie River, has abundant recruitment sources for large wood. As described for other rivers in the U.S. Pacific Northwest, the continuing recruitment and storage of large wood facilitates formation of logjams that influence the

distribution of hydraulics and sediment transport, commonly leading to a multithread channel planform and spatially heterogeneous floodplain geomorphology and floodplain forest (Fetherston et al., 1995; Collins et al., 2012). This represents design reference conditions for the South Fork McKenzie treatment site. When large wood is actively removed from the river corridor and/or deforestation removes wood recruitment sources, the loss of logjams in the channel and floodplain can lead to formation of a single channel flowing through a less diverse floodplain (Collins et al., 2002). This configuration represents degraded conditions for the South Fork McKenzie treatment site.

Measuring organic carbon: soil carbon

I anticipated within-reach heterogeneity in soil carbon content based on differences in hydrologic connectivity and soil moisture. Consequently, I differentiated wet and dry floodplain patches based on field conditions when sampling soil. I assigned these moisture conditions based on ground moisture at the time of field work and the type of vegetation present. For example, wetland vegetation such as sedges, rushes, or cattails characterize wet areas and more xeric vegetation such as reed canary grass (*Phalaris arundinacea*), cheatgrass (*Bromus tectorum*), or ponderosa pine (*Pinus ponderosa*) characterize dry areas. I randomized the exact sample location within a wet or dry area when choosing specific sample points.

I sampled soil carbon with a tubular soil corer of 3 cm diameter that collects 30-cm lengths of sample in each increment. At each soil sampling point, I sampled up to 1 m depth or refusal by cobbles in shallower soil. Previous research suggests that sampling bias and variance of organic carbon content cease to decrease after 11 samples within a floodplain along smaller rivers (Sutfin and Wohl, 2017) and within individual floodplain geomorphic units on larger rivers (Lininger et al., 2018). The case studies presented here involve smaller rivers, so I targeted 11 samples per moisture category in each floodplain class. This equates to 11 samples each in wet and dry soils per class per study area, for a total of 22

samples per class and 66 samples per study area. However, floodplains with degraded conditions were commonly hydrologically disconnected and dry. Consequently, fewer wet soil samples were collected from degraded floodplains. Additionally, some samples were lost during lab analysis. In total, I conducted statistical analyses on 59 soil samples from Deep Creek (12 dry and 2 wet from the degraded class, 11 dry and 13 wet from the treatment class, and 10 dry and 11 wet from the design reference class), and 53 samples from the South Fork McKenzie (11 dry from degraded, 11 dry and 10 wet from treatment, and 10 dry and 11 wet from design reference).

For final floodplain-scale estimation of soil carbon stocks, I weighted the estimated soil OC stocks for each moisture category by the approximate area of wet or dry soil in each floodplain. I determined wet versus dry conditions using National Agricultural Imagery Program (NAIP) aerial imagery from July 2020, the same month field samples were collected. Horse Creek, the design reference site for the South Fork McKenzie River, has too much forest vegetation to confidently estimate wet versus dry soil, so I used topography to estimate areas of wet and dry soil instead. Using a digital elevation model (resolution 1 m) made from airborne LiDAR data collected in 2016 and downloaded from Oregon Department of Geology and Mineral Resources, I assumed that soil below the average relative elevation above a channel surface (detrended by valley gradient) in the sampling area could be categorized as potentially wet. I validated this assumption with my sample locations of wet and dry soil. Through these analyses, I found the existing sample sizes to appropriately reflect area proportions of wet and dry soil, with roughly equal proportions in treatment and design reference floodplains, and little to no wet soil in degraded floodplains.

Soil samples were stored in a freezer and shipped to a commercial laboratory for analysis of organic carbon, total carbon, and texture with a hydrometer. Grain size percentages of silt, sand, and clay were used to categorize soil samples into soil types. Bulk density estimates were assigned based on soil type after evaluation of values according to soil type in comparison to two pedotransfer functions

(Leonaviciute, 2000; Ruehlmann and Korschens, 2009), three regression analyses of data from Chaudhari et al. (2013), and a constant density value. Estimates of bulk density were the median result of the seven methods evaluated and offered the most reasonable estimates of carbon stocks. The following formula was used to calculate carbon stocks from percent organic carbon:

$$soil\ organic\ carbon\ stock\ \left(\frac{Mg}{ha}\right) = \%OC \times bulk\ density\ \left(\frac{Mg}{m^3}\right) \times 1\ m\ depth \times 10{,}000\frac{m^2}{ha} \quad (1)$$

Measuring organic carbon: large wood carbon

Wood load was estimated via transects following the protocol of Van Wagner (1968) in the degraded and design reference reaches. Transects were evenly spaced where possible and extended either across the entire floodplain or across one half of the floodplain, depending on accessibility. I measured the diameter of each piece of large wood encountered along transects, and input diameters and lengths into the following equation to estimate volume per area of wood (Van Wagner, 1968):

$$\mathrm{V} = \frac{\pi^2 \Sigma \mathrm{d}^2}{8\mathrm{L}} \quad (2)$$

Where V = volume of wood per area, d = diameter of a piece of large wood >10 cm diameter and > 1 m length, L = transect length, and all metrics are in the same units of measurement. Wood volume in treatment floodplains was estimated with timber sale data from managing parties who completed the restoration projects, and from monitoring data in the South Fork McKenzie River (Hinshaw et al., in review). Monitoring data are from 2020 and include large wood volume measured in 23 plots randomly located in the South Fork McKenzie River treated floodplain. I calculated carbon stocks of large wood using average wood densities of the dominant tree species in each study area and the assumption that wood contains 50% organic carbon:

$$large\ wood\ organic\ carbon\ stock\ \left(\frac{Mg}{ha}\right) = wood\ load\ \left(\frac{m^3}{ha}\right) \times 50\%\ OC\ wood\ density\ \left(\frac{Mg}{m^3}\right) \quad (3)$$

For the South Fork McKenzie River, I averaged densities for the five dominant tree species mentioned above. Ponderosa pine density was used for Deep Creek degraded and treatment sites, and willow density was used for the Deep Creek design reference floodplain.

Statistical analyses

I used a type 3 ANOVA to determine whether there are differences between classes for each study site using a linear model of soil organic carbon stock predicted by class (degraded, treatment, and design reference). R version 4.0.3 was used to conduct the analysis with the car package (Fox and Weisberg, 2019; R Core Team, 2020). Separate models were fitted for the two study sites and two models were fit for Deep Creek: one model with class as the sole predictor, and one that included moisture. I used the emmeans package to conduct Tukey-adjusted pairwise comparisons between classes groups at the 95% confidence level (Lenth, 2020). Moisture was not included in the model for the South Fork McKenzie River because there were no wet samples in the degraded reach. Depth and texture, other potential predictors of carbon stocks, were not included because I assume they are adequately integrated into the calculation of soil organic carbon stocks. Moisture was included in a model for Deep Creek, but the sample size of n=2 wet samples in the degraded reach precludes reliable interpretation of comparisons of wet samples from the degraded class to other classes.

3.3 Results

I first tested whether there were significant differences in percent organic carbon in relation to moisture category (wet vs dry) at each of the six sites. I found significant differences at only two of the sites: percent organic carbon is significantly higher in (i) wet soils of the design reference site for South Fork McKenzie (p value 0.0275) and (ii) dry soils for the treatment site at Deep Creek (p value 0.036).

I then compared the six sites based on organic carbon stock. There were no significant differences between classes for Deep Creek when class was the sole predictor of soil organic carbon stock (Figure

3.6). When moisture and class were used to predict soil OC stocks, I found evidence of an interaction between class and moisture (p=0.04697). Among dry samples, there was a notable, but not statistically significant, difference between degraded and treated floodplain carbon stocks (p = 0.0782), and a significant difference between treated and design reference floodplain soil OC stocks (p = 0.0150). The estimated difference between treated and degraded dry floodplain OC stocks is 268 Mg/ha, with higher estimated carbon stocks in treated floodplains. My data in Deep Creek showed higher estimated OC stocks in dry treated than dry design reference conditions, with an estimated difference of 367 Mg/ha.

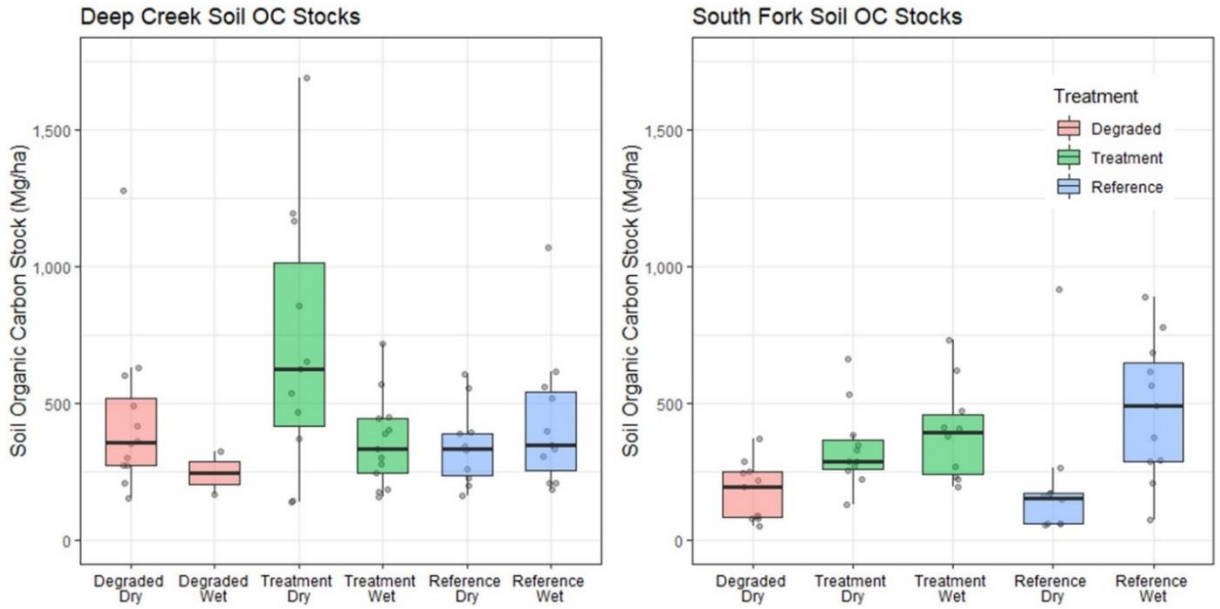

Figure 3.6. Box and whisker plots of soil organic carbon stock for wet and dry portions of each of the six classes. Line within each box indicates the median value, box ends are the upper and lower quartile, and whiskers are the 10th and 90th percentiles. Data points summarized by each box are also shown. Differences in South Fork McKenzie River organic carbon stocks were analyzed by class only due to a lack of wet samples from the degraded floodplain.

At the South Fork McKenzie site, there were no significant differences between class at the 95% confidence level, but there was a nonsignificant but notable estimated difference of 187 Mg/ha in mean values for OC stocks between the treated and degraded floodplains, with higher predicted soil OC stock in the treated floodplain (p = 0.0572). There was also a notable but nonsignificant difference between

the degraded and design reference floodplains for wet and dry combined (p = 0.0886), with estimated mean OC stocks in the design reference site predicted to be higher than the degraded site by 171 Mg/ha.

Estimates of large wood load and large wood carbon stocks varied depending on the method used and are presented in Table 3. Total estimated OC stocks, estimated by the sums of the simple mean soil OC stock of each class and large wood OC stocks, were greatest for the treated floodplain reaches in both study areas, and are also presented in Table 3.3. Basic organic carbon data are in Supplemental Table 3.

Table 3.3. Estimated carbon stocks in large wood and soil at the case study sites

Site & treatment	LW OC stock (Mg C/ha)	SOC stock (Mg C/ha)	Total OC stock (Mg C/ha)
Deep Creek			
degraded	21	416	437
treatment	7	521	528
reference	1	391	392
SF McKenzie			
degraded	39	177	225
treatment	136	364	500
reference	46	348	394

3.4 Discussion and Conclusions

My conceptual framework for quantifying carbon sequestration potential in river restoration involves the use of regional design reference and degraded floodplains for comparison to treated floodplains. The difference in measured carbon stocks between a degraded and design reference floodplain conceptually represents potential minimum differences in carbon storage that could be achieved through restoration actions, and measured carbon stocks in treatment areas indicate further potential for carbon storage. I illustrated application of the conceptual framework using two study areas, for both of which my results suggest higher organic carbon stocks in the treated areas than in

their respective degraded and design reference sites. I also estimated higher carbon stock in the degraded reach of the Deep Creek study area than in the design reference site.

The importance of large wood as a contributor to total carbon stock varies in relation to valley morphology and the presence of wood-trapping sites (Figure 3.2), and concentration of large wood in limited areas (e.g., beaver dams or very large logjams) can make it difficult to accurately estimate total wood load. I estimated the smallest carbon stocks in the form of large wood at the Gray's Creek site, for example, which is an active beaver meadow complex and design reference floodplain for Deep Creek. I expected a low wood load in the anastomosing grassed wetland of Gray's Creek, but the transect method of sampling large wood did not cross any beaver dams at this site, which may have caused us to underestimate wood load in the reach. Disproportionately high concentrations of wood are also located in large logjams at Horse Creek, the design reference floodplain for South Fork McKenzie. Because only one of 5 transects at Horse Creek crossed a logjam, the transect sampling method may have caused us to underestimate wood load at Horse Creek. In addition, high surface soil moisture and associated wood decay in Horse Creek likely kept us from measuring some buried, partially buried, decayed, and moss-covered pieces of wood from my transect surveys. Finally, the use of timber sale and project design data to estimate wood load in the treated Deep Creek floodplain likely led to an underestimate. Project design data provide an easy way to estimate wood loads in restoration reaches, but do not include pieces recruited since project construction.

Floodplain manipulation and other land use histories also influence large wood loads. The highest wood carbon stocks of my case studies occurred in the treated area of the South Fork McKenzie River. As part of the project implementation, large wood was placed in a lattice across the floodplain to create hydraulic roughness and encourage deposition. The use of large wood in restoration practices, such as the Stage 0 project at the South Fork McKenzie, increases the large wood carbon stocks in treated floodplains. At the degraded reach of the South Fork McKenzie, cut logs also increased measured wood

loads in the study area. I observed that many of the logs measured along transects in the degraded site were cut and accompanied by burn piles, presumably due to forest management practices such as hazardous fuel control. These cut logs increased my measured wood loads, but have separate, more static, geomorphic roles than large wood that more regularly interacts with water and sediment in dynamic floodplains such as Horse Creek.

I interpret the range of carbon stocks measured at all three sites in each case study as reflecting the potential range of floodplain carbon storage for the geographic and geomorphic setting of each case study. As described in the conceptual model, numerous factors interact to govern floodplain carbon accumulation rates through time and carbon stock at any point in time. This makes it both difficult to precisely predict floodplain carbon storage and difficult to use degraded and design reference reaches to demonstrate the effects of river restoration on carbon storage over short timespans of a few years. However, it is encouraging that the values of wood load and soil organic carbon at each of the design reference sites seem reasonable relative to preliminary carbon storage plots and summary tables developed from published values of floodplain large wood loads and soil carbon (Figure 3.3 and supplemental information). This suggests that the type of data reported in Table 3.1 and Figure 3.3 may eventually be useful in assessing potential floodplain carbon stocks following restoration, when the available data are expanded to include a larger number of sample sites across a wider range of climate and geomorphic conditions.

The optimal timeframes for monitoring organic carbon stock after restoration are not presently known but would presumably be at least several years to decades after restoration activities cease (e.g., Schiefer et al., 2018). This would allow newly (re)saturated floodplain soils time to accumulate organic matter. It would also allow time for large wood introduced to the site during restoration or trapped by the enhanced spatial heterogeneity of the restored site to accumulate in natural trapping sites such as bars, islands, or forested floodplain margins. Depending on the size and spatial heterogeneity of the

restored floodplain, I suggest that floodplain soil-carbon sampling be based on a stratified random design that, at a minimum, differentiates wet and dry floodplain surfaces and for larger rivers differentiates geomorphic patches (e.g., Lininger et al., 2018). Floodplain large-wood-carbon sampling using survey transects can also be based on a stratified random design where wood is known to be concentrated in large accumulations, including beaver dams.

Candidate sites for restoration are commonly chosen based on known or inferred historic conditions prior to excessive human disturbance and degradation. More specifically, in process-based and Stage 0 stream restoration, sites chosen for restoration activities are commonly wide, depositional valleys. This type of valley can be inferred, based on historic aerial imagery, local knowledge, relict hydric soils or floodplain landforms, to have historically possessed highly complex planforms with shallow groundwater tables, high degrees of lateral hydrologic connectivity, high wood loads, and floodplain wetlands. Abandoned beaver meadows are capable of retaining high carbon stocks for decades after abandonment (Laurel and Wohl, 2019). High measured soil carbon stocks of treatment floodplains in my case studies may primarily reflect past conditions, rather than the effects of recent restoration. In particular, the highest sampled soil carbon stocks from the Deep Creek treated floodplain (Figure 3.5) are from topographically high floodplain patches (referred to as “leave islands” during restoration) with old-growth ponderosa pines, suggesting the potential for prolonged organic matter input and accumulation.

There are many benefits associated with quantitatively estimating carbon stocks in degraded, treated, and design reference floodplains. I propose this conceptual model and study design as an example for practitioners, managers, scientists, investors, and other stakeholders to track changes of floodplains over time, collect baseline data in pre-treatment degraded areas, and build databases of design reference conditions that can be available to future stream restoration designers. At a broader scale, rivers play a role in the global carbon cycle, but the definition and quantification of carbon

sequestration potential in rivers remains largely unknown. I suggest that the type of quantitative estimations summarized here can be used to enhance the use of river restoration as a tool for carbon sequestration.

Chapter 4 Carbon sequestration potential of process-based river restoration

Summary

Certain methods of floodplain restoration enhance capacity for carbon sequestration by facilitating higher water tables, deposition of fine sediment, and increased input and residence time of organic matter. I measured floodplain soil carbon stocks in eight stream restoration projects across the western United States and compared them to nearby degraded and reference condition floodplains. Degraded floodplains had the lowest soil carbon stocks in the majority of floodplains measured, and reference stocks had the highest stocks of those with statistically significant differences between the three categories. Across all sites measured, stream restoration sites, referred to as treatment sites, had similar stocks to degraded condition floodplains. When modeled under degraded conditions, four out of eight of the treatment sites had significantly higher OC stocks than predicted. Climate and geologic variables are most influential in predicting carbon stocks, and floodplains in the interior western USA have the highest carbon stocks. As the demand for carbon sequestration is likely to increase due to society's response to climate change and the growing economic influence of the carbon market, ecologically responsible floodplain restoration provides a significant opportunity for carbon sequestration.

4.1 Introduction

There is a need for creative solutions to carbon sequestration with the ongoing and impending effects of climate change on our landscapes and societies. Stream restoration can potentially increase floodplain carbon stocks by enhancing processes of carbon deposition and storage. Within the global carbon cycle, potential magnitudes of organic carbon storage in the freshwater hydrosphere are not yet well constrained, and the uncertainty is particularly substantial for carbon storage in channels and their floodplains (Battin et al., 2009; Aufdenkampe et al., 2011). Within floodplains, stocks of carbon occur as

living biomass (i.e., vegetation and aquatic organisms), dissolved carbon in surface and ground water, dead biomass including large wood in the floodplain, and soil carbon (Sutfin et al., 2016; Wohl et al., 2017). Factors that influence carbon storage in floodplains include but are not limited to climate, geology, moisture, soil texture, residence time of sediment and biomass, and organic matter supply (Hinshaw and Wohl 2021). Soil carbon is typically the largest carbon stock in floodplains and is therefore the focus of this study. Optimal conditions for soil carbon storage in floodplains are wide, wet, relatively stable valley bottoms with long sediment residence times, cooler climates, and high organic matter inputs (Sutfin et al., 2016; Hinshaw and Wohl 2021). These conditions correspond to what are referred to as Stage 0 anastomosing wet woodland or anastomosing grassed wetland in the Cluer and Thorne (2014) stream evolution model. Reconfiguration and reconnection of river corridors to achieve Stage 0 conditions has been increasingly applied in the United States as part of stream restoration efforts within the past decade (Booth et al., 2009; Powers et al., 2019; Mattern et al., 2020).

Human alterations of river corridors including floodplain drainage, deforestation, flow regulation, artificial levees, and channelization can reduce carbon storage within floodplain vegetation, downed wood, and floodplain soil (Wohl et al., 2017). Stream restoration can potentially store carbon by enhancing processes that facilitate higher floodplain water tables and associated reducing conditions in the soil, as well as increased deposition of sediment and organic matter. Access to soil moisture from raised water tables facilitates new riparian vegetation growth that provides higher supply of organic matter via leaf litter. Residence time of floodplain sediment and associated soil organic carbon depend on fluvial erosion rates and vary from decades in small floodplains or locations close to the active channel(s) to thousands of years in larger floodplains and at locations farther from the channel (Wohl, 2015). Residence time of soil carbon also reflects rates of mineralization through microbial processing that releases CO_2 to the atmosphere and dissolved organic carbon to downstream transport and to groundwater (Bouillon et al., 2009; Handique, 2015). Although the process of stream restoration

implementation has a non-zero carbon footprint, estimated by Chiu et al. (2022) as 9-14 kg CO_2 per meter of stream restored, ecological restoration can transform the relative proportions of landscapes considered as carbon sources versus sinks and provide significant capacity to more efficiently sequester, rather than remain inactive or emit, carbon over decadal timescales (Zhou et al., 2020).

Riparian vegetation growth also increases the carbon stocks within aboveground biomass (e.g., Hanberry et al., 2015), but I do not account for living biomass (plants and vegetation) in this study. Rather, I focus solely on soil carbon as it is known to be abundant but highly spatially variable (Samaritani et al., 2011; Sutfin et al., 2016; Wohl et al., 2017).

Commonly, only a small portion of the project budget for most stream restoration projects is allocated to monitoring, and practically no budget is allocated to measure carbon content. However, incentives exist for practitioners to start measuring carbon. Other than the ethically satisfying quantification of carbon sequestered from the atmosphere, carbon credits in the units of tons of carbon can be sold on the carbon market (Wara, 2007; Schneider et al., 2019). This practice is widely applied within industries of agriculture and forestry (Ribaurdo et al., 2010; Paul et al., 2013), and it is only a matter of time before floodplain restoration could also qualify for carbon offsets (e.g., Matzek et al., 2015; Sapkota and White, 2020).

To my knowledge thus far, only one study has directly examined the effects of restoration on carbon stock in river corridors. Samaritani et al. (2011) compared soil carbon pools and fluxes in channelized and restored portions of the Thur River in Switzerland. This study investigated carbon in the context of increased spatial heterogeneity and temporal variability within the restored area but did not explicitly compare total carbon stock between restored and degraded areas. The restored floodplain had a larger range and higher heterogeneity of organic carbon pools and fluxes. Related studies indicate the effects of human alterations on river corridor carbon stock by comparing altered and natural river

corridors in the same region. Cabezas and Comin (2010) assessed the organic matter content of floodplain soils along Spain's Middle Ebro River in the context of land use. They found that floodplain soils with natural land cover have higher organic carbon stocks than agricultural portions of the floodplain, a pattern similar to that from Lininger and Polvi (2020), which showed decreasing floodplain organic carbon with increasing human alteration.

To begin the journey to bridge our understanding of carbon sequestration potential with quantified carbon stocks in stream restoration, we must address the following questions: Can measurable quantities of carbon be added to soil on short timescales? What framework works best to understand and measure carbon storage in stream restoration? Ideally, measurement of carbon in

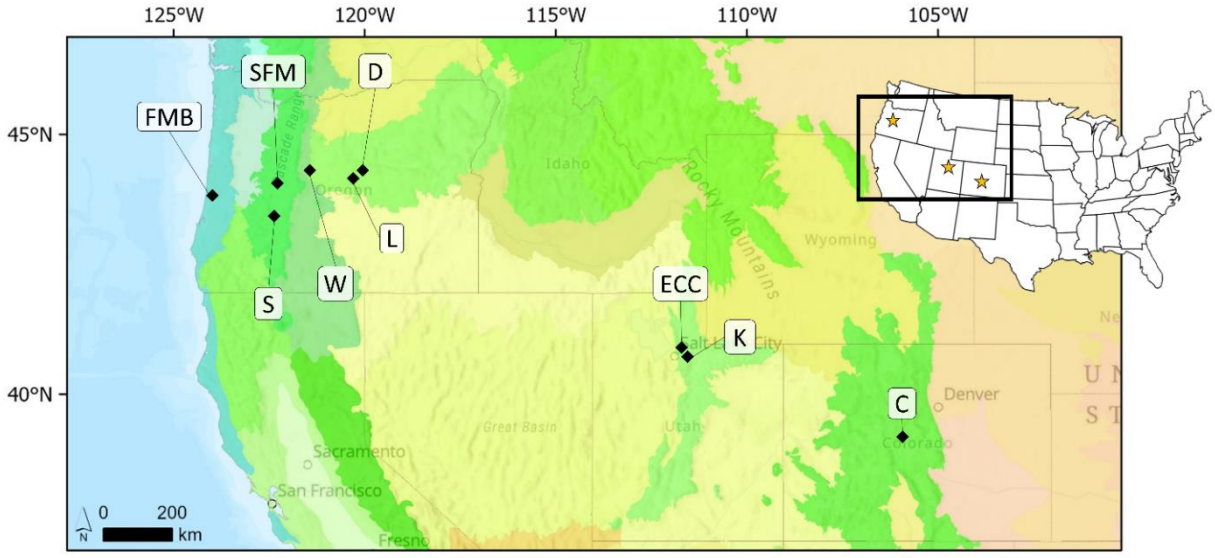

Figure 4.1. Context map of sampling areas in the western United States within boundaries of sites in Level III Ecoregions. Within each site, there are three or more floodplains corresponding to degraded, treatment, and reference categories. Labels correspond to treatment site names, i.e., FMB = Fivemile Bell, S = Staley Creek, SFM = South Fork McKenzie River, W = Whychus Creek, L = Lost Creek, D = Deep Creek, ECC = East Canyon Creek, K = Kimball Creek, C = Colorado sampling areas (Sheep Creek and Middle Fork South Platte River).

stream restoration would occur before and after restoration takes place. As a surrogate for pre and post restoration conditions, I use three alternative floodplain states to evaluate carbon sequestration: degraded, treatment, and reference. Alternative states are self-reinforcing states of equilibrium that can

exist simultaneously under the same environmental conditions (Holling, 1973; May, 1977). I choose the terminology of degraded, treatment, and reference to designate potential near-endmembers and an intermediate position on a spectrum of restoration, but recognize that 1) degraded and reference sites are not exact endmember positions, 2) the treatment, or stream restoration project category, is likely not in equilibrium and may fall anywhere along the spectrum, and 3) reference conditions are not always ideal conditions to restore to, and we may not be able to restore streams to a selected reference state (Dufour and Piegay 2009). I use the term treatment instead of restored because stream restoration sites are not "restored" as soon as construction takes place. The term degraded can encompass a range of impaired or impacted floodplain conditions and is not intended to assign blame to any particular person or group of people. I use it as a descriptive term and recognize that degraded floodplains can fall within a spectrum of conditions that may not be directly caused by one single type of floodplain alteration. Rather, floodplains chosen for the degraded category can represent the culmination of land or resource uses that may have limited floodplain function over the past few centuries. The primary objective of this study is to quantitatively compare floodplain organic carbon stocks in degraded, treatment, and reference stream corridors. Given the assumptions outlined above, I hypothesize that degraded sites contain the least carbon, treatment sites contain an intermediate amount of carbon, and reference sites contain the most carbon.

4.2 Study Areas

I include data from six stream restoration sites in Oregon, two stream restoration sites in Utah, and three floodplains in Colorado for this study (Figure 4.1). I henceforth refer to stream restoration projects as "treated" or "treatment" floodplains. I combined data for multiple treated reaches along the same stream where applicable, particularly in Fivemile Bell and Whychus Creek in Oregon and East Canyon Creek in Utah. Three treated sites in the South Park region of Colorado were intended to also be included in the study, but the soil samples from restoration projects were lost by UPS in transit to the

laboratory, leaving an incomplete dataset from Colorado including two degraded and one reference site. For analyses that do not rely primarily on floodplain class of degraded, treatment, and reference, Colorado soil samples are still included in the larger dataset. Associated with each treatment site is at least one reference condition site and at least one degraded site. Two sets of two projects, Deep Creek and Lost Creek in Oregon and Kimball Creek and East Canyon Creek in Utah, are within reasonable proximity to share the same reference site of Gray's Creek and McLeod Creek, respectively. Degraded sites represent intensive land uses that have degraded natural floodplain processes over time, and often include histories of levee construction, channel straightening, grazing, agriculture, timber harvest, or other methods of disconnecting channels from their floodplains. Some but not all degraded sites selected for this dataset are candidate sites for future restoration projects and can thus benefit from baseline data before restoration takes place. I chose each floodplain and assigned it to a category based on personal communications with local stakeholders and project designers, particularly scientists at the USDA Forest Service, Utah State University Swaner Preserve and EcoCenter, and the stream restoration company EcoMetrics Colorado. Individual site characteristics are listed in Table 4.1.

Table 4.1. Site characteristics of stream restoration projects considered in the study.

Restoration Project Stream Name	Sample Size[a]	Location	Year of Sampling Area Treatment	Average Elevation (m)	Ecoregion (Level III)[b]	Drainage Area (km^2)	Mean Annual Temperature (°C)	Mean Annual Precipitation (mm)
Fivemile Bell, OR	120	124.0097°W 43.8472°N	2018	15	Coast Range	21	11.3	2067
Staley Creek, OR	62	122.3828°W 43.4839°N	2017	687	Cascades	105	10.7	1378
South Fork McKenzie River, OR	53	122.2883°W 44.1596°N	2018	345	Cascades	560	10.9	1973
Whychus Creek, OR	82	121.4274°W 44.3623°N	2016	829	Blue Mountains	670	8.4	311
Deep Creek, OR	87	120.0585°W 44.3258°N	2018	1337	Blue Mountains	224	6.6	536
Lost Creek, OR	50	120.3348°W 44.1906°N	2012	1227	Blue Mountains	21	7.4	424
East Canyon Creek, UT	89	111.5487°W 40.7314°N	2015-19	1932	Wasatch and Uinta Mountains	130	6.3	541

Kimball Creek, UT	43	111.5181°W 40.7193°N	2019	1944	Wasatch and Uinta Mountains	77	6.3	535

[a]Sample sizes refer to number of floodplain soil samples collected and include shared reference samples for sites where references were shared, and do not include sites without a complete set of categories. The total sample size is 598. [b]From Esri US Federal Datasets and Omernik and Griffith (2014)

4.3 Methods

4.3.1 Field Methods

I followed the field methods described in Hinshaw and Wohl (2021) and collected 11 soil samples per moisture class (wet or dry) in each category (degraded, treatment, reference) of floodplain using a 3 cm diameter 22 cm length spoon sampling soil corer. The sample size of 11 per category is drawn from supplemental information in Sutfin and Wohl (2017), where bias and variance are shown to stabilize after 11 samples per geomorphic unit. Moisture categories were determined based on vegetation (riparian vs upland species), microtopography, and soil moisture conditions at the time of sampling. Moist soil with wetland vegetation (e.g., sedges, rushes) was categorized as wet. All sampling was conducted during relatively dry summer conditions. Dividing samples into separate moisture categories is intended to account for differences in carbon content of saturated vs dry soil found in previous literature (e.g., Moyano et al., 2012; Manning et al., 2015). At each sampling location, I noted vegetation present and sample depth. Samples were obtained at 30-cm vertical intervals at multiple depths to 90 cm from the same sampling hole where the floodplain sediment was sufficiently deep. In total, 598 samples collected over the summers of 2020 and 2021 were used in the analyses for this study (Table 4.1).

4.3.2 Data Analysis

4.3.2.1 Within-site comparisons

I examined relationships of carbon storage via within-site comparisons, where I compared carbon between degraded, treatment, and reference categories within one site. I first tested for within-site differences between degraded, treatment, and reference carbon content (%) and carbon stocks (Mg/ha). Without considering stream restoration intervention, the carbon sequestration potential at a particular site could be considered as the difference in carbon stocks between reference and degraded categories. I conducted Welch two-sample t-tests between degraded and reference carbon stocks for each site.

4.3.2.2 Modeled treatment stocks

I created unique models for each site that significantly estimated degraded category carbon content. I chose predictors for each site's degraded category floodplain based on what led to the model that best estimated degraded carbon content (Table S1). I used these degraded condition models to estimate treatment category carbon content at each restoration project. This process was intended to estimate carbon stored since restoration treatment, with the large assumption that pre-restoration conditions were similar to the degraded site associated with each restoration project. I recognize the centrality of the assumption and suggest that direct, repeat pre and post measurements would better represent the estimate of carbon stored since restoration. Using models associated with each degraded site to estimate treatment and reference and calculating the difference between measured carbon and estimated carbon provides a first-order approximation of how much carbon could be stored if environmental conditions are sufficiently similar between degraded, treatment, and reference sites.

4.3.2.3 *Across-site comparisons*

I tested for differences between degraded, treatment, and reference carbon content (%) and carbon stocks (Mg/ha) for sites combined by Level III Ecoregion (Omernik and Griffith, 2014) and for all sites combined. I categorized Ecoregions by where the treatment floodplain was located for a set of

degraded, treatment, and reference floodplains within a site. Five Type III Ecoregions were represented by the treatment sites sampled (Table 4.1). Two of the five Ecoregions consisted of only one site and thus have the same comparisons as the individual site results. The Cascades, Blue Mountains, and Wasatch and Uinta Mountain Ecoregions contained multiple sites combined. Staley and South Fork McKenzie River sites are both in the Cascades Ecoregion; Deep Creek, Lost Creek, and Whychus Creek fall into the Blue Mountains Ecoregion, and East Canyon Creek and Kimball Creek are within the Mountain Valleys Ecoregion. Within Whychus Creek, a treatment reach (Camp Polk) and reference site (Indian Ford) fell into the adjacent Ecoregion (Eastern Cascades Slopes and Foothills) but were grouped into the Blue Mountains with the remainder of Whychus samples for simplicity.

I conducted tests on all data combined and explored models that best explain carbon content for the entire dataset. I ran ANOVA tests to determine differences in categories for all sites combined. Then, using the combined dataset, I investigated correlations between carbon content and potential numeric predictor variables listed in Table S1. Using variables with significant correlations and additional categorical predictor variables of research interest, I used three types of models to estimate carbon content (%). I split the dataset using 80% of sample points for model building and the remaining 20% for model evaluation.

I began with a linear mixed model. To account for the lack of independence of samples from the same floodplains, lack of independence of samples from different depths from the same hole, and the availability-based nature of the stream restoration projects I chose to sample, I modeled carbon as a mixed model with random and fixed effects with a nested block study design using the lmer function from the lme4 package in R version 4.1.3 (R Core Team, 2022). Due to the large number of complexities to be considered in the mixed generalized linear model, I also modeled carbon using a gradient boosted regression tree model that utilizes elements of decision trees and machine learning to account for characteristics of the dataset without the need to account for the same linear model sensitivities. The

gradient boosting model was built with the dismo package in R (Hijmans et al., 2021). Parameters for this model were those suggested by Elith et al. (2008). In addition, I modeled the data with a random forest model using regression decision trees with the randomForest package in R (Liaw and Wiener 2002). I compared results from the three models with the root mean square error (RMSE) and the coefficient of determination (R^2) between 20% of the data reserved for model evaluation and the model predictions.

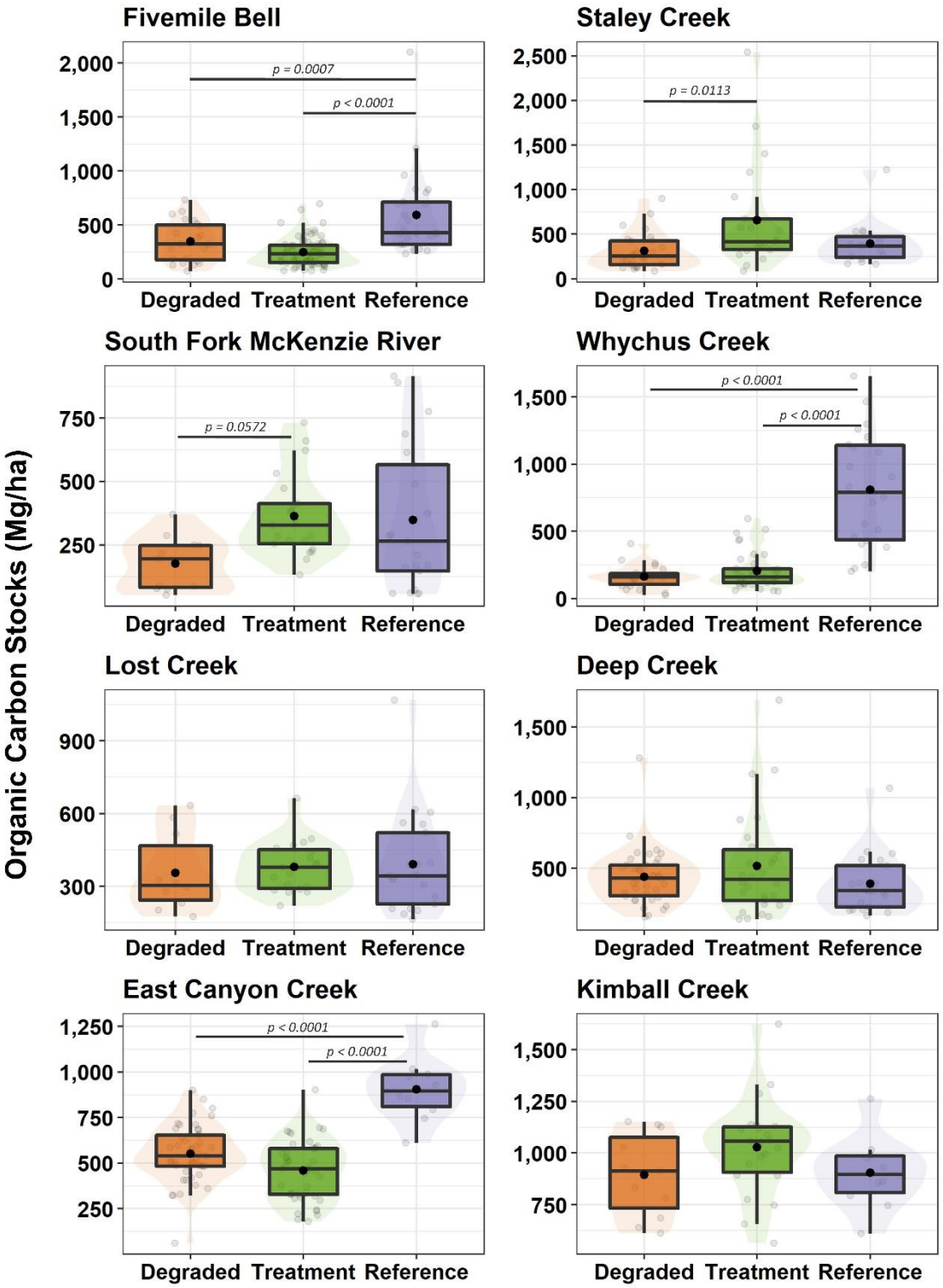

Figure 4.2. Box and whisker plots of carbon stocks at each site. Black dots show the mean of each category and y-axis scales vary for each plot. Transparent dots show stocks from individual samples, and violin shading behind boxes represents the relative density of samples. Significant differences between categories are noted with black lines and labeled with Tukey-adjusted p-values.

4.4 Results

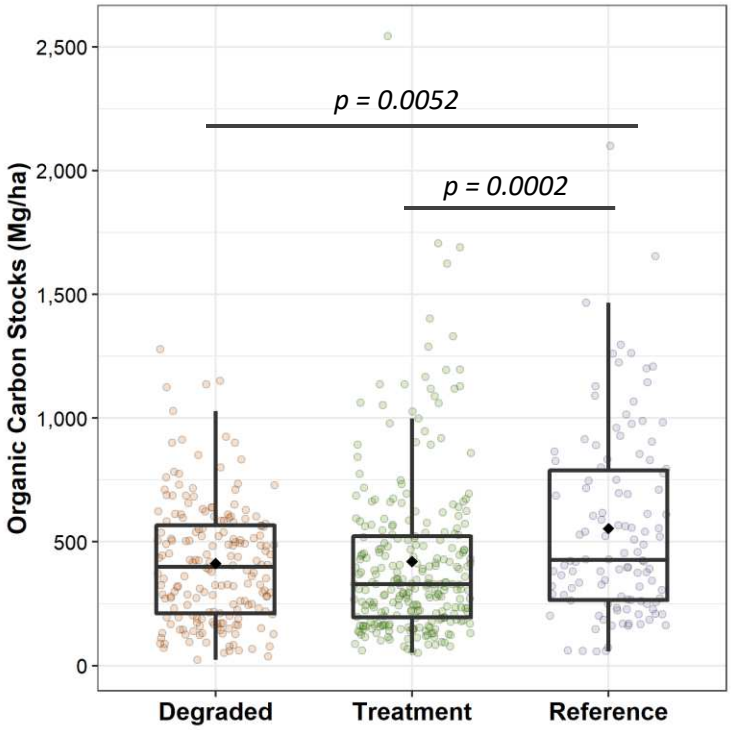

Figure 4.3. Box and whisker plot of all Oregon and Utah sites combined. Colorado is not included due to an incomplete dataset. Black dots indicate the mean of each category. Black bars indicate significant differences and are labeled with Tukey-adjusted p-values.

Table 4.2. Results of measured carbon stocks in each category of floodplain at all sites.

Site	Degraded Stocks (Mg/ha)				Treatment Stocks (Mg/ha)				Reference Stocks (Mg/ha)
	Reach 1	Reach 2	Reach 3	Mean	Reach 1	Reach 2	Reach 3	Mean	
Fivemile Bell	397 ± 52	293 ± 57		347 ± 39	247 ± 23	283 ± 23	228 ± 31	249 ± 15	**593 ± 81***
Staley Creek	279 ± 59	338 ± 56		313 ± 40				**659 ± 131****	396 ± 68
South Fork McKenzie				177 ± 32				**364 ± 35**	348 ± 62
Whychus Creek	154 ± 19	170 ± 36		161 ± 19	176 ± 21	249 ± 46		203 ± 22	**811 ± 92***
Lost Creek				355 ± 51				380 ± 24	**391 ± 46**
Deep Creek	421 ± 67	452 ± 28		439 ± 32				**515 ± 69**	391 ± 46
East Canyon Creek	538 ± 48	564 ± 31	551 ± 40	552 ± 23	430 ± 36	488 ± 35		458 ± 25	**904 ± 56***
Kimball Creek				894 ± 60				**1028 ± 49**	904 ± 56
All OR & UT Sites	413 ± 18				421 ± 21				**554 ± 35**
Colorado Sites (incomplete)	768 ± 54	763 ± 118		766 ± 49				NA	645 ± 118

Bolded values are highest of dataset for each site. * represents a significant (Tukey adjusted p<0.05) difference in an ANOVA test comparing the 3 categories. **In Staley Creek, treatment stocks are significantly higher than degraded (p<0.05) but not reference.

Table 4.3. Ranked categories of floodplains

Site	Degraded Stocks	Treatment Stocks	Reference Stocks
Fivemile Bell	intermediate	Lowest	highest*
Staley Creek	lowest	highest	intermediate
South Fork McKenzie River	lowest	highest	intermediate
Whychus Creek	lowest	intermediate	highest*
Lost Creek	lowest	intermediate	highest
Deep Creek	intermediate	highest	lowest
East Canyon Creek	intermediate	Lowest	highest*
Kimball Creek	lowest	highest	intermediate

* indicates significance at the 95% confidence level

4.4.1 Within-site comparisons

Results for carbon stocks are shown in Table 4.2 and Figure 4.2. Patterns of significance were the same between tests run on organic carbon (%) and organic carbon stocks, therefore I describe only carbon stocks. In all sites except Colorado, which lacks a treatment sample set, either treatment or reference stocks are highest. Degraded stocks were not the highest of any site but were intermediate at three of the eight sites with complete datasets (Table 4.3). Degraded floodplains had the lowest stocks in five of the eight complete datasets. Three out of four of the sites with highest reference carbon stocks were significantly higher than both other categories at the 95% confidence level when tested with an ANOVA. Moisture was not included in the ANOVA tests between floodplain categories at each site. Among tests for differences in moisture categories between categories at each site, only three floodplains (East Canyon Creek Degraded Reach 1, Staley Creek Degraded Reach 2, and South Fork McKenzie Reference Reach) have significant differences between carbon stocks for wet versus dry samples, and therefore I conduct simple comparisons of degraded, treatment, and reference carbon stocks only.

In the t-tests between degraded and reference within each site to determine carbon sequestration potential without the treatment category, half of the sites sampled (South Fork McKenzie, Staley Creek, Fivemile Bell, and East Canyon Creek) had significantly higher reference carbon stocks than degraded stocks. In all sites except one (Deep Creek), reference floodplains have higher mean carbon stocks than degraded stocks, although the result is not statistically significant for Whychus Creek, Lost Creek, and Kimball Creek. Six sites have higher mean stocks in treatment than degraded, but only two sites, Staley Creek and South Fork McKenzie River, have statistically significant higher treatment stocks than degraded stocks.

In summary, of the eight sites with complete datasets, degraded floodplains had the lowest soil organic carbon stock at five sites and reference floodplains had the highest carbon stock at four sites (Table 4.3). These results provide partial support for the original hypothesis.

4.4.2 Modeled treatment stocks

When treatment stocks were estimated with a degraded model fitted to each site, the four sites of Staley Creek, South Fork McKenzie River, Whychus Creek, and Kimball Creek showed higher measured than predicted treatment stocks at the 95% confidence level (Figure 4.4). Two sites had lower than predicted stocks, and two did not show significant differences. The estimated differences between measured and predicted treatment stocks for sites where measured stocks exceeded predicted stocks

are 354 Mg/ha, 132 Mg/ha, 56 Mg/ha, and 118 Mg/ha for Staley Creek, South Fork McKenzie River, Whychus Creek, and Kimball Creek, respectively (Figure 4.4).

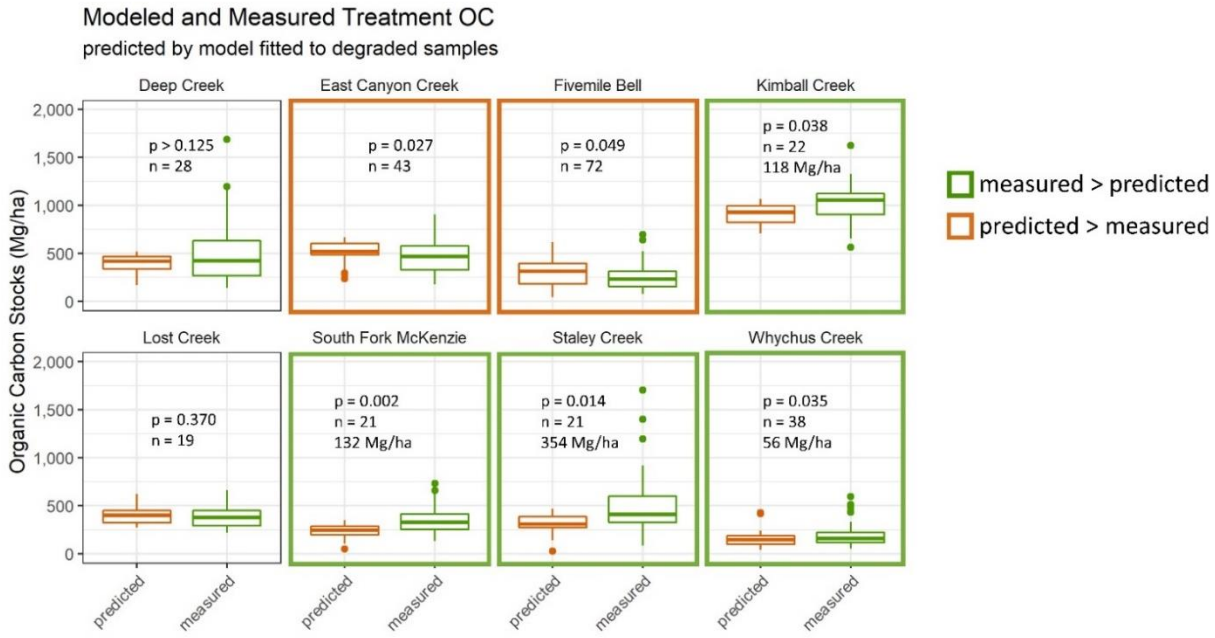

Figure 4.4. Box and whisker plots of modeling results and measured treatment stocks at each site. Green boxes outline sites where the measured carbon stocks exceed predicted stocks at the 95% confidence level, and orange boxes outline sites where predicted carbon stocks exceed measured stocks at the 95% confidence level. p-values and sample sizes for each category (measured and predicted) are given, and the estimated difference between measured and predicted carbon stocks is listed for sites that had higher measured than predicted treatment stocks.

4.4.3 Across-site comparisons

When analyzing all sites together, I found the largest magnitude correlation between carbon stocks and grain size, particularly between percent sand content (ρ= -0.532, p = 4E-45), which is directly inversely related to the sum of silt and clay content (Table 4.4). Correlations between organic carbon stocks and location data, climate data, ad elevation are also significant and suggest that carbon stocks are higher in the high elevation mountain ranges in the interior of the continent that have cooler climates.

Across all Ecoregions, carbon stocks for ecoregions in Oregon were significantly lower than the combined Colorado and Utah Ecoregions ($p<0.0001$) when the sites were analyzed in an ANOVA. When degraded, treatment, and reference categories were compared within each Ecoregion, results were as follows: Cascades sites had highest stocks in the treatment category with a significant difference between treatment and degraded, but no significant difference between treatment and reference or reference and degraded. Blue Mountains sites had significantly higher reference stocks than degraded and treatment, and the Wasatch and Uinta Mountain sites in Utah also had highest stocks in the reference category.

Combining all samples from all sites revealed significantly higher reference carbon stocks than degraded and treatment, and no significant difference between degraded and treatment (Figure 4.3). This result was the same for a simple comparison of the three treatment categories and an ANOVA comparison that accounted for moisture, site, sample location, and depth (p-values range from 0.0002 – 0.0052).

Table 4.4. Correlations between organic carbon stock and numeric variables. All correlations are significant except for distance to stream.

Variable	Pearson Correlation with Carbon Stock	p-value
% Sand	-0.532	<0.0001
% Silt	0.530	<0.0001
% Clay	0.314	<0.0001
Depth	-0.279	<0.0001
elevation	0.388	<0.0001
Drainage area	-0.238	<0.0001
x (longitude)	0.403	<0.0001
y (latitude)	-0.397	<0.0001
NDVI	0.135	<0.0001
Mean annual precipitation	-0.236	<0.0001
Mean annual temperature	-0.343	<0.0001
Distance to stream	-0.041	0.313
Grain size	-0.531	<0.0001

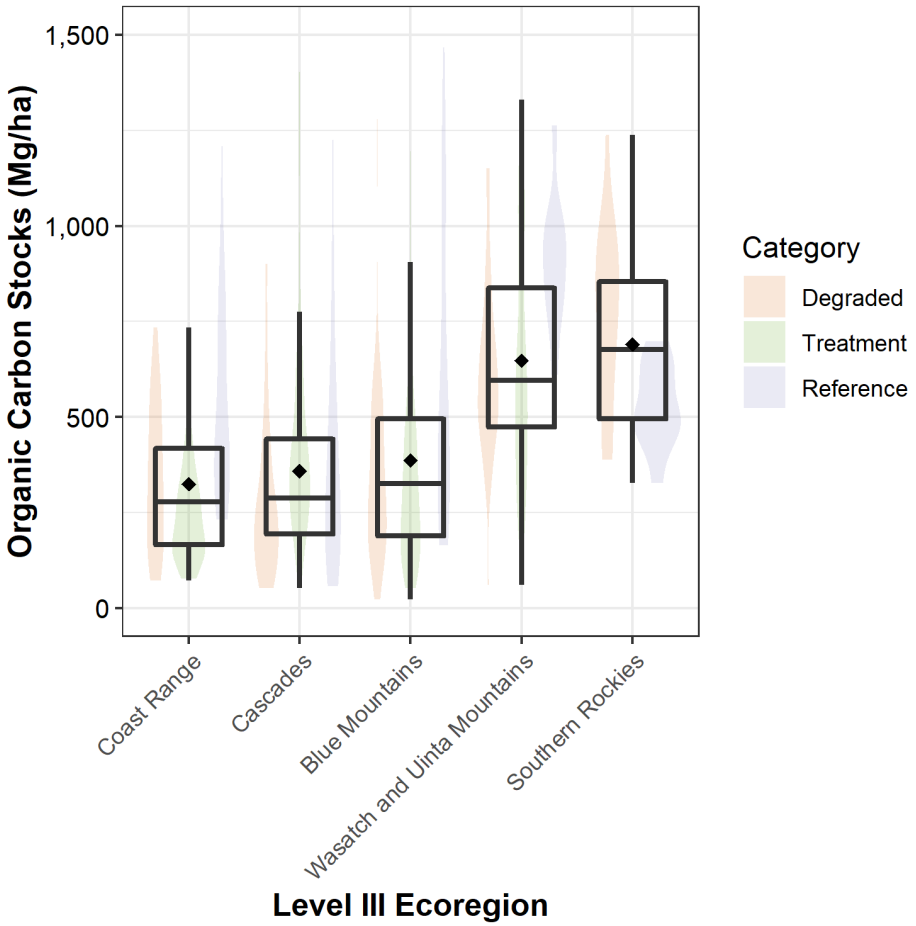

Figure 4.5. Box and whisker plot of samples within each Ecoregion. Black dots indicate the mean OC stocks and violin plot shading behind boxes shows the relative density of sample points.

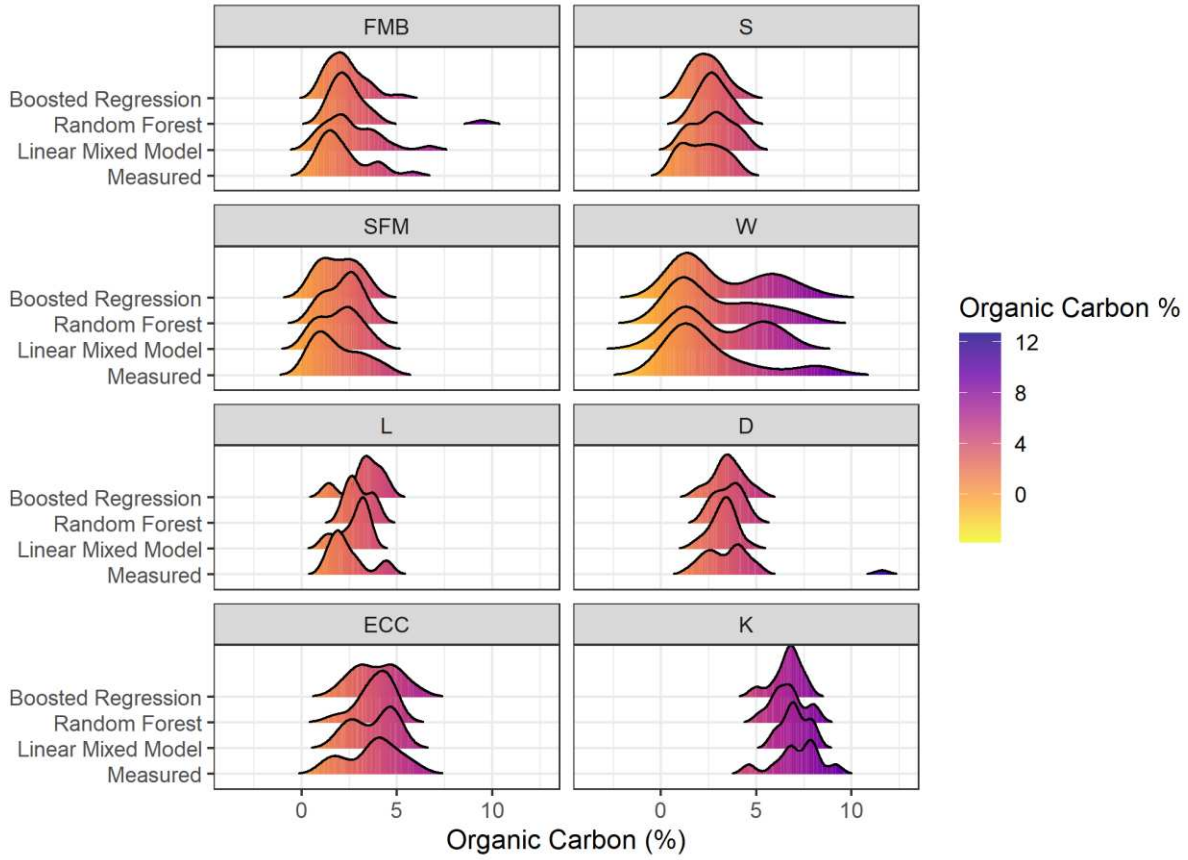

Figure 4.6. Density histograms of organic carbon concentration for each site with 3 models. The three models were used to estimate 20% of the dataset that was reserved for model validation, while 80% of the data were used to create the models. Sites are labeled with codes as follows: FMB = Fivemile Bell, S = Staley Creek, SFM = South Fork McKenzie River, W = Whychus Creek, L = Lost Creek, D = Deep Creek, ECC = East Canyon Creek, K = Kimball Creek.

4.4.4 Regional modeling

I modeled data from all locations combined using a linear mixed model, a random forest model, and a gradient boosted regression model (Figure 4.6). I included 80% of the dataset in all three models and reserved 20% of the dataset for model evaluation. I compared the models with the root mean square error and coefficient of determination (R^2) between the measured and predicted data. The random forest model had the lowest root mean square error (RMSE) of the 3 models at 1.26 % OC and the highest R^2 of 0.68. All models tended to overestimate degraded and reference carbon content of the dataset. Model descriptions and results are shown in Table 5.

Table 4.5. Model predictors, results, and errors from linear mixed, random forest, and boosted regression models built to predict % organic carbon in randomly selected 20% proportion of the total data.

Model	Predictor Variables	% OC Estimates			RMSE	R^2, modeled vs measured data
		Deg	Treat	Ref		
Measured Data	NA	3.09	2.83	3.93	NA	NA
Linear Mixed Model	Site, reach sample hole, depth, mean annual temperature, NDVI, silt+clay, soil type	3.19	2.78	4.26	1.33	0.64
Random Forest Model	treatment, depth, texture, elevation, NDVI, mean annual temperature, drainage area, land cover class, geology, Ecoregion, silt+clay, vegetation	3.36	2.93	4.01	1.26	0.68
Boosted Regression Model	treatment, depth, texture, elevation, NDVI, mean annual temperature, drainage area, land cover class, geology, Ecoregion, silt+clay, vegetation	3.30	2.73	4.10	1.36	0.62

4.5 Discussion

The sites selected for soil sampling represent a geographic range of elevation, climate, and lithology for the western United States. My goal was to determine whether there are detectable differences in floodplain carbon stock between the categorized floodplain states of degraded, treatment, and reference, and to assess the carbon sequestration potential of stream restoration within the context of these simple categories. A secondary goal was to examine factors that influence carbon content within floodplain soil at a larger, regional scale.

4.5.1 Within-site comparisons

Degraded floodplains have the lowest carbon stocks in the majority of sites, which supports my hypothesis. Among sites with complete datasets, treatment and reference were tied for having the

highest carbon stocks, but the reference category has more statistically significant higher stocks than the treatment category.

Deep Creek is the only site where reference soil carbon stocks are lower than both treatment and degraded stocks. The reference site chosen for Deep Creek was Gray's Creek, a beaver meadow about 15 km away from Deep Creek. Gray's Creek and Deep Creek are within same North Fork Crooked River watershed, but the two sites are underlain by different geology. Gray's Creek lies within Eocene- to Oligocene-aged volcaniclastic tuff in the John Day Formation, while Deep Creek overlies the Columbia River Basalt formation of Miocene age. Basalt weathers to clay minerals, while tuff contains higher silica content and is more resistant to weathering than basalt. Within my samples, floodplain soils underlain by basalt bedrock geology contained a higher proportion of silt and clay. The results from correlation of numerical predictor variables show that grain size has the largest magnitude of negative correlation to carbon content, indicating that silt and clay content are significant contributors to carbon storage, as demonstrated in previous work (e.g., Cai et al., 2016). Gray's Creek also has smaller drainage area than Deep Creek, with 42 km^2 and 224 km^2, respectively. Deep Creek hosts large ponderosa pine (*Pinus ponderosa)* trees and is classified as Evergreen Forest in the National Land Cover Dataset (Homer et al., 2012), while Gray's Creek is classified as Emergent Vegetation and contains no large trees other than willows. Gray's Creek is also the reference site chosen for Lost Creek. Lost Creek is within the same geological formation as Gray's Creek and trends from least to greatest mean carbon content in degraded, treatment, and reference stocks. In hindsight, a different reference condition should have been chosen for Deep Creek and future iterations of this study design should consider the underlying geology when associating categories of floodplain.

Staley Creek treatment area had the most variable soil carbon stocks by an order of magnitude compared to all other categories of stocks in all other sites that had complete datasets (i.e., not Colorado). Soil carbon stocks in the Colorado sites had the same order of magnitude of variance but

were not complete sample sets. This variability could reflect another desired aspect of restoration: floodplain heterogeneity. Heterogeneity enhances diversity of habitats and in turn supports more biodiverse and resilient floodplains (Wohl, 2016), but many sequences of disturbance and succession induced by frequent lateral channel migration can also lead to a variety of patches with different soil carbon contents (Lininger et al., 2018; Sutfin et al., 2021).

4.5.2 Modeled treatment stocks

Predicted treatment stocks were lower than measured treatment stocks in four sites when models using degraded category data were used to estimate OC stocks in treatment floodplains. Models made separately for each site are intended to minimize variability in climate, geology, and soil formation processes. The input of degraded data to make these models utilizes the assumption that treatment sites were similar to degraded sites before restoration took place. However, magnitudes of differences in carbon stocks in treated versus degraded, divided by the number of years since restoration, reveals carbon sequestration rates that may be too good to be true. If the difference between measured and predicted carbon stocks serves as an estimate of carbon sequestered since treatment, granted the assumption that pre-restoration conditions are well represented by degraded sites, the magnitude of carbon stored since restoration in Staley Creek, South Fork McKenzie River, Whychus Creek, and Kimball Creek is 354 Mg ha^{-1}, 132 Mg ha^{-1}, 56 Mg ha^{-1}, and 118 Mg ha^{-1}, respectively. These four sites also contained higher treatment stocks than degraded stocks. Divided by the number of years since restoration, the per-year carbon sequestration approximations for the four sites are 118 Mg ha^{-1} $year^{-1}$ for Staley Creek, 66 Mg ha^{-1} $year^{-1}$ for South Fork McKenzie, 14 Mg ha^{-1} $year^{-1}$ for Whychus Creek, and 59 Mg ha^{-1} $year^{-1}$ for Kimball Creek. Table 3 in Sutfin et al. (2016) lists accumulation rates ranging from 0.03-8 Mg C ha^{-1} $year^{-1}$, an order of magnitude lower than the estimated differences from this study. I cannot accurately estimate carbon accumulation rates in the sites for this study because there are no measurements of antecedent conditions, but the substantial difference between my inferred rates and

the range of published rates for diverse environments around the world suggests that my inferred rates are too high. Thus, I infer that the sites with measured treatment stocks that were higher than degraded stocks, or higher than modeled treatment stocks, likely contained more carbon than degraded floodplains before treatment, facilitated by historic conditions prior to degradation that likely factored into the choice to select the area for stream restoration. In future studies, it would be beneficial to consider time since degradation, specific manner of degradation, and further information about historic conditions prior to degradation when comparing the categories of degraded, treatment, and reference. Although floodplains such as South Fork McKenzie River and Staley Creek underwent large scale regrading of the floodplain as part of restoration, it is promising that their soil carbon stocks were not destroyed by the disturbance within the organic-rich upper layer. Instead, these sites either retained their existing carbon stocks or gained more carbon since treatment. For purposes other than research, such as carbon offset verification, I recommend that direct comparisons to estimate magnitude of carbon stored since restoration be made on repeat pre-post data rather than assuming degraded conditions can directly reflect pre-treatment conditions.

4.5.3 Across-site comparisons

The Colorado and Utah sites show significant carbon stocks compared to other regions. This is likely explained by high elevation and low mean annual temperature compared to other areas. It is pertinent to consider mountain valleys of the interior western USA as zones of high potential carbon storage. Floodplain drainage, development for agriculture, and associated degradation of wide, wet valley bottoms with potential for high carbon storage (i.e., beaver meadow complexes and other wetlands) could have disproportionately high impacts on carbon sequestration (Wohl et al., 2018). Considering that US states such as Colorado likely have lower total budgets for stream restoration compared to states in the Pacific Northwest that are greatly driven by funding from fisheries conservation, carbon sequestration can serve as an additional added benefit and enhanced return on

investment in stream restoration within the Intermountain West. Entry into the carbon market and the sale of carbon offsets could provide a source for further funding of ecological restoration.

Both sites within the Cascades ecoregion, Staley Creek and South Fork McKenzie River, contained higher carbon stocks at treatment sites than at degraded or reference sites. Because the data in this study do not directly compare pre-and post-restoration stocks, my ability to quantify carbon stored directly as a result of restoration is limited. However, both projects in this region utilized similar methods of stream restoration, in which the valley bottom was regraded to fill incised channels and to lower high-elevation surfaces, and large wood was laid across the valley bottom to maintain hydraulic roughness as vegetation reestablishes. In both cases, surface water was spread across the valley bottom, and field observations of declining upland species and early succession wetland vegetation suggest water tables were raised. Whether recent increases in soil carbon storage took place at each site or persisted from former valley conditions, the manner of restoration sampled in this ecoregion facilitated the development of river corridors with processes and planforms that support carbon sequestration. In addition, carbon stocks in the form of large wood were greatly increased at both sites via the project designs.

The most influential factors contributing to carbon storage are climate and geology, as outlined in the conceptual framework for floodplain carbon storage in Hinshaw and Wohl (2021) and further illuminated by correlations between my sample set and environmental variables. Correlations between grain size, temperature, and elevation support patterns of carbon in existing literature (Wang et al., 2013; Cai et al., 2016; Qi et al., 2016). Generally, carbon increases with (i) elevation and associated climate trends toward cooler temperatures in all study areas and (ii) higher proportion of silt and clay. Geographically, carbon content increased toward the center of the continent. Potential carbon content in soil depends primarily on intermediate to long term processes such as soil formation from weathering of underlying lithology and gradual organic matter input from vegetation, but local hydrologic and

geomorphic conditions, especially those influenced by floodplain restoration, can set the stage for carbon transport or leakage versus soil carbon enhancement and storage. Elevated concentrations of soil carbon can persist for decades after degradation or drying (Laurel and Wohl, 2019), but rather than optimizing carbon storage potential, dry, degraded floodplains gradually decrease in carbon storage capacity over time (Ferre et al., 2014; Hanberry et al., 2015; Limpert et al., 2020; Lininger and Polvi, 2020).

4.5.4 Regional modeling

Given that methods to verify carbon offsets often rely on models and encounter substantial uncertainty (Smith et al., 2020), the three models that I used estimated carbon content with reasonable performance. Of the three models, the Random Forest model performed the best. Although the linear mixed model results aligned well with the measured carbon and the other model results, this model relies on information about the specific sites to account for my study design and therefore would be more laborious to use in a predictive setting in contrast to the estimation setting used here to evaluate the models. In general, it is my goal to create a model that uses climate and landscape variables that are easily obtainable, such as remote sensing data, to generate a first-order estimate of carbon content. Remote indices do exist to estimate carbon content (e.g., Angelopoulou et al., 2019) but are commonly developed on barren or agricultural soils that do not contain the same level of complexity as river corridors. Future steps for the application of these models would be to test or incorporate validation data from outside of my study areas.

4.6 Conclusion and Future Directions

Demand for carbon credits within the carbon market is likely to increase as large, economically impactful organizations strive toward carbon neutral practices, and as compliance standards for releasing carbon into the atmosphere become stricter (e.g., Lindstad and Bø, 2018). Currently, carbon

offsets fall into two categories: emission reduction (e.g., Sinha and Chaturvedi, 2019) and carbon sequestration (e.g., Lal, 2007). I suggest that stream restoration can offer both. By revitalizing hydrologic conditions that limit the decomposition and extend the residence time of carbon, stream restoration involving hydrologic reconnection prevents gradual or rapid loss of carbon that is stored in soil and released during floodplain degradation. By enhancing organic matter input from regenerated riparian vegetation and creating conditions for fine sediment deposition, the potential for new carbon sequestration increases.

The current estimated fluxes of carbon into and out of floodplain-wetland corridors show some carbon release through methane emissions from wetlands (e.g., Saarnio et al., 2009), carbon dioxide emissions to the atmosphere (Butman and Raymond, 2011), and some export of carbon out of floodplains via dissolved carbon in water and transport of large wood. The magnitude of carbon storage versus carbon transport within individual river corridors or on regional to global scales remains poorly constrained, but the potential for net carbon sequestration in river corridors is likely to be notable in the context of climate change. My results show that floodplains in reference conditions tend to contain higher carbon stocks, and therefore river restoration offers an opportunity to sequester more carbon. However, the continuum of degraded, treatment, and reference alternative states is not linear, and does not always follow the assumed temporal order of degraded, treatment, and reference. Disturbance associated with stream restoration construction can reset carbon content in treatment floodplains to lower values than carbon content of degraded conditions, or the disturbance may not affect persistent carbon stocks with the floodplain chosen for restoration. Acknowledging this variability, the environment created by restoration that encourages raised water tables, deposition, and wetland formation increases the carbon sequestration potential by setting the stage for faster carbon accumulation rates combined with slower decomposition. This study shows that reference carbon stocks in anastomosing grassed wetlands and anastomosing wet woodlands are generally higher than degraded

and treatment stocks within the same regions, giving the restoration community something to work toward as we strive for resilient, functioning floodplains and creative solutions to climate change.

Chapter 5 Conclusion

I view stream restoration as a natural experiment. Through this lens, stream restoration offers lessons and scientific insight to the landscape's natural response to human perturbation, whether the perturbation involves floodplain impairment or rehabilitation. The science to support and improve stream restoration practices is obtained through monitoring. Thus, short- and long-term monitoring is essential to restore, conserve, and protect floodplains that offer bountiful resources and ecosystem services to humans and other species, as well as their own intrinsic value. Environmental manipulation by humans is not always desirable, but stream restoration provides opportunities to study effects of various magnitudes of environmental manipulation that are intended to restore function rather than degrade it. Stream restoration and subsequent monitoring also offer continuous lessons about what works and what does not. Although practices and styles of river restoration have improved greatly over recent decades, there is still a long way to go. The magnitude of restoration, or the position on the "PBR continuum" of restoration actions, depends on the expected trajectory of the river corridor considered for treatment. Some sites may only need a nudge, and some may need a process reset. Reference conditions are useful examples but may not always be realistic goals.

As climate change plagues landscapes, organisms, and societies, the value of floodplains will only increase. Floodplains attenuate the effects of drought, fire, flood, pollutants, and other environmental disturbances. In addition, they store carbon disproportionately for their relative fraction of the landscape (Wohl et al., 2012; Wohl, 2013; Sutfin et al., 2016). With restoration of river-wetland corridors, there is an opportunity to enhance carbon sequestration even more.

In this dissertation, I have presented a monitoring strategy for a complex floodplain enhancement project, developed a conceptual model and protocol for identifying drivers and measuring

carbon sequestration in river restoration, and tested the latter protocol in the western USA. Both monitoring protocols offered in the chapters of this dissertation are pilot strategies in which I encourage multiple adaptations over several iterations to improve the methods from their initial presentation in this dissertation. The application and analysis of carbon within degraded, treatment, and reference floodplains not only aims to contribute to the understanding of floodplain response to river restoration, but also contributes to the context of floodplains' roles in the global carbon cycle.

The first method presented in Chapter 2 is a plot-based geomorphic monitoring strategy that is applicable to large floodplains with multiple channels. This method can be scalable for different sized floodplains (e.g., via plot deconstruction and the use of individual subplots over larger or smaller areas) and can be efficiently linked to remote sensing data collection methods such as photo plots and multispectral aerial imagery. Substrate, large wood, organic cover, canopy cover, and water depth and velocity are the primary measurements within the monitoring plots. Over the first two years of monitoring after project implementation, I detected reduced canopy cover, finer substrate size, and changes in heterogeneity.

The second method and pilot study presented in Chapters 3 and 4 aim to estimate carbon sequestration potential of restored river-wetland corridors, and utilize a comparison of degraded, treatment, and reference floodplains. In these studies, I found that reference sites have significantly higher carbon stocks than treatment and degraded floodplains when all data are combined, and that degraded floodplains have the lowest stocks in the majority of sites measured. My literature-derived conceptual framework that describes drivers of soil and large wood carbon stocks supports the methods that are proposed and tested. I intend for this method to be approachable for practitioners, scientists, and managers who are also interested in estimating carbon sequestration in the context of river restoration.

Future directions of this work could begin to navigate the official verification process for carbon offset credits earned with floodplain restoration. Caution is necessary in this process to avoid encouraging more emissions while emitted carbon is "balanced" with offsets; i.e., more carbon sequestration is needed than emission in order to mitigate climate change. This research shows the highly variable nature of carbon content in the landscape and exemplifies the highly uncertain nature of humans' quantifiable alteration of the carbon cycle. However, measurement of carbon in stream restoration is the first step to understanding how stream restoration can enhance carbon storage. Whether monitoring carbon content or geomorphic site response, I have learned through this dissertation that monitoring is imperative to the process of interpreting and restoring streams. The science and practice of stream restoration will only continue to progress when adequate time and resources are allotted to monitoring efforts (Wohl et al., 2015).

References

Aberle, J., and Järvelä, J. 2013. Flow resistance of emergent rigid and flexible floodplain vegetation. Journal of Hydraulic Research 51: 33-45.

Adame, M.F., Reef, R., Wong, V.N.L., Balcombe, S.R., Turschwell, M.P., Kavehei, E., Rodriguez, D., Kelleway, J.J., Masque, P., and Ronan, M. 2020. Carbon and nitrogen sequestration of *Melaleuca* floodplain wetlands in tropical Australia. Ecosystems 23: 454-466.

Angelopoulou, T., N. Tziolas, A. Balafoutis, G. Zalidis, D. Bochtis. 2019. Remote sensing techniques for soil organic carbon estimation: a review. Remote Sensing 11: 676. https://doi.org/10.23390/rs11060676

Appling, A.P. 2012. Connectivity drives function: carbon and nitrogen dynamics in a floodplain-aquifer ecosystem. PhD dissertation, Duke University, Durham, North Carolina.

Assine, M.L., Merino, E.R., Pupim, F.N., Warren, L.V., Guerreiro, R.L., and McGlue, M.M. 2015. "Geology and geomorphology of the Pantanal Basin," in Dynamics of the Pantanal Wetland in South America, eds. I. Bergier and M.L. Assine (Cham, Switzerland: Springer: 23-50.

Atha, J.B. 2014. Identification of fluvial wood using Google Earth. River Research and Applications 30: 857-864.

Atha, J.B., and Dietrich, W.E. 2016. Detecting fluvial wood in forested watersheds using LiDAR data: a methodological assessment. River Research and Applications 32: 1587-1596.

Aufdenkampe, A.K., Mayorga, E., Raymond, P.A., Melack, J.M., Doney, S.C., Alin, S.R., Aalto, R.E. and Yoo, K., 2011. Riverine coupling of biogeochemical cycles between land, oceans, and atmosphere. Frontiers in Ecology and the Environment 9(1): 53-60.

Baron JS, Poff NL, Angermeier PL, Dahm CN, Gleick PH, Hairston Jr NG, Jackson RB, Johnston CA, Richter BD, Steinman AD. 2002. Meeting ecological and societal needs for freshwater. Ecological Applications. 12:1247-1260.

Battin, T.J., Luyssaert, S., Kaplan, L.A., Aufdenkampe, A.K., Richter, A. and Tranvik, L.J., 2009. The boundless carbon cycle. Nature Geoscience 2(9): 598-600.

Bechtold WA, Patterson PL. 2005. The enhanced forest inventory and analysis program-national sampling design and estimation procedures. Gen. Tech. Rep. SRS-80. Asheville, NC: US Department of Agriculture, Forest Service, Southern Research Station. 85 p., 80.

Beechie, T.J., Sear, D.A., Olden, J.D., Pess, G.R., Buffington, J.M., Moir, H., Roni, P. and Pollock, M.M., 2010. Process-based principles for restoring river ecosystems. BioScience 60(3): 209-222.

Bellmore, J.R., Baxter, C.V., Connolly PJ. 2015. Spatial complexity reduces interaction strengths in the meta-food web of a river floodplain mosaic. Ecology 96: 274-283.

Bellmore JR, Baxter CV, Martens K, Connolly PJ. 2013. The floodplain food web mosaic: a study of its importance to salmon and steelhead with implications for their recovery. Ecological Applications 23: 189-207.

Bellmore, J.R., Duda, J.J., Craig, L.S., Greene, S.L., Torgersen, C.E., Collins, M.J., Vittum, K. 2017. Status and trends of dam removal research in the United States. Wiley Interdisciplinary Reviews: Water 4: e1164.

Benda, L., and Sias, J.C. 2003. A quantitative framework for evaluating the mass balance of in-stream organic debris. Forest Ecology and Management 172: 1-16.

Bernhardt, E.S., Palmer, M.A., Allan, J.D., Alexander, G., Barnas, K., Brooks, S., Carr, J., Clayton, S., Dahm, C., Follstad-Shah, J. and Galat, D., 2005. Synthesizing US river restoration efforts. Science 308(5722): 636-637.

Bernhardt, E.S., Sudduth, E.B., Palmer, M.A., Allan, J.D., Meyer, J.L., Alexander, G., Follastad-Shah, J., Hassett, B., Jenkinson, R., Lave, R. and Rumps, J., 2007. Restoring rivers one reach at a time: results from a survey of US river restoration practitioners. Restoration Ecology 15(3): 482-493.

Boivin, M., Buffin-Belanger, T., and Piegay, H. 2015. The raft of the Saint-Jean River, Gaspé (Québec, Canada): a dynamic feature trapping most of the wood transported from the catchment. Geomorphology 231: 270-280.

Booth, E.G., Loheide, S.P. and Hansis, R.D., 2009. Postsettlement alluvium removal: A novel floodplain restoration technique (Wisconsin). Ecological Restoration 27(2): 136-139.

Bouillon, S., Abril, G., Borges, A.V., Dehairs, F., Govers, G., Hughes, H.J., Merckx, R., Meysman, F.J.R., Nyunja, J., Osburn, C. and Middelburg, J.J., 2009. Distribution, origin and cycling of carbon in the Tana River (Kenya): a dry season basin-scale survey from headwaters to the delta. Biogeosciences 6(11): 2475-2493.

Bridge, J.S. 2003. Rivers and Floodplains. Oxford, UK: Blackwell.

Brierley GJ, Fryirs KA. 2016. The use of evolutionary trajectories to guide 'moving targets' in the management of river futures. River Research and Applications 32: 823-835.

Briggs, M.A., and Hare, D.K. 2018. Explicit consideration of preferential groundwater discharges as surface water ecosystem control points. Hydrological Processes 2018: 1-6.

Brinson, M.M., Bradshaw, H.D., Holmes, R.N., and Elkins, J.B. 1980. Litterfall, stemflow, and throughfall nutrient fluxes in an alluvial swamp forest. Ecology 61: 827-835.

Brown AG, Lespez L, Sear DA, Macaire JJ, Houben P, Klimek K, Brazier RE, Van Oost K, Pears B. 2018. Natural vs anthropogenic streams in Europe: History, ecology and implications for restoration, river rewilding and riverine ecosystem services. Earth-Science Reviews 180: 185-205.

Butman, D., P.A. Raymond. 2011. Significant efflux of carbon dioxide from streams and rivers in the United States. Nature Geoscience 4: 839-842. doi:10.1038/ngeo1294.

Cabezas, A., Comin, F.A., and Walling, D.E. 2009. Changing patterns of organic carbon and nitrogen accretion on the middle Ebro floodplain NE Spain. Ecological Engineering 35: 1547-1558.

Cabezas, A., F.A. Comin. 2010. Carbon and nitrogen accretion in the topsoil of the Middle Ebro River floodplains (NE Spain): Implications for their ecological restoration. Ecological Engineering 36: 640-652.

Cai, A., Feng, W., Zhang, W. and Xu, M., 2016. Climate, soil texture, and soil types affect the contributions of fine-fraction-stabilized carbon to total soil organic carbon in different land uses across China. Journal of Environmental Management 172: 2-9.

Camara dos Reis M, Bagatini IL, de Oliveira Vidal L, Bonnet MP, da Motta Marques D, Sarmento H. 2019. Spatial heterogeneity and hydrological fluctuations drive bacterioplankton community composition in an Amazon floodplain system. PLOS ONE 15: e0228721.

Carnell, P.E., Windecker, S.M., Brenker, M., Baldock, J., Masque, P., Brunt, K., and Macreadie, P.I. 2018. Carbon stocks, sequestration, and emissions of wetlands in south eastern Australia. Global Change Biology 24: 4173-4184.

Castro, J.M. and Thorne, C.R., 2019. The stream evolution triangle: Integrating geology, hydrology, and biology. River Research and Applications 35(4): 315-326.

Chan, K.M., Guerry, A.D., Balvanera, P., Klain, S., Satterfield, T., Basurto, X., Bostrom, A., Chuenpagdee, R., Gould, R., Halpern, B.S. and Hannahs, N., 2012. Where are cultural and social in ecosystem services? A framework for constructive engagement. BioScience 62(8): 744-756.

Chiu, Y., Yang, Y. and Morse, C., 2022. Quantifying carbon footprint for ecological river restoration. Environment, Development and Sustainability 24(1): 952-970.

Christensen, C.W., Hayashi, M., and Bentley, L.R. 2020. Hydrogeological characterization of an alpine aquifer system in the Canadian Rocky Mountains. Hydrogeology Journal 28: 1871-1890.

Cierjacks, A., Kleinschmitt, B., Babinsky, M., Kleinschroth, F., Markert, A., Menzel, M., Ziechmann, U., Schiller, T., Graf, M., and Lang, F. 2010. Carbon stocks of soil and vegetation on Danubian floodplains. Journal of Plant Nutrition and Soil Science 173, 644-653.

Clark, D.B., Clark, D.A., Brown, S., Oberbauer, S.F., and Veldkamp, E. 2002. Stocks and flows of coarse woody debris across a tropical rain forest nutrient and topography gradient. Forest Ecology and Management 164: 237-248.

Cluer, B. and Thorne, C., 2014. A stream evolution model integrating habitat and ecosystem benefits. River Research and Applications 30(2): 135-154.

Collins, B.D., Montgomery D.R., and Haas, A.D. 2002. Historical changes in the distribution and functions of large wood in Puget Lowland rivers. Canadian Journal of Fisheries and Aquatic Sciences 59: 66-76.

Collins, B.D., Montgomery, D.R., Fetherston, K.L., and Abbe, T.B. 2012. The floodplain large-wood cycle hypothesis: a mechanism for the physical and biotic structuring of temperate forested alluvial valleys in the North Pacific coastal ecoregion. Geomorphology 139-140: 460-470.

Comiti, F., Andreoli, A., Mao, L. and Lenzi, M.A. 2008. Wood storage in three mountain streams of the southern Andes and its hydro-morphological effects. Earth Surface Processes and Landforms 33: 244-262.

Craft, C., Vymazal, J., and Kröpfelova, L. 2018. Carbon sequestration and nutrient accumulation in floodplain and depressional wetlands. Ecological Engineering 114: 137-145.

Craft, C.B. and Casey, W.P. 2000. Sediment and nutrient accumulation in floodplain and depressional freshwater wetlands of Georgia, USA. Wetlands 20: 323-332.

D'Elia, A.H., Liles, G.C., Viers, J.H., and Smart, D.R. 2017. Deep carbon storage potential of buried floodplain soils. Scientific Reports 7: 8181. Doi:10.1038/s41598-017-06494-4

Daily, G.C., 1997. Introduction: what are ecosystem services. Nature's services: Societal dependence on natural ecosystems 1(1).

DesRoches, A., Danielescu, S., and Butler, K. 2014. Structural controls on groundwater flow in a fractured bedrock aquifer underlying an agricultural region of northwestern New Brunswick, Canada. Hydrogeology Journal 22: 1067-1086.

Dixon, S.J., Sear, D.A., Odoni, N.A., Sykes, T., and Lane, S.N. 2016. The effects of river restoration on catchment scale flood risk and flood hydrology. Earth Surface Processes and Landforms 41: 997-1008.

Doughty M., Sawyer A.H., Wohl E., Singha K. 2020. Mapping increases in hyporheic exchange from channel-spanning logjams. Journal of Hydrology 587: 124931.

Dufour, S. and Piégay, H., 2009. From the myth of a lost paradise to targeted river restoration: forget natural references and focus on human benefits. River Research and Applications 25(5): 568-581.

Ehlen, J., and Wohl, E. 2002. Joints and landform evolution in bedrock canyons. Trans. Japanese Geomorphol. Union 23: 237-255.

Elith, J., Leathwick, J.R. and Hastie, T., 2008. A working guide to boosted regression trees. Journal of animal ecology 77(4): 802-813.

England J., Skinner K.S., Carter M.G. 2008. Monitoring, river restoration and the Water Framework Directive. Water and Environment Journal 22: 227-234.

Erwin S.O., Schmidt J.C., Allred T.M. 2016. Post-project assessment of a large process-based river restoration project. Geomorphology 270: 145-158.

Everitt, B.L. 1968. Use of the cottonwood in an investigation of the recent history of a flood plain. American Journal of Science 266: 417-439.

Falloon, P., Jones, C.D., Ades, M., and Paul, K. 2011. Direct soil moisture controls of future global soil carbon changes: An important source of uncertainty. Global Biogeochemical Cycles 25: 1– 14.

Fausch KD, Northcote TG. 1992. Large woody debris and salmonid habitat in a small coastal British Columbia stream. Canadian Journal of Fisheries and Aquatic Sciences 49: 682-693.

Ferré, C., Comolli, R., Leip, A. and Seufert, G., 2014. Forest conversion to poplar plantation in a Lombardy floodplain (Italy): effects on soil organic carbon stock. Biogeosciences 11(22): 6483-6493.

Fetherston, K.L., Naiman, R.J., and Bilby, R.E. 1995. Large woody debris, physical process, and riparian forest development in montane forest networks of the Pacific Northwest. Geomorphology 13: 133-144.

Fox, J. and Weisberg, S. 2019. An {R} Companion to Applied Regression, Third Edition. Thousand Oaks CA: Sage. URL: https://socialsciences.mcmaster.ca/jfox/Books/Companion/

Fox, M., and Bolton, S. 2007. A regional and geomorphic reference for quantities and volumes of instream wood in unmanaged forest basins of Washington State. North American Journal of Fisheries Management 27: 342-359.

Friedlingstein, P., O'Sullivan, M., Jones, M.W., Andrew, R.M., Hauck, J., Olsen, A., and others. 2020. Global carbon budget 2020. Earth System Science Data 12: 3269-3340.

Gifford, L. 2020. "You can't value what you can't measure": a critical look at forest carbon accounting. Climatic Change 161: 291-306.

Graf, W.L., 1999. Dam nation: A geographic census of American dams and their large-scale hydrologic impacts. Water resources research 35(4): 1305-1311.

Grill, G., Lehner, B., Thieme, M., Geenen, B., Tickner, D., Antonelli, F., Babu, S., Borrelli, P., Cheng, L., Crochetiere, H. and Ehalt Macedo, H., 2019. Mapping the world's free-flowing rivers. Nature 569(7755): 215-221.

Gurnell AM, Corenblit D, Garcia de Jalon D, Gonzalez del Tanago M, Grabowski RC, O'Hare MT, Szewczyk M. 2016. A conceptual model of vegetation-hydromorphology interactions within river corridors. River Research and Applications 32: 142-163.

Gurnell, A.M., Petts, G.E., Harris, N., Ward, J.V., Tockner, K., Edwards, P.J., and Kollmann, J. 2000. Large wood retention in river channels: the case of the Fiume Tagliamento, Italy. Earth Surface Processes and Landforms 25: 255-275.

Guyette, R.P., Dey, D.C., and Stambaugh, M.C. 2008. The temporal distribution and carbon storage of large oak wood in streams and floodplain deposits. Ecosystems 11: 643-653.

Hall, J.E., Holzer, D.M., and Beechie, T.J. 2007. Predicting river floodplain and lateral channel migration for salmon habitat conservation. Journal of the American Water Resources Association 43: 786-797.

Hanberrry, B.B., Kabrick, J.M., and He, H.S. 2015. Potential tree and soil carbon storage in a major historical floodplain forest with disrupted ecological function. Perspectives in Plant Ecology, Evolution and Systematics 17: 17-23.

Handique, S. 2015. A review on the riverine carbon sources, fluxes and perturbations. In M. Ramkumar, K. Kuamaraswamy, R. Mohanraj, eds., Environmental Management of River Basin Ecosystems. Springer Earth System Sciences, Switzerland, 417-428.

Hanna, D.E., Tomscha, S.A., Ouellet Dallaire, C. and Bennett, E.M., 2018. A review of riverine ecosystem service quantification: Research gaps and recommendations. Journal of Applied Ecology 55(3): 1299-1311.

Hardie, M.A., Doyle, R.B., Cotching, W.E., and Lisson, S. 2012. Subsurface lateral flow in texture-contrast (duplex) soils and catchments with shallow bedrock. Applied and Environmental Soil Science 2012: 861358.

Hartranft JL, Merritts DJ, Walter RC, Rahnis M. 2011. Big Spring Run restoration experiment: policy, geomorphology, and aquatic ecosystems in the Big Spring Run watershed, Lancaster County, PA. Sustain 24: 24-34.

Hijmans, R.J., S. Phillips, J. Leathwick, J. Elith 2021. dismo: Species Distribution Modeling. R package version 1.3-5. https://CRAN.R-project.org/package=dismo

Hinshaw, S. and Wohl, E., 2021. Quantitatively Estimating Carbon Sequestration Potential in Soil and Large Wood in the Context of River Restoration. Frontiers in Earth Science 9: 975.

Hinshaw, S., Wohl, E., Burnett, J.D. and Wondzell, S., 2022. Development of a geomorphic monitoring strategy for stage 0 restoration in the South Fork McKenzie River, Oregon, USA. Earth Surface Processes and Landforms. https://doi.org/10.1002/esp.5356

Hoffmann, T., Erkens, G., Cohen, K.M., Houben, P., Seidel, J., and Dikau, R. 2007. Holocene floodplain sediment storage and hillslope erosion within the Rhine catchment. The Holocene 17: 105-118.

Hoffmann, T., Glatzel, S., and Dikau, R. 2009. A carbon storage perspective on alluvial sediment storage in the Rhine catchment. Geomorphology 108: 127-137.

Holling CS. 1973. Resilience and stability of ecological systems. Annual Review of Ecology, Evolution, and Systematics 4: 1–23.

Hood, G.A., and Bayley, S.E. 2008. Beaver (*Castor canadensis*) mitigate the effects of climate on the area of open water in boreal wetlands in western Canada. Biological Conservation 141: 556-567.

Hupp, C.R., Demas, C.R., Kroes, D.E., Day, R.H., and Doyle, T.W. 2008. Recent sedimentation patterns within the central Atchafalaya Basin, Louisiana. Wetlands 28: 125-140.

Hupp, C.R., Kroes, D.E., Noe, G.B., Schenk, E.R., and Day, R.H. 2019. Sediment trapping and carbon sequestration in floodplains of the lower Atchafalaya Basin, LA: allochthonous versus autochthonous carbon sources. Journal of Geophysical Research Biogeosciences 124: 663-677.

James, L.A. and Marcus, W.A., 2006. The human role in changing fluvial systems: Retrospect, inventory and prospect. Geomorphology 79(3-4): 152-171.

Jaramillo, V.J., Kauffmann, J.B., Renteria-Rodriguez, L., Cummings, D.L., and Ellingson, L.J. 2003. Biomass, carbon, and nitrogen pools in Mexican tropical dry forest landscapes. Ecosystems 6: 609-629.

Jiang Y, He X, Lee MLT, Rosner D, Yan J. 2017. Wilcoxon rank-based tests for clustered data with r package clusrank. arXiv preprint arXiv:1706.03409.

Jobbágy, E.G., and Jackson, R.B. 2000. The vertical distribution of soil organic carbon and its relation to climate and vegetation. Ecological Applications 10: 423–436.

Johnson, M.F., Thorne, C.R., Castro, J.M., Kondolf, G.M., Mazzacano, C.S., Rood, S.B. and Westbrook, C., 2020. Biomic river restoration: A new focus for river management. River Research and Applications 36(1): 3-12.

Kaiser, K., and Guggenberger, G. 2000. The role of DOM sorption to mineral surfaces in the preservation of organic matter in soils. Organic Geochemistry 31: 711–725.

Kaiser, N.N., Feld, C.K. and Stoll, S., 2020. Does river restoration increase ecosystem services? Ecosystem Services 46: 101206.

Knox, R.L., Morrison, R.R. and Wohl, E.E., 2022. Identification of artificial levees in the contiguous United States. Water Resources Research, 58(4).

Koltzer, N., Scheck-Wenderoth, M., Cacace, M., Frick, M., and Bott, J. 2019. Regional hydraulic model of the Upper Rhine Graben. Advances in Geosciences 49: 197-206.

Kondolf GM, Wolman MG. 1993. The sizes of salmonid spawning gravels. Water Resources Research 29: 2275-2285.

Lal, R., 2007. Carbon management in agricultural soils. Mitigation and adaptation strategies for global change, 12(2), pp.303-322.

Lal, R., 2008. Carbon sequestration. Philosophical Transactions of the Royal Society B: Biological Sciences 363(1492): 815-830.

Larsen, A., May, J.H., Moss, P., and Hacker, J. 2016. Could alluvial knickpoint retreat rather than fire drive the loss of alluvial wet monsoon forest, tropical northern Australia? Earth Surface Processes and Landforms 41: 1583-1594.

Larsen, L.G., and Harvey, J.W. 2010. How vegetation and sediment transport feedbacks drive landscape change in the Everglades and wetlands worldwide. The American Naturalist 176: E66-E79.

Lassettre, N.S., Piegay, H., Dufour, S., and Rollet, A.J. 2008. Decadal changes in distribution and frequency of wood in a free meandering river, the Ain River, France. Earth Surface Processes and Landforms 33: 1098-1112.

Laurel, D. and Wohl, E., 2019. The persistence of beaver-induced geomorphic heterogeneity and organic carbon stock in river corridors. Earth Surface Processes and Landforms 44(1): 342-353.

Lautz, L., Kelleher, C., Vidon, P., Coffman, J., Riginos, C. and Copeland, H., 2019. Restoring stream ecosystem function with beaver dam analogues: Let's not make the same mistake twice. Hydrological Processes, 33(1): 174-177.

Lautz, L.K., Siegel, D.I., and Bauer, R.L. 2006. Impact of debris dams on hyporheic interaction along a semi-arid stream. Hydrological Processes 20: 183-196.

Lave, R.A., 2008. The Rosgen wars and the shifting political economy of expertise. University of California, Berkeley.

Lave, R. and Doyle, M., 2021. Streams of revenue: the restoration economy and the ecosystems it creates. MIT Press.

Lenth, R.V. 2020. emmeans: Estimated Marginal Means, aka Least-Squares Means. R package version 1.5.3. https://CRAN.R-project.org/package=emmeans

Leopold LB. 1962. The Vigil network. Hydrological Sciences Journal 7: 5-9.

Liaw, A., M. Wiener. 2002. Classification and regression by randomForest. R News 2(3): 18—22.

Limpert, K.E., Carnell, P.E., Trevathan-Tackett, S.M. and Macreadie, P.I., 2020. Reducing emissions from degraded floodplain wetlands. Frontiers in Environmental Science 8:8.

Lindstad, E., T.I. Bø. 2018. Potential power setups, fuels and hull designs capable of satisfying future EEDI requirements. Transportation Research Part D: Transport and Environment 63: 276-290.

Lininger, K.B., E. Wohl, J.R. Rose. 2018. Geomorphic controls on floodplain soil organic carbon in the Yukon Flats, interior Alaska, from reach to river basin scales. Water Resources Research 54: 1934-1951.

Lininger, K.B., L.E. Polvi. 2020. Evaluating floodplain organic carbon across a gradient of human alteration in the boreal zone. Geomorphology 370: 107390.

Lininger, K.B., Wohl, E., Rose, J.R., and Leisz, S.J. 2019. Significant floodplain soil organic carbon storage along a large high-latitude river and its tributaries. Geophysical Research Letters 46: 2121-2129.

Livers, B., and Wohl, E. 2015. An evaluation of stream characteristics in glacial versus fluvial process domains in the Colorado Front Range. Geomorphology 231: 72-82.

Lohr, SL. 1999. Sampling: design and analysis. Brooks.

Lumley T, 2020. survey: analysis of complex survey samples. R package version 4.0.

Maguire DA. 1994. Branch mortality and potential litterfall from Douglas-fir trees in stands of varying density. Forest Ecology and Management 70: 41-53.

Malone, B.P., McBratney, A.B., Minasny, B., and Laslett, G.M. 2009. Mapping continuous depth functions of soil carbon storage and available water capacity. Geoderma 154: 138-152.

Manning, P., de Vries, F.T., Tallowin, J.R., Smith, R., Mortimer, S.R., Pilgrim, E.S., Harrison, K.A., Wright, D.G., Quirk, H., Benson, J. and Shipley, B., 2015. Simple measures of climate, soil properties and plant traits predict national-scale grassland soil carbon stocks. Journal of Applied Ecology 52(5): 1188-1196.

Martens KD, Connolly PJ. 2014. Juvenile anadromous salmonid production in Upper Columbia River side channels with different levels of hydrological connection. Transactions of the American Fisheries Society 143: 757-767.

Martin, A.R., Doraisami, M., and Thomas, S.C. 2018. Global patterns in wood carbon concentration across the world's trees and forests. Nature Geoscience 11: 915-920.

Mattern, K., Lutgen, A., Sienkiewicz, N., Jiang, G., Kan, J., Peipoch, M. and Inamdar, S., 2020. Stream restoration for legacy sediments at Gramies Run, Maryland: early lessons from implementation, water quality monitoring, and soil health. Water 12(8): 2164.

Matzek, V., C. Puleston, J. Gunn. 2015. Can carbon credits fund riparian forest restoration? Restoration Ecology 23: 7-14.

May RM. 1977. Thresholds and breakpoints in ecosystems with a multiplicity of stable states. Nature 269: 471–47

McNeely C, Finlay JC, Power ME. 2007. Grazer traits, competition, and carbon sources to a headwater-stream food web. Ecology 88: 391-401.

Merz JE, Setka JD. 2003. Evaluation of a spawning habitat enhancement site for Chinook salmon in a regulated California river. North American Journal of Fisheries Management 24: 397-407.

Meyer K, Hammons B, Hogervorst J, Powers P, Weybright J, Bair B, Robertson G, Mazullo C. 2018. Lower South Fork McKenzie River Floodplain Enhancement Project 80% Design Report. McKenzie Watershed Council. https://www.mckenziewc.org/?page_id=884

Meyer K. 2019. Scaling Up: Stage 0 Restoration on a Large River in the Western Cascades of Oregon. Presentation for River Restoration Northwest conference. https://www.rrnw.org/wp-content/uploads/7.1-RRNW-Kate-Meyer-2019.pdf

Micheli, E.R., and Kirchner, J.W. 2002. Effects of wet meadow riparian vegetation on streambank erosion. 2. Measurements of vegetated bank strength and consequences for failure mechanics. Earth Surface Processes and Landforms 27: 687-697.

Miller, J.R., Lord, M.L., Villarroel, L.F., Germanoski, D., and Chambers, J.C. 2012. Structural organization of process zones in upland watersheds of central Nevada and its influence on basin connectivity, dynamics, and wet meadow complexes. Geomorphology 139-140: 384-402.

Mitsch, W.J., Dorage, C.L., and Wiemhoff, J.R. 1979. Ecosystem dynamics and a phosphorus budget of an alluvial cypress swamp in southern Illinois. Ecology 30: 1116-1124.

Montgomery DR, Collins BD, Buffington JM. 2003. Geomorphic effects of wood in rivers. In: Gregory, S.V., Boyer, K.L., and Gurnell, A.M., eds., The Ecology and Management of Wood in World Rivers. American Fisheries Society Symposium 37, pp. 21-47.

Montgomery, D.R. 2002. Valley formation by fluvial and glacial erosion. Geology 30: 1047-1050.

Moore D. 2002. NRCS Frequency Determination Curve Spreadsheet. United States Natural Resources Conservation Service Bulletin 17b Guidelines for Determining Flood Flow Frequency. Version 306. http://go.usa.gov/KS6

Moreira-Turcq, P., Jouanneau, J.M., Turcq, B., Seyler, P., Weber, O., and Guyot, J.L. 2004. Carbon sedimentation at Lago Grande de Curuai, a floodplain lake in the low Amazon region: insights into sedimentation rates. Palaeogeography, Palaeoclimatology, Palaeoecology 214: 27-40.

Mosisch TD, Bunn SE, Davies PM. 2001. The relative importance of shading and nutrients on algal production in subtropical streams. Freshwater Biology 46: 1269-1278.

Moyano, F.E., Vasilyeva, N., Bouckaert, L., Cook, F., Craine, J., Curiel Yuste, J., Don, A., Epron, D., Formanek, P., Franzluebbers, A. and Ilstedt, U., 2012. The moisture response of soil heterotrophic respiration: interaction with soil properties. Biogeosciences 9(3): 1173-1182.

Muldoon, M.A., Simo, J.A., and Bradbury, K.R. 2001. Correlation of hydraulic conductivity with stratigraphy in a fractured-dolomite aquifer, northeastern Wisconsin, USA. Hydrogeology Journal 9: 570-583.

Mulholland, P.J. 1981. Organic carbon flow in a swamp-stream ecosystem. Ecological Monographs 51: 307-322.

Nahlik, A.M., and Fennessy, M.S. 2016. Carbon storage in US wetlands. Nature Communications 7: 13835. Doi:10.1038/ncomms13835.

Naiman, R.J., Melillo, J.M., Lock, M.A., Ford, T.E., and Reice, S.R. 1987. Longitudinal patterns of ecosystem processes and community structure in a subarctic river continuum. Ecology 68: 1139-1156.

Nardi, F., Annis, A., Di Baldassare, G., Vivoni, E.R., and Grimaldi, S. 2019. GFPLAIN250m, a global high-resolution dataset of Earth's floodplains. Scientific Data 6: 180309.

National Land Cover Database: Homer, C.H., Fry, J.A., and Barnes C.A., 2012, The National Land Cover Database, U.S. Geological Survey Fact Sheet 2012-3020

Nelson, G.A. 2022. fishmethods: Fishery Science Methods and Models. R package version 1.11-3. https://CRAN.R-project.org/package=fishmethods

Nelson G.A. 2014. Cluster sampling: a pervasive, yet little recognized survey design in fisheries research. Transactions of the American Fisheries Society 143: 926-938.

Noe, G.B. and Hupp, C.R. 2009. Retention of riverine sediment and nutrient lands by coastal plain floodplains. Ecosystems 12: 728-746.

Norton, B.G. 2012. Valuing ecosystems. Nature Education Knowledge 3(10):2

Ogston L, Gidora S, Foy M, Rosenfeld J. 2014. Watershed-scale effectiveness of floodplain habitat restoration for juvenile coho salmon in the Chilliwack River, British Columbia. Canadian Journal of Fisheries and Aquatic Sciences 72: 479-490.

O'Connor, J.E., Jones, M.A., and Haluska, T.L. 2003. Flood plain and channel dynamics of the Quinault and Queets Rivers, Washington, USA. Geomorphology 51: 31-59.

Omernik, J.M., and G.E. Griffith. 2014. Ecoregions of the conterminous United States: evolution of a hierarchical spatial framework. Environmental Management 54(6):1249-1266, http://dx.doi.org/10.1007/s00267-014-0364-1

Osterkamp WR, Emmett WW, Leopold LB. 1991. The Vigil network: a means of observing landscape change in drainage basins. Hydrological Sciences Journal 36: 331-344.

Oswald, E.B., and Wohl, E. 2008. Wood-mediated geomorphic effects of a jökulhlaup in the Wind River Mountains, Wyoming. Geomorphology 100: 549-562.

Palmer MA, Hondula KL, Koch BA. 2014. Ecological restoration of streams and rivers: shifting strategies and shifting goals. Annual Review of Ecology, Evolution, and Systematics 45: 247-269.

Patalano, A., García, C.M., Rodríguez, A., 2017. Rectification of Image Velocity Results (RIVeR): A simple and user-friendly toolbox for large scale water surface. Particle Image Velocimetry (PIV) and Particle Tracking Velocimetry (PTV) 109: 323–330. doi:10.1016/j.cageo.2017.07.009

Paul, K.I., Reeson, A., Polglase, P., Crossman, N., Freudenberger, D. and Hawkins, C., 2013. Economic and employment implications of a carbon market for integrated farm forestry and biodiverse environmental plantings. Land use policy 30(1): 496-506.

Perignon, M.C., Tucker, G.E., Griffin, E.R., and Friedman, J.M. 2013. Effects of riparian vegetation on topographic change during a large flood event, Rio Puerco, New Mexico, USA. Journal of Geophysical Research Earth Surface 118: 1193-1209.

Piégay, H. 1993. Nature, mass and preferential sites of coarse woody debris deposits in the lower Ain Valley (Mollon reach), France. Regulated Rivers: Research and Management 8: 359-372.

Piégay, H. and Gurnell, A.M. 1997. Large woody debris and river geomorphological pattern: Examples from S.E. France and S. England. Geomorphology 19: 99-116.

Poff N.L., Allan JD, Bain MB, Karr JR, Prestegaard KL, Richter BD, Sparks RE, Stromberg JC. 1997. The natural flow regime. BioScience 47: 769-784.

Pollock, M.M., Beechie, T.J., Wheaton, J.M., Jordan, C.E., Bouwes, N., Weber, N., and Volk, C. 2014. Using beaver dams to restore incised stream ecosystems. BioScience 64: 279-290.

Polvi L.E., Lind L, Persson H, Miranda-Melo A, Pilotto F, Su X, Nilsson C. 2020. Facets and scales in river restoration: nestedness and interdependence of hydrological, geomorphic, ecological, and biogeochemical processes. Journal of Environmental Management 265: 110288.

Polvi, L.E., and Wohl, E. 2012. The beaver meadow complex revisited – the role of beavers in post-glacial floodplain development. Earth Surface Processes and Landforms 37: 332-346.

Powers, P.D., Helstab, M. and Niezgoda, S.L., 2019. A process-based approach to restoring depositional river valleys to Stage 0, an anastomosing channel network. River Research and Applications 35(1): 3-13.

Pringle C.M. 2001. Hydrologic connectivity and the management of biological reserves: a global perspective. Ecological Applications 11: 981-998.

Qi, R., Li, J., Lin, Z., Li, Z., Li, Y., Yang, X., Zhang, J. and Zhao, B., 2016. Temperature effects on soil organic carbon, soil labile organic carbon fractions, and soil enzyme activities under long-term fertilization regimes. Applied Soil Ecology 102: 36-45.

R Core Team 2020, 2022. R: A language and environment for statistical computing. R Foundation for Statistical Computing, Vienna, Austria. URL https://www.R-project.org/.

Rasmussen, C., Heckman, K., Wider, W.R., Keiluweit, M., Lawrence, C.R., Berhe, A.A., Blankinship, J.C., Crow, S.E., et al. 2018. Beyond clay: towards an improved set of variables for predicting soil organic matter content. Biogeochemistry 137: 297-306.

Rathburn, S.L., Rubin, Z.K., Wohl, E.E. 2011. Evaluating channel response to an extreme sedimentation event in the context of historical range of variability: Upper Colorado River, USA. Earth Surface Processes and Landforms 38: 391-406.

Remy N, Boucher A, Wu J. 2009. Applied geostatistics with SGeMS: a user's guide. Cambridge University Press.

Ribaudo, M., Greene, C., Hansen, L. and Hellerstein, D., 2010. Ecosystem services from agriculture: Steps for expanding markets. Ecological economics 69(11): 2085-2092.

Ricker, M.C., and Lockaby, B.G. 2015. Soil organic carbon stocks in a large eutrophic floodplain forest of the southeastern Atlantic Coastal Plain, USA. Wetlands 35: 291-301.

Ricker, M.C., Donohue, S.W., Stolt, M.H., and Zavada, M.S. 2012. Development and application of multi-proxy indices of land use change for riparian soils in southern New England, USA. Ecological Applications 22: 487-501.

Rosgen, D.L., 2011. Natural channel design: fundamental concepts, assumptions, and methods. Stream Restoration in Dynamic Fluvial Systems: Scientific Approaches, Analyses, and Tools, Geophysical Monographs Series 194: 69-93.

Saarnio, S., W. Winiwarter, J. Leitao. 2009. Methane release from wetlands and watercourses in Europe. Atmospheric Environment 43: 1421-1429.

Samaritani, E., J. Shrestha, B. Fournier, E. Frossard, F. Gillet, C. Guenat, P.A. Niklaus, N. Pasquale, K. Tockner, E.A.D. Mitchell, J. Luster. 2011. Heterogeneity of soil carbon pools and fluxes in a channelized and restored floodplain section (Thur River, Switzerland). Hydrogy and Earth System Sciences 15: 1757-1769.

Sanders, L.M., Taffs, K.H., Stokes, D.J., Sanders, C.J., Smoak, J.M., Enrich-Prast, A., Macklin, P.A., Santos, I.R., and Marotta, H. 2017. Carbon accumulation in Amazonian floodplain lakes: a significant component of Amazon budgets? Limnology and Oceanography Letters 2: 29-35.

Sapkota, Y. and White, J.R., 2020. Carbon offset market methodologies applicable for coastal wetland restoration and conservation in the United States: A review. Science of the Total Environment 701: 134497.

Sawyer, A.H., and Cardenas, M.B. 2012. Effect of experimental wood addition on hyporheic exchange and thermal dynamics in a losing meadow stream. Water Resources Research 48: W10537. Doi: 10.1029/2011WR011776.

Scharlemann, J.P.W., Tanner, E.V.J., Hiederer, R., and Kapos, V. 2014. Global soil carbon: understanding and managing the largest terrestrial carbon pool. Carbon Management 5: 81-91.

Schiefer, J., Lair, G.J., Lüthgens, C., Wild, E.M., Steier, P., and Blum, W.E.H. 2018. The increase of soil organic carbon as proposed by the "4/1000 initiative" is strongly limited by the status of soil development – A case study along a substrate age gradient in central Europe. Science of the Total Environment 628-629: 840-847.

Schneider, L. and La Hoz Theuer, S., 2019. Environmental integrity of international carbon market mechanisms under the Paris Agreement. Climate Policy 19(3): 386-400.

Schumm SA, Harvey MD, Watson CC. 1984. Incised Channels: Morphology, Dynamics, and Control. Water Resources Publications: Littleton, CO.

Scott D. 2019. Aerial drone imagery of South Fork McKenzie River at high flow in April 2019.

Scott, D.N., and Wohl, E.E. 2018a. Geomorphic regulation of floodplain soil organic carbon concentration in watersheds of the Rocky and Cascade Mountains, USA. Earth Surface Dynamics 6: 1101-1114.

Scott, D.N., and Wohl, E.E. 2018b. Natural and anthropogenic controls on wood loads in river corridors of the Rocky, Cascade, and Olympic Mountains, USA. Water Resources Research 54: 7893-7909.

Scott, D.N., and Wohl, E.E. 2020. Geomorphology and climate interact to control organic carbon stock and age in mountain river valley bottoms. Earth Surface Processes and Landforms 45: 1911-1925.

Scrucca L, Fop M, Murphy TB, Raftery AE. 2016. mclust 5: clustering, classification and density estimation using Gaussian finite mixture models, The R Journal, 8/1, pp. 205-233. https://journal.r-project.org/archive/2016/RJ-2016-021/RJ-2016-021.pdf

Sear DA, Millington CE, Kitts DR, Jeffries R. 2010. Logjam controls on channel:floodplain interactions in wooded catchments and their role in the formation of multi-channel patterns. Geomorphology 116: 305-319.

Sedell JR. Froggatt JL. 1984. Importance of streamside forests to large rivers: the isolation of the Willamette River, Oregon, USA, from its floodplain by snagging and streamside forest removal. Internationale Vereinigung fur Theoretische und Angewandte Limnologie 22: 1828-1834.

Sinha, R.K. and Chaturvedi, N.D., 2019. A review on carbon emission reduction in industries and planning emission limits. Renewable and Sustainable Energy Reviews 114: 109304.

Smith, P., Soussana, J.F., Angers, D., Schipper, L., Chenu, C., Rasse, D.P., Batjes, N.H., Van Egmond, F., McNeill, S., Kuhnert, M. and Arias-Navarro, C., 2020. How to measure, report and verify soil

carbon change to realize the potential of soil carbon sequestration for atmospheric greenhouse gas removal. Global Change Biology 26(1): 219-241.

Smith, R.F., Neideigh, E.C., Rittle, A.M., and Wallace, J.R. 2020. Assessing macroinvertebrate community response to restoration of Big Spring Run: expanded analysis of before-after-control-impact sampling designs. River Research and Applications 36: 79-90.

Soil Survey Staff. 2021. Natural Resources Conservation Service, US Department of Agriculture. Web Soil Survey. Available online at https://websoilsurvey.nrcs.usda.gov/. Accessed [February 5, 2021].

Stanford JA, Ward JV. 1993. An ecosystem perspective of alluvial rivers: connectivity and the hyporheic corridor. Journal of the North American Benthological Society 12: 48-60.

Structx. 2021. https://structx.com/Soil_Properties_002.html, accessed 16 April 2021.

Sutfin, N.A., Wohl, E.E. and Dwire, K.A., 2016. Banking carbon: a review of organic carbon storage and physical factors influencing retention in floodplains and riparian ecosystems. Earth Surface Processes and Landforms 41(1) 38-60.

Sutfin, N.A. and Wohl, E., 2017. Substantial soil organic carbon retention along floodplains of mountain streams. Journal of Geophysical Research: Earth Surface 122(7): 1325-1338.

Sutfin, N.A., and Wohl, E. 2019. Elevational differences in hydrogeomorphic disturbance regime influence sediment residence times within mountain river corridors. Nature Communications 10: 2221. Doi:10.1038/s41467-019-0986-4-w

Sutfin, N.A., E. Wohl, T. Fegel, N. Day, L. Lynch. 2021. Logjams and channel morphology influence sediment storage, transformation of organic matter, and carbon storage within mountain stream corridors. Water Resources Research 57: e2020WR028046.

Swinnen, W., Daniels, T., Maurer, E., Broothaerts, N., and Verstraeten, G. 2020. Geomorphic controls on floodplain sediment and soil organic carbon storage in a Scottish mountain river. Earth Surface Processes and Landforms 45: 207-223.

Tangen, B.A., and Bansal, S. 2020. Soil organic carbon stocks and sequestration rates of inland, freshwater wetlands: Sources of variability and uncertainty. Science of the Total Environment 749, 141444. Doi.org/10.1016/j.scitotenv.2020.141444

Tank JL, Rosi-Marshall EJ, Griffiths NA, Entrekin SA, Stephen ML. 2010. A review of allochthonous organic matter dynamics and metabolism in streams. Journal of the North American Benthological Society 29: 118-146.

Tappel PD, Bjornn TC. 1983. A new method of relating size of spawning gravel to salmonid embryo survival. North American Journal of Fisheries Management 3: 123-135.

Thorson TD, Bryce SA, Lammers DA, Woods AJ, Omernik JM, Kagan J, Pater DE, Comstock JA. 2003. Ecoregions of Oregon (color poster with map, descriptive text, summary tables, and photographs): Reston, Virginia, U.S. Geological Survey (map scale 1:1,500,000).

Tockner, K., Pennetzdorfer, D., Reiner, N., Schiemer, F., and Ward, J.V. 1999. Hydrological connectivity, and the exchange of organic matter and nutrients in a dynamic river-floodplain system (Danube, Austria). Freshwater Biology 41: 521-535.

Tooth, S., and McCarthy, T.S. 2007. Wetlands in drylands: geomorphological and sedimentological characteristics, with emphasis on examples from southern Africa. Progress in Physical Geography 31: 3-41.

Triska, F.J. 1984. Role of wood debris in modifying channel geomorphology and riparian areas of a large lowland river under pristine conditions: A historical case study. Verhandlung Internationale Vereinigung Limnologie 22: 1876–1892.

Villa, J.A., and Bernal, B. 2018. Carbon sequestration in wetlands, from science to practice: an overview of the biogeochemical process, measurement methods, and policy framework. Ecological Engineering 114: 115-128.

Walling, D.E. 2006. Human impact on land-ocean sediment transfer by the world's rivers. Geomorphology 79: 192-216.

Walter, R.C. and Merritts, D.J., 2008. Natural streams and the legacy of water-powered mills. Science 319(5861): 299-304.

Wang, G., Zhou, Y., Xu, X., Ruan, H. and Wang, J., 2013. Temperature sensitivity of soil organic carbon mineralization along an elevation gradient in the Wuyi Mountains, China. PLoS One 8(1): 53914.

Wara, M., 2007. Is the global carbon market working? Nature 445(7128): 595-596.

Westbrook, C.J., Cooper, D.J., and Baker, B.W. 2006. Beaver dams and overbank floods influence groundwater-surface water interactions of a Rocky Mountain riparian area. Water Resources Research 42: W06404. Doi:10.1029/2005WR004560.

Wheaton J.M., Bennett S.N., Bouwes, N., Maestas J.D. and Shahverdian S.M. (Editors), 2019. Low-Tech Process-Based Restoration of Riverscapes: Design Manual. Version 1.0. Utah State University Restoration Consortium. Logan, UT. DOI: 10.13140/RG.2.2.19590.63049/2.

Whiting, G.J., and Chanton, J.P. 2001. Greenhouse carbon balance of wetlands: methane emission versus carbon sequestration. Tellus B 53: 521-528.

Wipfli MS, Baxter CV. 2010. Linking ecosystems, food webs, and fish production: subsidies in salmonid watersheds. Fisheries 35: 373-387.

Wittmann, H., and von Blanckenburg, F. 2009. Cosmogenic nuclide budgeting of floodplain sediment transfer. Geomorphology 109: 246-256.

Wohl, E. 2011. What should these rivers look like? Historical range of variability and human impacts in the Colorado Front Range, USA. Earth Surface Processes and Landforms 36: 1378-1390.

Wohl, E., and Cadol, D. 2011. Neighborhood matters: patterns and controls on wood distribution in old-growth forest streams of the Colorado Front Range, USA. Geomorphology 125: 132-146.

Wohl, E., Dwire, K., Sutfin, N., Polvi, L. and Bazan, R., 2012. Mechanisms of carbon storage in mountainous headwater rivers. Nature communications, 3(1): 1-8.

Wohl, E., 2013. Landscape-scale carbon storage associated with beaver dams. Geophysical research letters 40(14): 3631-3636.

Wohl E. 2014. A legacy of absence: wood removal in US rivers. Progress in Physical Geography 38: 637-663.

Wohl E, Beckman ND. 2014. Leaky rivers: implications of the loss of longitudinal fluvial disconnectivity in headwater streams. Geomorphology 205: 27-35.

Wohl, E. 2015. Particle dynamics: The continuum of bedrock to alluvial river segments. Geomorphology 241: 192-208.

Wohl E, Lane SN, Wilcox AC. 2015. The science and practice of river restoration. Water Resources Research 51(8): 5974-5997.

Wohl, E. 2016. Spatial heterogeneity as a component of river geomorphic complexity. Progress in Physical Geography 40: 598-615.

Wohl E. 2017a. Bridging the gaps: an overview of wood across time and space in diverse rivers. Geomorphology 279: 3-26.

Wohl E. 2017b. Connectivity in rivers. Progress in Physical Geography 41: 345-362.

Wohl, E., Hall, R.O., Lininger, K.B., Sutfin, N.A., and Walters, D.M. 2017. Carbon dynamics of river corridors and the effects of human alterations. Ecological Monographs 87: 379-409.

Wohl, E., Cadol, D., Pfeiffer, A., Jackson, K., and Laurel, D. 2018a. Distribution of large wood within river corridors in relation to flow regime in the semiarid western US. Water Resources Research 54: 1890-1904.

Wohl, E., K.B. Lininger, D.N. Scott. 2018. River beads as a conceptual framework for building carbon storage and resilience to extreme climate events into river management. Biogeochemistry 141: 365-383.

Wohl, E., and Pfeiffer, A. 2018. Organic carbon storage in floodplain soils of the U.S. prairies. River Research and Applications 34: 406-416.

Wohl, E., Scott, D.N., and Lininger, K.B. 2018b. Spatial distribution of channel and floodplain large wood in forested river corridors of the Northern Rockies. Water Resources Research 54: 7879-7892.

Wohl E, Kramer N, Ruiz-Villanueva V, Scott DN, Comiti F, Gurnell AM, Piegay H, Lininger KB, Jaeger KL, Walters DM, Fausch KD. 2019. The natural wood regime in rivers. BioScience 69: 259-273.

Wohl, E. 2020. Wood process domains and wood loads on floodplains. Earth Surface Processes and Landforms 45: 144-156.

Wolf, E.C., Cooper, D.J., and Hobbs, N.T. 2007. Hydrologic regime and herbivory stabilize an alternative state in Yellowstone National Park. Ecological Applications 17: 1572-1587.

Wood SN. 2011. Fast stable restricted maximum likelihood and marginal likelihood estimation of semiparametric generalized linear models. Journal of the Royal Statistical Society (B), 73: 3-36.

Wyzga, B., and Zawiejska, J. 2005. Wood storage in a wide mountain river: case study of the Czarny Dunajec, Polish Carpathians. Earth Surface Processes and Landforms 30: 1475-1494.

Zeug SC, Winemiller KO. 2008. Relationships between hydrology, spatial heterogeneity, and fish recruitment dynamics in a temperate floodplain river. River Research and Applications 24: 90-102

Zhou, J., Zhao, Y., Huang, P., Zhao, X., Feng, W., Li, Q., Xue, D., Dou, J., Shi, W., Wei, W. and Zhu, G., 2020. Impacts of ecological restoration projects on the ecosystem carbon storage of inland river basin in arid area, China. Ecological Indicators 118: 106803.

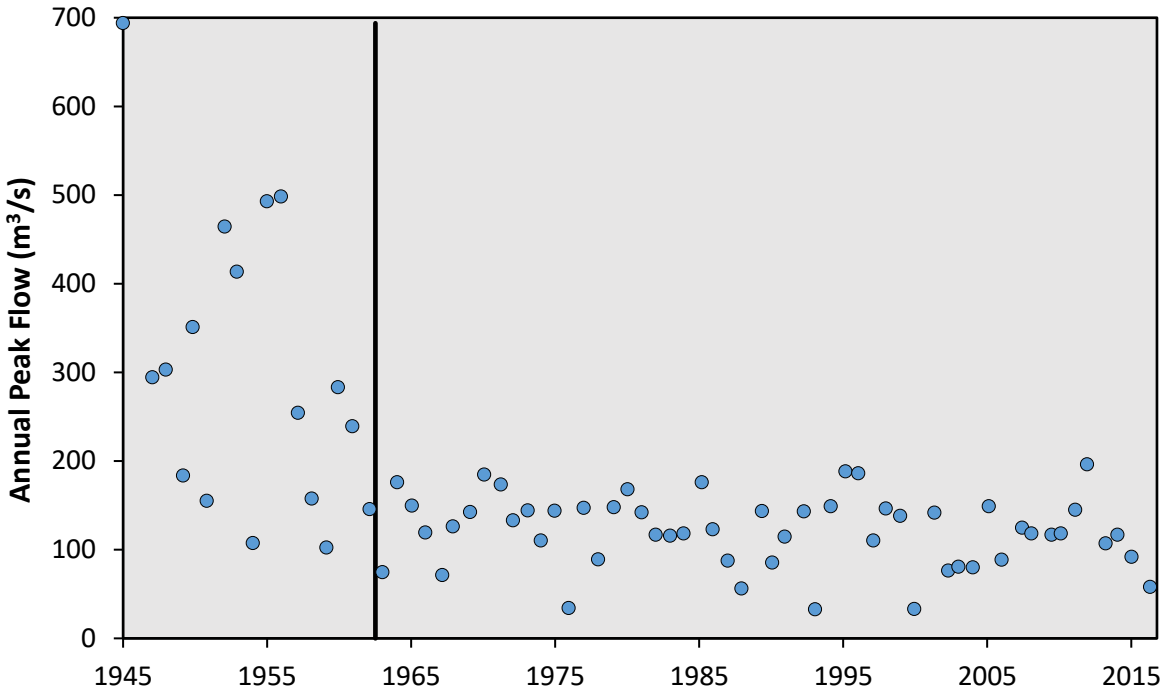

Figure S1. Annual peak discharge of the South Fork McKenzie River has decreased significantly (p = 0.0004) since the construction of Cougar Dam in 1963.

Table S1. Sediment frequencies by category of all plots combined at the SFMR.

	Mean Percentage within plots	
Size Class	**2019**	**2020**
Silt	8%	8%
Sand	40%	43%
Gravel	28%	28%
Cobble	21%	20%
Boulder	3%	1%

Table S2. 2019 Data from SFMR plots and subplots, denoted by azimuth, used for analyses presented in the study.

Plot Number	Azimuth	X	Y	Daily Discharge (cms)	Canopy Cover	Organic Cover	Scaled Water Depth (cm)	Scaled Surface Velocity (m/s)	Scaled Velocity at 60% Depth (m/s)	Unit	Median Grain Size (mm)
1	center	-122.2945	44.1581	9.34	0.97	0.4	37	0.01	0.01	ff flooded forest	0.0625
1	30	-122.2945	44.1581	9.34	0.71	0.75	38	0.07	0.07	ff flooded forest	0.0625
1	150	-122.2945	44.1580	9.34	0.88	0.4	49	0.05	0.05	ff flooded forest	0.0625
1	270	-122.2945	44.1581	9.34	0.85	0.4	0	0	0	ff flooded forest	
2	center	-122.2937	44.1577	9.34	0.60	0.35	18	0.24	0.23	sc secondary channel	0.5
2	30	-122.2936	44.1577	9.34	0.38	0.3	8	0.15	0.16	sc secondary channel	0.375
2	150	-122.2937	44.1577	9.34	0.53	0.35	31	0.38	0.32	sc secondary channel	0.09375
2	270	-122.2937	44.1577	9.34	0.40	0.3	66	0.22	0.27	sc secondary channel	
3	center	-122.2932	44.1592	9.34	0.93	0	0	0	0	vb vegetated bank	32.125
3	30	-122.2932	44.1592	9.34	0.96	0	0	0	0	vb vegetated bank	0.25
3	150	-122.2932	44.1592	9.34	0.93	0	0	0	0	vb vegetated bank	90
3	270	-122.2932	44.1592	9.34	0.91	0.1	0	0	0	vb vegetated bank	
4	center	-122.2928	44.1595	9.34	0.25	0.01	0	0	0	vb vegetated bank	128
4	30	-122.2928	44.1595	9.34	0.94	0.05	0	0	0	vb vegetated bank	154
4	150	-122.2928	44.1594	9.34	1.00	0.01	3	0	0	vb vegetated bank	64
4	270	-122.2929	44.1595	9.34	0.44	0.02	0	0	0	vb vegetated bank	0.25
5	center	-122.2924	44.1597	9.34	0.06	0	67	0.38	0.36	run	95.5
5	30	-122.2924	44.1598	9.34	0.00	0	67	0.36	0.09	run	180
5	150	-122.2924	44.1597	9.34	0.16	0.2	34	0.25	0.22	run	0.5
5	270	-122.2925	44.1597	9.34	0.01	0	67	0.23	0.15	run	180
6	center	-122.2922	44.1566	9.32	1.00	0	0	0	0	forest	
6	30	-122.2922	44.1567	9.32	0.99	0	0	0	0	forest	
6	150	-122.2921	44.1566	9.32	1.00	0	0	0	0	forest	
6	270	-122.2922	44.1566	9.32	0.97	0	0	0	0	forest	

7	center	-122.2918	44.1564	9.32	0.51	0.25	38	0.28	0.32	fm flooded meadow	0.0625
7	30	-122.2918	44.1564	9.32	1.00	0.15	48	0.32	0.23	fm flooded meadow	0.0625
7	150	-122.2920	44.1565	9.32	0.50	0.4	41	0.15	0.07	fm flooded meadow	0.0625
7	270	-122.2919	44.1564	9.32	0.87	0.1	49	0.28	0.2	fm flooded meadow	0.0625
8	center	-122.2910	44.1600	9.46	0.19	0.4	15	0.06	0.05	riffle	64
8	30	-122.2909	44.1600	9.46	0.07	0.6	18	0.01	0	riffle	154
8	150	-122.2909	44.1600	9.46	0.09	0.1	10	0.16	0.15	riffle	27.3
8	270	-122.2910	44.1600	9.46	0.10	0	10	0.31	0.3	riffle	27.3
9	center	-122.2906	44.1603	9.46	0.24	0.1	35	0.37	0.25	run	64
9	30	-122.2906	44.1603	9.46	0.60	0	42	0.35	0.41	run	77
9	150	-122.2906	44.1603	9.46	0.06	0	27.5	0.72	0.7	run	64
9	270	-122.2907	44.1603	9.46	0.31	0	50	0.38	0.43	run	128
10	center	-122.2900	44.1574	9.20	0.94	0.05	0	0	0	fm flooded meadow	56.3
10	30	-122.2900	44.1574	9.20	0.99	0.3	35	0.18	0.18	fm flooded meadow	0.0625
10	150	-122.2901	44.1573	9.20	0.71	0.02	85	0.01	0.03	fm flooded meadow	109
10	270	-122.2901	44.1574	9.20	0.85	0.07	38	0.27	0.25	fm flooded meadow	0.0625
11	center	-122.2899	44.1604	9.46	0.07	0	37	0.4	0.52	run	10
11	30	-122.2898	44.1605	9.46	0.01	0.03	44.5	0.64	0.67	run	64
11	150	-122.2898	44.1604	9.46	0.06	0	30.5	0.37	0.33	run	109
11	270	-122.2899	44.1604	9.46	0.07	0.01	38	0.51	0.4	run	77
12	center			9.46						deep pool	
12	30			9.46							
12	150			9.46							
12	270			9.46							
13	center	-122.2894	44.1603	9.46	0.34	0.02	0	Dry	0	vb vegetated bank	0.25
13	30	-122.2894	44.1603	9.46	0.24	0.05	0	0	0	vb vegetated bank	0.25
13	150	-122.2894	44.1603	0.00					0		0.25
13	270	-122.2895	44.1603	0.00					0		0.25
14	center	-122.2894	44.1580	9.15	0.50	0.45	57	0.01	0.15	pool	109
14	30	-122.2893	44.1580	9.15	0.40	0.17	52	0.23	0.19	pool	109

14	150	-122.2893	44.1580	9.15	0.37	0.07	58	0.13	0.25	pool	8.3
14	270	-122.2894	44.1580	9.15	0.43	0.3	47	0.1	0.1	pool	64
15	center	-122.2889	44.1594	9.15	0.13	0.5	57	0.08	0.12	pool	9.5
15	30	-122.2888	44.1594	9.15	0.07	0.3	52	0.05	0.04	pool	18.8
15	150	-122.2888	44.1594	9.15	0.00	0.25	57	0.05	0.07	pool	0.75
15	270	-122.2889	44.1594	9.15	0.09	0.15	50	0.12	0.1	pool	27.3
16	center	-122.2887	44.1571	9.20	0.78	0.25	63	0	0	ff flooded forest	
16	30	-122.2887	44.1569	9.20	0.74	0.15	53	0	0	ff flooded forest	0.125
16	150	-122.2887	44.1570	9.20	0.74	0.1	61	0	0	ff flooded forest	
16	270	-122.2888	44.1568	9.20	0.66	0.1	52	0	0	ff flooded forest	
17	center	-122.2885	44.1596	9.40	0.38	0.55	24	0.01	0.02	jam	0.25
17	30	-122.2885	44.1597	9.40	0.50	0.3	36	0.2	0.16	run	0.75
17	150	-122.2885	44.1596	9.40	0.12	0.2	24	0.2	0.19	run	2
17	270	-122.2886	44.1596	9.40	0.19	0.2	25	0.01	0.01	pool	1.5
18	center	-122.2884	44.1588	9.15	0.47	0.3	0	0	0	terrace	
18	30	-122.2884	44.1588	9.15	0.18	0.15	20	0	0	margin	0.5
18	150			9.15							
18	270	-122.2884	44.1588	0.00	0.13	0.15	15	0.02	0.03	margin	1
19	center	-122.2882	44.1599	9.46	0.49	0.15	19.5	0	0	island	67.5
19	30	-122.2881	44.1599	9.46	0.09	0.07	0	0	0	island	64
19	150	-122.2882	44.1599	9.46	0.34	0	21	0.41	0.36	pool	45
19	270	-122.2882	44.1599	9.46	0.69	0.25	14	0	0	island	16
20	center	-122.2873	44.1572	9.20						forest	
20	30			0.00						forest	
20	150			0.00						forest	
20	270			0.00						forest	
21	center	-122.2870	44.1594	9.12	0.25	0.01	14	0.22	0.24	run	64
21	30	-122.2869	44.1595	9.12	0.34	0.02	20	0.18	0.21	run	27.3
21	150	-122.2869	44.1594	9.12	0.26	0.01	26	0.22	0.21	run	32
21	270	-122.2870	44.1595	9.12	0.21	0.01	6	0.01	0.01	run	54.5

22	center			0.00							
22	30			0.00							
22	150			0.00							
22	270			0.00							
23	center	-122.2869	44.1591	9.12	0.16	0.01	7	0.03	0.03	riffle	22.6
23	30	-122.2868	44.1591	9.12	0.12	0.07	19	0.72	0.28	riffle	32
23	150	-122.2868	44.1591	9.12	0.13	0.05	7	0.15	0.15	riffle	54.5
23	270	-122.2869	44.1591	9.12	0.10	0.02	22	0.04	0.01	riffle	19.3
24	center	-122.2867	44.1563	9.20	0.59	0.05	35	0.36	0.19	sc secondary channel	1
24	30	-122.2867	44.1563	9.20	0.40	0.08	61	1.1	0.6	sc secondary channel	5
24	150	-122.2867	44.1563	9.20	0.31	0.02	27	0.11	0.1	sc secondary channel	0.5
24	270	-122.2867	44.1563	9.20	0.49	0.4	71	0.68	0.27	sc secondary channel	0.5
25	center	-122.2864	44.1585	9.12	0.24	0.02	7	0.12	0.12	riffle	0.5
25	30	-122.2864	44.1586	9.12	0.28	0.1	0	0	0	bar	0.5
25	150	-122.2863	44.1585	9.12	0.24	0	7	0.31	0.31	riffle	32
25	270	-122.2864	44.1585	9.12	0.18	0.1	15	0.16	0.15	riffle	45
26	center	-122.2863	44.1600	9.17	0.10	0.15	1.5	0	0	bar	0.5
26	30	-122.2862	44.1601	9.17	0.06	0.2	1.5	0	0	bar	19.3
26	150	-122.2862	44.1600	9.17	0.10	0.1	10	0.33	0.29	riffle	38.5
26	270	-122.2863	44.1600	9.17	0.09	0.02	3.5	0	0	bar	45
27	center	-122.2863	44.1581	9.20	0.24	0.65	23	0.02	0	margin	0.125
27	30	-122.2863	44.1581	9.20	0.06	0.1	24	0.04	0.04	margin	0.125
27	150	-122.2863	44.1581	9.20	0.19	0.5	34	0.01	0.01	margin	0.125
27	270	-122.2863	44.1580	9.20	0.29	0.15	16	0	0	margin	0.125
28	center	-122.2859	44.1600	9.17	0.13	0.2	7	0	0	bar	0.25
28	30	-122.2859	44.1600	9.17	0.09	0.17	7	0.01	0.01	bar	0.1875
28	150	-122.2859	44.1599	9.17	0.10	0.25	0	0	0	bar	0.125
28	270	-122.2860	44.1600	9.17	0.15	0.07	0	0	0	bar	0.5
29	center	-122.2858	44.1595	9.40	0.76	0.04	96.5	0.09	0.09	ff flooded forest	0.25
29	30	-122.2858	44.1595	9.40	0.63	0.3	88	0.19	0.11	ff flooded forest	0.25

29	150	-122.2858	44.1595	9.40	0.96	0.04	55	0.17	0.16	pool	0.25
29	270	-122.2858	44.1595	9.40	0.62	0.17	68	0.14	0.06	ff flooded forest	0.25
30	center	-122.2855	44.1583	9.20	0.09	0.6	39	0.13	0.28	run	54.5
30	30	-122.2855	44.1582	9.20	0.04	0.2	31	0.3	0.25	run	19.3
30	150	-122.2855	44.1582	9.20	0.15	0.3	27	0.55	0.4	run	45
30	270	-122.2856	44.1582	9.20	0.10	0.45	27	0.23	0.21	run	64
31	center	-122.2854	44.1594	9.15	0.40	0.35	0	0	0	island	0.5
31	30	-122.2853	44.1594	9.15	0.28	0.45	0	0	0	island	0.5
31	150	-122.2853	44.1593	9.15	0.29	0.12	0	0	0	island	0.5
31	270	-122.2854	44.1594	9.15	0.41	0.2	63	0.14	0.12	pool	0.25
32	center	-122.2853	44.1589	9.40	0.28	0.3	31	0.66	0.44	run	64
32	30	-122.2853	44.1589	9.40	0.16	0.3	14	0.4	0.4	run	13.5
32	150	-122.2852	44.1589	9.40	0.37	0.35	35	0.17	0.11	run	4.5
32	270	-122.2853	44.1589	9.40	0.34	0.6	16	0.25	0.17	run	
33	center	-122.2849	44.1592	9.26	0.50	0.2	9	0	0	margin	0.5
33	30	-122.2849	44.1592	9.26	0.51	0.27	0	0	0	island	
33	150	-122.2849	44.1591	9.26	0.44	0.03	0	0	0	island	0.5
33	270	-122.2850	44.1591	9.26	0.56	0.18	0	0	0	island	0.5
34	center	-122.2848	44.1568	9.20	0.37	0.12	17	0.11	0.08	sc secondary channel	0.5
34	30	-122.2848	44.1568	9.20	0.57	0.15	20	0.24	0.27	sc secondary channel	38.5
34	150	-122.2847	44.1567	9.20	0.54	0.05	16	0.11	0.08	sc secondary channel	0.5
34	270	-122.2849	44.1569	9.20	0.53	0.2	15	0.11	0.13	sc secondary channel	0.25
35	center	-122.2844	44.1586	9.26	0.00	0.01	14	0.24	0.25	riffle	54.5
35	30	-122.2844	44.1586	9.26	0.00	0	20	0.19	0.18	riffle	22.6
35	150	-122.2844	44.1586	9.26	0.00	0.17	16	0.07	0.07	riffle	27.3
35	270	-122.2844	44.1586	9.26	NA	0.01	15	0.47	0.43	riffle	54.5
36	center	-122.2844	44.1602	9.17	0.34	0.4	52	0	0	pool	54.5
36	30	-122.2843	44.1602	9.17	0.50	0.3	25	0	0	pool	90
36	150	-122.2843	44.1602	9.17	0.43	0.1	0.5	0	0	pool	0.25
36	270	-122.2844	44.1602	9.17	0.32	0.05	10	0	0	pool	90

37	center	-122.2839	44.1581	9.34	0.78	0.1	26	0.02	0.04	ff flooded forest	33.8
37	30	-122.2839	44.1581	9.34	0.90	0.15	36	0.04	0.01	ff flooded forest	0.75
37	150	-122.2839	44.1580	9.34	0.09	0.7	6	0.05	0.06	ff flooded forest	0.25
37	270	-122.2840	44.1581	9.34	0.00	0.02	16	0.06	0.08	ff flooded forest	16.8
38	center	-122.2834	44.1575	9.34	0.63	0.85	29	0	0	jam	
38	30	-122.2833	44.1575	9.20	0.90	0.4	16	0.01	0.01	margin	1.525
38	150	-122.2834	44.1574	9.20	0.69	0.45	0	0	0	vegetated bank	
38	270	-122.2834	44.1575	9.20	0.91	0.7	50	0.01	0.08	margin	
40	center	-122.2828	44.1585	9.34	0.51	0.02	0	0	0	island	54.5
40	30	-122.2828	44.1586	9.15	0.62	0.3	0	0	0	island	22.6
40	150	-122.2828	44.1585	9.15	0.72	0.6	0	0	0	island	38.5
40	270	-122.2829	44.1585	9.15	0.56	0.1	0	0	0	island	45

Table S3. 2020 Data from SFMR plots and subplots, denoted by azimuth, used for analyses presented in the study.

Plot Number	Azimuth	Daily Discharge 2020 (cms)	X	Y	Canopy Cover	Organic Cover	Scaled Water Depth (cm)	Scaled Surface Velocity (m/s)	Scaled Velocity at 60% Depth (m/s)	Unit	Median Grain Size (mm)
1	center	14.16	-122.2945	44.1581	0.87	0.4	29	0.04	0.07	pool	0.25
1	30	14.16	-122.2945	44.1581	0.79	0.2	48	0.17	0.18	pool	0.25
1	150	14.16	-122.2945	44.1580	0.81	0.15	41.5	0.09	0.08	pool	0.25
1	270	14.16	-122.2946	44.1581	NA	NA	0	0	0	pool	
2	center	14.16	-122.2937	44.1577	0.22	0.2	32	0.15	0.14	riffle	0.25
2	30	14.16	-122.2936	44.1577	0.25	0.02	35	0.53	0.31	riffle	0.09375
2	150	14.16	-122.2937	44.1577	0.21	0.1	43	0.3	0.27	riffle	0.0625
2	270	14.16	-122.2937	44.1577	0.22	NA	92	0.29	0.27	riffle	0.25
3	center	14.22	-122.2932	44.1592	0.85	0.01	0	0	0	island	0.25
3	30	14.22	-122.2932	44.1592	0.79	0.01	0	0	0	island	0.25
3	150	14.22	-122.2931	44.1591	0.85	0	0	0	0	island	0.5
3	270	14.22	-122.2932	44.1592	0.87	0.08	0	0	0	island	0.5
4	center	14.22	-122.2928	44.1594	0.76	0	16	0.01	0.01	margin	109
4	30	14.22	-122.2928	44.1594	0.76	0	4	0	0	margin	1.5
4	150	14.22	-122.2928	44.1594	0.91	0.02	9.5	0.01	0.01	margin	109
4	270	14.22	-122.2929	44.1594	0.50	0	0	0	0	margin	0.5
5	center	14.22	-122.2924	44.1597	0.00	0.02	67	0.63	0.44	run	256
5	30	14.22	-122.2924	44.1597	0.01	0.01	52	0.35	0.31	run	9.5
5	150	14.22	-122.2924	44.1597	0.07	0.15	34	0.34	0.32	run	0.75
5	270	14.22	-122.2924	44.1597	0.04	0.02	80	0.59	0.51	run	256
6	center										
6	30										
6	150										
6	270										
7	center	14.16	-122.2918	44.1564	0.35	0.25	51	0.33	0.29	pool	0.0625

7	30	14.16	-122.2918	44.1564	0.65	0	65	0.27	0.26	pool	0.0625
7	150	14.16	-122.2918	44.1564	0.16	0.15	45	0.2	0.05	pool	0.0625
7	270	14.16	-122.2919	44.1564	0.18	0.01	60	0.54	0.55	pool	0.0625
8	center	14.19	-122.2910	44.1600	0.01	0.1	18	0.33	0.33	riffle	24
8	30	14.19	-122.2909	44.1600	0.00	0.45	21	0.13	0.14	riffle	96
8	150	14.19	-122.2909	44.1600	0.01	0.35	8	0.16	0.16	riffle	34
8	270	14.19	-122.2910	44.1600	0.00	0.2	17	0.3	0.21	riffle	45
9	center	14.19	-122.2906	44.1603	0.07	0.15	47	0.77	0.64	riffle	54.5
9	30	14.19	-122.2906	44.1603	0.07	0	50	0.65	0.66	riffle	90
9	150	14.19	-122.2906	44.1603	0.06	0	42	1.01	0.96	riffle	90
9	270	14.19	-122.2907	44.1603	0.03	NA	57	0.65	0.67	riffle	90
10	center										
10	30										
10	150										
10	270										
11	center	14.19	-122.2898	44.1604	0.00	0	48	0.58	0.63	riffle	45
11	30	14.19	-122.2898	44.1605	0.00	0	54	0.43	0.36	riffle	109
11	150	14.19	-122.2898	44.1604	0.00	0	39	0.68	0.38	riffle	90
11	270	14.19	-122.2899	44.1605	0.00	0.4	51	0.63	0.53	riffle	64
12	center										
12	30										
12	150										
12	270										
13	center	14.19	-122.2894	44.1603	0.29	0.01	0	0	0	island	0.25
13	30	14.19	-122.2894	44.1603	0.15	0	0	0	0	island	3.05
13	150	14.19	-122.2894	44.1603	0.25	0.25	0	0	0	island	0.25
13	270	14.19	-122.2895	44.1603	0.32	0.06	0	0	0	island	0.25
14	center	14.16	-122.2894	44.1580	0.22	0.7	59	0.04	0.02	pool	90
14	30	14.16	-122.2893	44.1580	0.19	0.4	58	0.25	0.15	pool	90
14	150	14.16	-122.2894	44.1580	0.16	0.03	53	0.29	0.3	pool	2.4

14	270	14.16	-122.2894	44.1580	0.28	0.25	50	0.19	0.06	pool	64
15	center										
15	30										
15	150										
15	270										
16	center										
16	30										
16	150										
16	270										
17	center	14.67	-122.2885	44.1596	0.10	0.45	29	0.1	0.03	pool	0.5
17	30	14.67	-122.2885	44.1596	0.06	0.05	42	0.08	0.06	pool	0.375
17	150	14.67	-122.2885	44.1596	0.09	0.3	34	0.13	0.18	pool	0.5
17	270	14.67	-122.2886	44.1596	0.12	0.06	30	0.03	0.02	pool	0.1875
18	center										
18	30										
18	150										
18	270										
19	center	14.19	-122.2881	44.1599	0.21	0.2	14.5	0.05	0.07	island	77
19	30	14.19	-122.2881	44.1599	0.37	0	0	0	0	island	0.75
19	150	14.19	-122.2881	44.1599	0.09	0.4	42	0.18	0.14	island	2.8
19	270	14.19	-122.2881	44.1599	0.25	0.1	0	0	0	island	54.5
20	center										
20	30										
20	150										
20	270										
21	center										
21	30										
21	150										
21	270										
22	center										

22	30										
22	150										
22	270										
23	center										
23	30										
23	150										
23	270										
24	center										
24	30										
24	150										
24	270										
25	center										
25	30										
25	150										
25	270										
26	center	14.22	-122.2862	44.1601	0.00	0.25	7	0.08	0.08	riffle	13.5
26	30	14.22	-122.2862	44.1600	0.00	0.25	6.8	0.23	0.23	riffle	27.3
26	150	14.22	-122.2863	44.1601	0.00	0.25	13	0.19	0.15	riffle	13.5
26	270	14.22			0.00	0.02	9	0.32	0.32	riffle	27.3
27	center										
27	30										
27	150										
27	270										
28	center	14.07	-122.2859	44.1600	0.01	0.4	16	0.03	0	pool	0.375
28	30	14.07	-122.2859	44.1600	0.00	0.25	20	0.02	0.01	pool	0.125
28	150	14.07	-122.2859	44.1599	0.03	0.45	4	0	0	pool	0.125
28	270	14.07	-122.2860	44.1600	0.03	0.01	2	0	0	pool	0.3125
29	center										
29	30										
29	150										

29	270										
30	center										
30	30										
30	150										
30	270										
31	center	14.07	-122.2854	44.1594	0.16	0.15	0	0	0	island	0.25
31	30	14.07	-122.2853	44.1594	0.18	0.35	18	0	0	island	0.5
31	150	14.07	-122.2853	44.1593	0.22	0.1	8	0	0	island	0.25
31	270	14.07	-122.2854	44.1594	0.16	0.5	68	0.08	0.2	island	0.5
32	center	14.07	-122.2853	44.1589	0.00	0.4	35	0.49	0.36	riffle	54.5
32	30	14.07	-122.2853	44.1589	0.01	0.45	33	0.46	0.55	riffle	22.6
32	150	14.07	-122.2853	44.1589	0.10	0.7	51	0.3	0.12	riffle	109
32	270	14.07	-122.2853	44.1589	0.01	0.8	20	0.67	0.45	riffle	24
33	center	14.07	-122.2849	44.1592	0.59	0.25	0	0	0	island	0.09375
33	30	14.07	-122.2849	44.1592	0.53	0.04	1	0	0	island	0.5
33	150	14.07	-122.2849	44.1592	0.44	0.03	9	0.25	0.25	island	0.5
33	270	14.07	-122.2849	44.1592	0.53	0.07	16	0.28	0.06	island	0.5
34	center										
34	30										
34	150										
34	270										
35	center	14.07	-122.2844	44.1586	0.00	0.35	16	0.24	0.21	riffle	22.6
35	30	14.07	-122.2844	44.1586	0.00	0.2	17	0.24	0.21	riffle	22.6
35	150	14.07	-122.2844	44.1586	0.00	0.4	40	0.19	0.19	riffle	7.5
35	270	14.07	-122.2844	44.1586	0.00	0	25	0.85	0.82	riffle	54.5
36	center	14.07	-122.2844	44.1602	0.29	0.7	110	0.11	0.25	pool	128
36	30	14.07	-122.2843	44.1602	0.41	0.45	87	0.12	0.09	pool	128
36	150	14.07	-122.2843	44.1602	0.26	0.1	55	0.26	0.43	pool	77
36	270	14.07	-122.2844	44.1602	0.31	0.03	60	0.16	0.17	pool	128
37	center	14.07	-122.2839	44.1581	0.07	0.25	29	0.01	0.01	pool	0.125

37	30	14.07	-122.2839	44.1581	0.18	0.6	21	0.04	0.03	pool	0.25
37	150	14.07	-122.2839	44.1580	0.09	0.9	5	0	0	pool	0.125
37	270	14.07	-122.2840	44.1581	0.04	0.15	24	0.13	0.11	pool	0.09375
38	center	14.07	-122.2835	44.1575	0.62	0.95	15	0	0	vb	0.1875
38	30	14.07	-122.2834	44.1575	0.32	0.6	6	0.01	0.01	vb	8.0625
38	150	14.07	-122.2835	44.1575	0.88	0.07	0	0	0	vb	0.25
38	270	14.07	-122.2835	44.1574	0.51	0.7	38	0.02	0.02	vb	2.4
40	center	14.07	-122.2829	44.1585	0.50	0.1	0	0	0	island	19.3
40	30	14.07	-122.2829	44.1586	0.56	0.7	0	0	0	island	77
40	150	14.07	-122.2829	44.1585	0.35	0.55	0	0	0	island	27.3
40	270	14.07	-122.2829	44.1586	0.69	0.02	0	0	0	island	27.3

Table S4. Water characteristics from geomorphic field plots, 2019-2020

Year	Plot Number	Plot Azimuth	Water Depth (cm)	Surface Velocity (m/s)	Velocity at 60% Depth (m/s)
2019	1	center	37	0.01	0.01
2019	1	30	38	0.07	0.07
2019	1	150	49	0.05	0.05
2019	1	270	0	0	0
2019	2	center	18	0.24	0.23
2019	2	30	8	0.15	0.16
2019	2	150	31	0.38	0.32
2019	2	270	66	0.22	0.27
2019	3	center	0	0	0
2019	3	30	0	0	0
2019	3	150	0	0	0
2019	3	270	0	0	0
2019	4	center	0	0	0
2019	4	30	0	0	0
2019	4	150	3	0	0
2019	4	270	0	0	0
2019	5	center	67	0.38	0.36
2019	5	30	67	0.36	0.09
2019	5	150	34	0.25	0.22
2019	5	270	67	0.23	0.15
2019	6	center	0	0	0
2019	6	30	0	0	0
2019	6	150	0	0	0
2019	6	270	0	0	0
2019	7	center	38	0.28	0.32
2019	7	30	48	0.32	0.23
2019	7	150	41	0.15	0.07
2019	7	270	49	0.28	0.2
2019	8	center	15	0.06	0.05
2019	8	30	18	0.01	0
2019	8	150	10	0.16	0.15
2019	8	270	10	0.31	0.3
2019	9	center	35	0.37	0.25
2019	9	30	42	0.35	0.41
2019	9	150	27.5	0.72	0.7
2019	9	270	50	0.38	0.43
2019	10	center	0	0	0
2019	10	30	35	0.18	0.18
2019	10	150	85	0.01	0.03
2019	10	270	38	0.27	0.25

2019	11	center	37	0.4	0.52
2019	11	30	44.5	0.64	0.67
2019	11	150	30.5	0.37	0.33
2019	11	270	38	0.51	0.4
2019	12	center	NA	NA	NA
2019	12	30	NA	NA	NA
2019	12	150	NA	NA	NA
2019	12	270	NA	NA	NA
2019	13	center	0	0	0
2019	13	30	0	0	0
2019	13	150	NA	NA	0
2019	13	270	NA	NA	0
2019	14	center	57	0.01	0.15
2019	14	30	52	0.23	0.19
2019	14	150	58	0.13	0.25
2019	14	270	47	0.1	0.1
2019	15	center	57	0.08	0.12
2019	15	30	52	0.05	0.04
2019	15	150	57	0.05	0.07
2019	15	270	50	0.12	0.1
2019	16	center	63	0	0
2019	16	30	53	0	0
2019	16	150	61	0	0
2019	16	270	52	0	0
2019	17	center	24	0.01	0.02
2019	17	30	36	0.2	0.16
2019	17	150	24	0.2	0.19
2019	17	270	25	0.01	0.01
2019	18	center	0	0	0
2019	18	30	20	0	0
2019	18	150	NA	NA	NA
2019	18	270	15	0.02	0.03
2019	19	center	19.5	0	0
2019	19	30	0	0	0
2019	19	150	21	0.41	0.36
2019	19	270	14	0	0
2019	20	center	NA	NA	NA
2019	20	30	NA	NA	NA
2019	20	150	NA	NA	NA
2019	20	270	NA	NA	NA
2019	21	center	14	0.22	0.24
2019	21	30	20	0.18	0.21
2019	21	150	26	0.22	0.21

2019	21	270	6	0.01	0.01
2019	22	center	NA	NA	NA
2019	22	30	NA	NA	NA
2019	22	150	NA	NA	NA
2019	22	270	NA	NA	NA
2019	23	center	7	0.03	0.03
2019	23	30	19	0.72	0.28
2019	23	150	7	0.15	0.15
2019	23	270	22	0.04	0.01
2019	24	center	35	0.36	0.19
2019	24	30	61	1.1	0.6
2019	24	150	27	0.11	0.1
2019	24	270	71	0.68	0.27
2019	25	center	7	0.12	0.12
2019	25	30	0	0	0
2019	25	150	7	0.31	0.31
2019	25	270	15	0.16	0.15
2019	26	center	1.5	0	0
2019	26	30	1.5	0	0
2019	26	150	10	0.33	0.29
2019	26	270	3.5	0	0
2019	27	center	23	0.02	0
2019	27	30	24	0.04	0.04
2019	27	150	34	0.01	0.01
2019	27	270	16	0	0
2019	28	center	7	0	0
2019	28	30	7	0.01	0.01
2019	28	150	0	0	0
2019	28	270	0	0	0
2019	29	center	96.5	0.09	0.09
2019	29	30	88	0.19	0.11
2019	29	150	55	0.17	0.16
2019	29	270	68	0.14	0.06
2019	30	center	39	0.13	0.28
2019	30	30	31	0.3	0.25
2019	30	150	27	0.55	0.4
2019	30	270	27	0.23	0.21
2019	31	center	0	0	0
2019	31	30	0	0	0
2019	31	150	0	0	0
2019	31	270	63	0.14	0.12
2019	32	center	31	0.66	0.44
2019	32	30	14	0.4	0.4

2019	32	150	35	0.17	0.11
2019	32	270	16	0.25	0.17
2019	33	center	9	0	0
2019	33	30	0	0	0
2019	33	150	0	0	0
2019	33	270	0	0	0
2019	34	center	17	0.11	0.08
2019	34	30	20	0.24	0.27
2019	34	150	16	0.11	0.08
2019	34	270	15	0.11	0.13
2019	35	center	14	0.24	0.25
2019	35	30	20	0.19	0.18
2019	35	150	16	0.07	0.07
2019	35	270	15	0.47	0.43
2019	36	center	52	0	0
2019	36	30	25	0	0
2019	36	150	0.5	0	0
2019	36	270	10	0	0
2019	37	center	26	0.02	0.04
2019	37	30	36	0.04	0.01
2019	37	150	6	0.05	0.06
2019	37	270	16	0.06	0.08
2019	38	center	29	0	0
2019	38	30	16	0.01	0.01
2019	38	150	0	0	0
2019	38	270	50	0.01	0.08
2019	40	center	0	0	0
2019	40	30	0	0	0
2019	40	150	0	0	0
2019	40	270	0	0	0
2020	1	center	29	0.04	0.07
2020	1	30	48	0.17	0.18
2020	1	150	41.5	0.09	0.08
2020	1	270	0	0	0
2020	2	center	32	0.15	0.14
2020	2	30	35	0.53	0.31
2020	2	150	43	0.3	0.27
2020	2	270	92	0.29	0.27
2020	3	center	0	0	0
2020	3	30	0	0	0
2020	3	150	0	0	0
2020	3	270	0	0	0
2020	4	center	16	0.01	0.01

2020	4	30	4	0	0
2020	4	150	9.5	0.01	0.01
2020	4	270	0	0	0
2020	5	center	67	0.63	0.44
2020	5	30	52	0.35	0.31
2020	5	150	34	0.34	0.32
2020	5	270	80	0.59	0.51
2020	6	center	NA	NA	NA
2020	6	30	NA	NA	NA
2020	6	150	NA	NA	NA
2020	6	270	NA	NA	NA
2020	7	center	51	0.33	0.29
2020	7	30	65	0.27	0.26
2020	7	150	45	0.2	0.05
2020	7	270	60	0.54	0.55
2020	8	center	18	0.33	0.33
2020	8	30	21	0.13	0.14
2020	8	150	8	0.16	0.16
2020	8	270	17	0.3	0.21
2020	9	center	47	0.77	0.64
2020	9	30	50	0.65	0.66
2020	9	150	42	1.01	0.96
2020	9	270	57	0.65	0.67
2020	10	center	NA	NA	NA
2020	10	30	NA	NA	NA
2020	10	150	NA	NA	NA
2020	10	270	NA	NA	NA
2020	11	center	48	0.58	0.63
2020	11	30	54	0.43	0.36
2020	11	150	39	0.68	0.38
2020	11	270	51	0.63	0.53
2020	12	center	NA	NA	NA
2020	12	30	NA	NA	NA
2020	12	150	NA	NA	NA
2020	12	270	NA	NA	NA
2020	13	center	0	0	0
2020	13	30	0	0	0
2020	13	150	0	0	0
2020	13	270	0	0	0
2020	14	center	59	0.04	0.02
2020	14	30	58	0.25	0.15
2020	14	150	53	0.29	0.3
2020	14	270	50	0.19	0.06

2020	15	center	NA	NA	NA
2020	15	30	NA	NA	NA
2020	15	150	NA	NA	NA
2020	15	270	NA	NA	NA
2020	16	center	NA	NA	NA
2020	16	30	NA	NA	NA
2020	16	150	NA	NA	NA
2020	16	270	NA	NA	NA
2020	17	center	29	0.1	0.03
2020	17	30	42	0.08	0.06
2020	17	150	34	0.13	0.18
2020	17	270	30	0.03	0.02
2020	18	center	NA	NA	NA
2020	18	30	NA	NA	NA
2020	18	150	NA	NA	NA
2020	18	270	NA	NA	NA
2020	19	center	14.5	0.05	0.07
2020	19	30	0	0	0
2020	19	150	42	0.18	0.14
2020	19	270	0	0	0
2020	20	center	NA	NA	NA
2020	20	30	NA	NA	NA
2020	20	150	NA	NA	NA
2020	20	270	NA	NA	NA
2020	21	center	NA	NA	NA
2020	21	30	NA	NA	NA
2020	21	150	NA	NA	NA
2020	21	270	NA	NA	NA
2020	22	center	NA	NA	NA
2020	22	30	NA	NA	NA
2020	22	150	NA	NA	NA
2020	22	270	NA	NA	NA
2020	23	center	NA	NA	NA
2020	23	30	NA	NA	NA
2020	23	150	NA	NA	NA
2020	23	270	NA	NA	NA
2020	24	center	NA	NA	NA
2020	24	30	NA	NA	NA
2020	24	150	NA	NA	NA
2020	24	270	NA	NA	NA
2020	25	center	NA	NA	NA
2020	25	30	NA	NA	NA
2020	25	150	NA	NA	NA

2020	25	270	NA	NA	NA
2020	26	center	7	0.08	0.08
2020	26	30	6.8	0.23	0.23
2020	26	150	13	0.19	0.15
2020	26	270	9	0.32	0.32
2020	27	center	NA	NA	NA
2020	27	30	NA	NA	NA
2020	27	150	NA	NA	NA
2020	27	270	NA	NA	NA
2020	28	center	16	0.03	0
2020	28	30	20	0.02	0.01
2020	28	150	4	0	0
2020	28	270	2	0	0
2020	29	center	NA	NA	NA
2020	29	30	NA	NA	NA
2020	29	150	NA	NA	NA
2020	29	270	NA	NA	NA
2020	30	center	NA	NA	NA
2020	30	30	NA	NA	NA
2020	30	150	NA	NA	NA
2020	30	270	NA	NA	NA
2020	31	center	0	0	0
2020	31	30	18	0	0
2020	31	150	8	0	0
2020	31	270	68	0.08	0.2
2020	32	center	35	0.49	0.36
2020	32	30	33	0.46	0.55
2020	32	150	51	0.3	0.12
2020	32	270	20	0.67	0.45
2020	33	center	0	0	0
2020	33	30	1	0	0
2020	33	150	9	0.25	0.25
2020	33	270	16	0.28	0.06
2020	34	center	NA	NA	NA
2020	34	30	NA	NA	NA
2020	34	150	NA	NA	NA
2020	34	270	NA	NA	NA
2020	35	center	16	0.24	0.21
2020	35	30	17	0.24	0.21
2020	35	150	40	0.19	0.19
2020	35	270	25	0.85	0.82
2020	36	center	110	0.11	0.25
2020	36	30	87	0.12	0.09

2020	36	150	55	0.26	0.43
2020	36	270	60	0.16	0.17
2020	37	center	29	0.01	0.01
2020	37	30	21	0.04	0.03
2020	37	150	5	0	0
2020	37	270	24	0.13	0.11
2020	38	center	15	0	0
2020	38	30	6	0.01	0.01
2020	38	150	0	0	0
2020	38	270	38	0.02	0.02
2020	40	center	0	0	0
2020	40	30	0	0	0
2020	40	150	0	0	0
2020	40	270	0	0	0

Appendix B: Supplemental information for Chapter 3

Basic data for the case studies

Data for this chapter are a subset of Deep Creek and South Fork McKenzie River data. The data for the two sites are included in the comprehensive dataset that is located in the Mountain Scholar Repository and can be searched for with the author name Sarah Hinshaw.

The data are also temporarily available at the following link to a csv document on Google Drive:

Link to data on Google Drive

Table 2. Data used to generate response surfaces

- maP is mean annual precipitation, in mm
- maT is mean annual temperature, in degrees C
- SOC is soil organic carbon, in Mg C/ha

Table S5. Data used to generate response surfaces				
soil organic carbon data				
location	**reference**	**maP**	**maT**	**SOC**
North St Vrain Creek, Colorado, USA	Wohl et al., 2012	800	4	370
Danube River, Austria	Cierjacks et al., 2010	533	9.8	183
River Dee, eastern Scotland	Swinnen et al., 2020	950	3	323
Oklahoma	Wohl & Pfeiffer, 2018	1194	13.9	166
Kansas 1	Wohl & Pfeiffer, 2018	914	13.3	410
Kansas 2	Wohl & Pfeiffer, 2018	914	13.3	517
Missouri 1	Wohl & Pfeiffer, 2018	1245	13.3	332
Missouri 2	Wohl & Pfeiffer, 2018	1245	13.3	324
Arikaree River, Colorado	Wohl & Pfeiffer, 2018	462	10.4	129
Bijou Creek, Colorado	Wohl & Pfeiffer, 2018	538	7	326
Kiowa Creek, Colorado	Wohl & Pfeiffer, 2018	340	9.3	223
Big Sandy Creek, Colorado	Wohl & Pfeiffer, 2018	538	7	133
Spring Creek, Colorado	Wohl & Pfeiffer, 2018	538	7	14
South Fork Republican River, Colorado	Wohl & Pfeiffer, 2018	465	10.1	4
Mexico	Jaramillo et al., 2003	680	25	114
central Alaska	Lininger et al., 2019	170	-1	277
Congaree River, South Carolina	Ricker & Lockaby, 2015	1220	18	236
Middle Fork Snoqualmie River, WA	Scott & Wohl, 2020	3040	5.4	193

Big Sandy, Wyoming	Scott & Wohl, 2020	720	2.3	94
Deep Creek, Oregon	this paper	468	5.7	391
South Fork McKenzie River, Oregon	this paper	1882	10.6	348

Reference citations: soil

- Cierjacks, A., Kleinschmit, B., Babinsky, M., Kleinschroth, F., Markert, A., Menzel, M., Ziechmann, U., Schiller, T., Graf, M., and Lang F. (2010). Carbon stocks of soil and vegetation on Danubian floodplains. Journal of Plant Nutrition and Soil Science 173, 644-653.
- Jaramillo, V.J., Kauffmann, J.B., Renteria-Rodriguez, L., Cummings, D.L., and Ellingson, L.J. (2003). Biomass, carbon, and nitrogen pools in Mexican tropical dry forest landscapes. Ecosystems 6, 609-629.
- Lininger, K.B., Wohl, E., Rose, J.R., and Leisz, S.J. (2019). Significant floodplain soil organic carbon storage along a large high-latitude river and its tributaries. Geophysical Research Letters 46, 2121-2129.
- Ricker, M.C., and Lockaby, B.G. (2015). Soil organic carbon stocks in a large eutrophic floodplain forest of the southeastern Atlantic coastal plain, USA. Wetlands 35, 291-301.
- Scott, D.N., and Wohl, E. (2020). Geomorphology and climate interact to control organic carbon stock and age in mountain river valley bottoms. Earth Surface Processes and Landforms 45, 1911-1925.
- Swinnen, W., Daniels, T., Maurer, E., Broothaerts, N., and Verstraeten, G. (2020). Geomorphic controls on floodplain sediment and soil organic carbon storage in a Scottish mountain river. Earth Surface Processes and Landforms 45, 207-223.
- Wohl, E., Dwire, K., Sutfin, N., Polvi, L., and Bazan, R. (2012). Mechanisms of carbon storage in mountainous headwater rivers. Nature Communications 3, 1263.
- Wohl, E., and Pfeiffer, A. (2018). Organic carbon storage in floodplain soils of the U.S. prairies. River Research and Applications 34, 406-416.

Table S5 continued

wood load data				
location	**reference**	**maP**	**maT**	**wood**
Peru, Amazon lowlands	Chao et al., 2008	2700	27	10
Mexico, dry tropics	Jaramillo et al., 2003	680	25	15
Sweden, boreal forest	Dahlstrom & Nilsson, 2006	800	2	27
Alaska, boreal forest	Lininger et al., 2017	170	-1	42
South Carolina, subtropical	Wohl et al., 2011	1220	18	50
New Mexico	Wohl et al., 2018a	700	7	68
northern Montana	Wohl et al., 2018c	2000	2	490
southeastern Australia	Robinson, 1997; MacNally et al., 2001	435	16	250

western Oregon	Nakamura & Swanson, 1994	2500	8	380
northern Colorado	Jackson, 2014	550	8	66
northern Colorado	Livers et al., 2018	800	4	70
southern Colorado	Wohl et al., 2018a	800	9	128
southwestern Colorado	Wohl, 2020	580	6	198
northern Wyoming	Wohl, 2020	1000	3	190
Washington	Laterell et al., 2006	4500	11	187
northern California	Keller et al., 1995	975	10	740

Reference citations: wood

- Chao, K.J., Phillips, O.L., and Baker, T.R. (2008). Wood density and stocks of coarse woody debris in a northwestern Amazonian landscape. Canadian Journal of Forest Research 38, 795-805.
- Dahlstrom, N., and Nilsson, C. (2006). The dynamics of coarse woody debris in boreal Swedish forests are similar between stream channels and adjacent riparian forests. Canadian Journal of Forest Research 36, 1139-1148.
- Jackson, K. (2014). Instream wood loads in old-growth and non-old-growth montane forests. MS thesis, Colorado State University, Fort Collins, CO.
- Jaramillo, V.J., Kauffmann, J.B., Renteria-Rodriguez, L., Cummings, D.L., and Ellingson, L.J. (2003). Biomass, carbon, and nitrogen pools in Mexican tropical dry forest landscapes. Ecosystems 6, 609-629.
- Keller, E.A., Macdonald, A., Tally, T., and Merrit, N.J. (1995). Effects of large organic debris on channel morphology and sediment storage in selected tributaries of Redwood Creek, northern California. U.S. Geological Survey Professional Paper 1454-P.
- Laterell, J.J., Bechtold, J.S., O'Keefe, T.C., Van Pelt, R., and Naiman, R.J. (2006). Dynamic patch mosaics and channel movement in an unconfined river valley of the Olympic Mountains. Freshwater Biology 51, 523-544.
- Lininger, K.B., Wohl, E., Sutfin, N.A., and Rose, J.R. (2017). Floodplain downed wood volumes: a comparison across three biomes. Earth Surface Processes and Landforms 42, 1248-1261.
- Livers, B., Wohl, E., Jackson, K.J., and Sutfin, N.A. (2018). Historical land use as a driver of alternative states for stream form and function in forested mountain watersheds of the Southern Rocky Mountains. Earth Surface Processes and Landforms 43, 669-684.
- MacNally, R., Parkinson, A., Horrocks, G., Conole, L., and Tzaros, C. (2001). Relationships between terrestrial vertebrate diversity, abundance and availability of coarse woody debris on south-eastern Australian floodplains. Biological Conservation 99, 191-205.
- Nakamura, F., and Swanson, F.J. (1994). Distribution of coarse woody debris in a mountain stream, western Cascade Range, Oregon. Canadian Journal of Forest Research 24, 2395-2403.

- Robinson, R. (1997). Dynamics of coarse woody debris in floodplain forests: impacts of forest management and flood frequency. BSc thesis, Charles Sturt University [cited in MacNally et al., 2001]
- Wohl, E., Polvi, L.E., and Cadol, D. (2011). Wood distribution along streams draining old-growth floodplain forests in Congaree National Park, South Carolina, USA. Geomorphology 126, 108-120.
- Wohl, E., Cadol, D., Pfeiffer, A., Jackson, K., and Laurel, D. (2018a). Distribution of large wood within river corridors in relation to flow regime in the semiarid western US. Water Resources Research 54, 1890-1904.
- Wohl, E., Scott, D.N., and Lininger, K.B. (2018c). Spatial distribution of channel and floodplain large wood in forested river corridors of the Northern Rockies. Water Resources Research 54, 7879-7892.
- Wohl, E. (2020). Wood process domains and wood loads on floodplains. Earth Surface Processes and Landforms 45, 144-156.

Appendix C: Supplemental information for Chapter 4

Data: Soil carbon data and associated sample characteristics are submitted and will be available and searchable on the Mountain Scholar Data Repository and associated with the author Sarah Hinshaw.

The data are also temporarily available via the following link: https://drive.google.com/file/d/1yx_O8lzYgdNCgVLt1LC78GCnmpaE0iRl/view?usp=sharing

Table S6. Measured treatment and predicted treatment stocks using a degraded model for each site to predict Treatment Stocks.

Site	Degraded Model Predictors	OC Stocks (Mg/ha) Measured	Predicted	Measured - Predicted
Fivemile Bell	depth, silt+clay	249	295	-46
Staley	depth, silt+clay	659	305	354
Lost	silt	380	410	-30
South Fork McKenzie	depth, silt+clay	364	232	132
Deep Creek	depth, silt+clay	515	403	112
Whychus Creek	depth, silt+clay	203	147	56
East Canyon Creek	depth, silt+clay, moisture	458	525	-67
Kimball Creek	depth, silt+clay	1028	910	118

Table S7. Years of restoration treatment at each site with verification information.

Site	Year of Restoration	Year Sampled	Years Since	Verified?
South Fork McKenzie	2018	2020	2	Personal communication, US Forest Service staff
Whychus Canyon	2016	2020	4	Whychus Creek Remote Sensing Report
Whychus Camp Polk	2012	2020	8	https://www.deschuteslandtrust.org/protected-lands/camp-polk-meadow-preserve/cpm-restoration/camp-polk-whychus-restoration
Kimball Creek	2019	2021	2	Personal communication, Swaner Preserve staff
East Canyon Creek Downstream (T1)	2015	2021	6	Personal communication, Swaner Preserve staff
East Canyon Creek Upstream (T2)	2019	2021	2	Personal communication, Swaner Preserve staff
Fivemile Bell R1	2018	2020	2	Paul Burns personal communication and presentation handout, USFS Report
Staley Creek	2017	2020	3	https://www.middleforkwillamette.org/restore/rivers-and-streams/staley-creek/
Deep Creek	2018	2020	2	Paul Powers personal communication
Lost Creek	2012	2020	8	https://stagezeroriverrestoration.com/Lost_creek.html

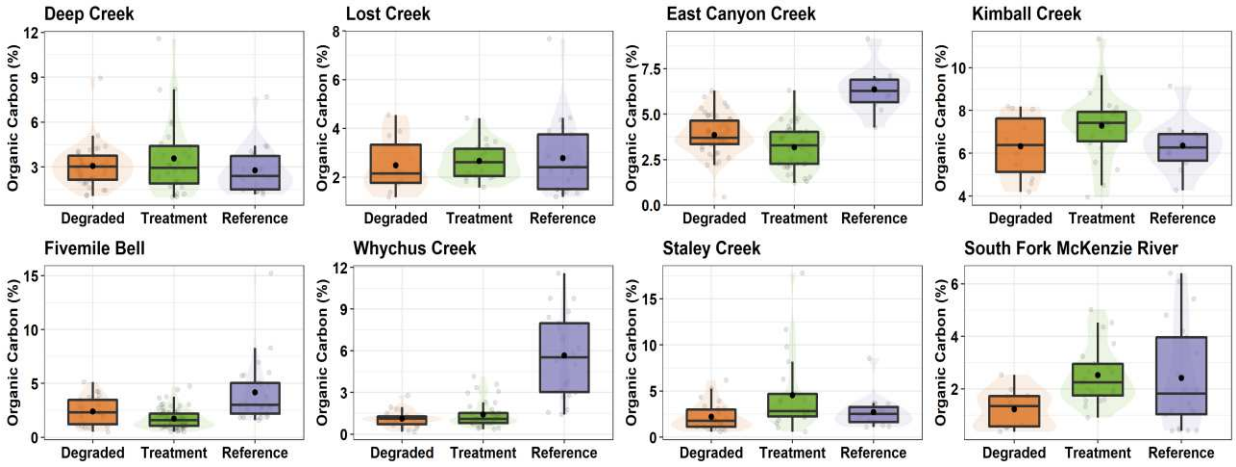

Figure S1.Box and whisker plots of percent organic concentration at each of the 8 sites measured.

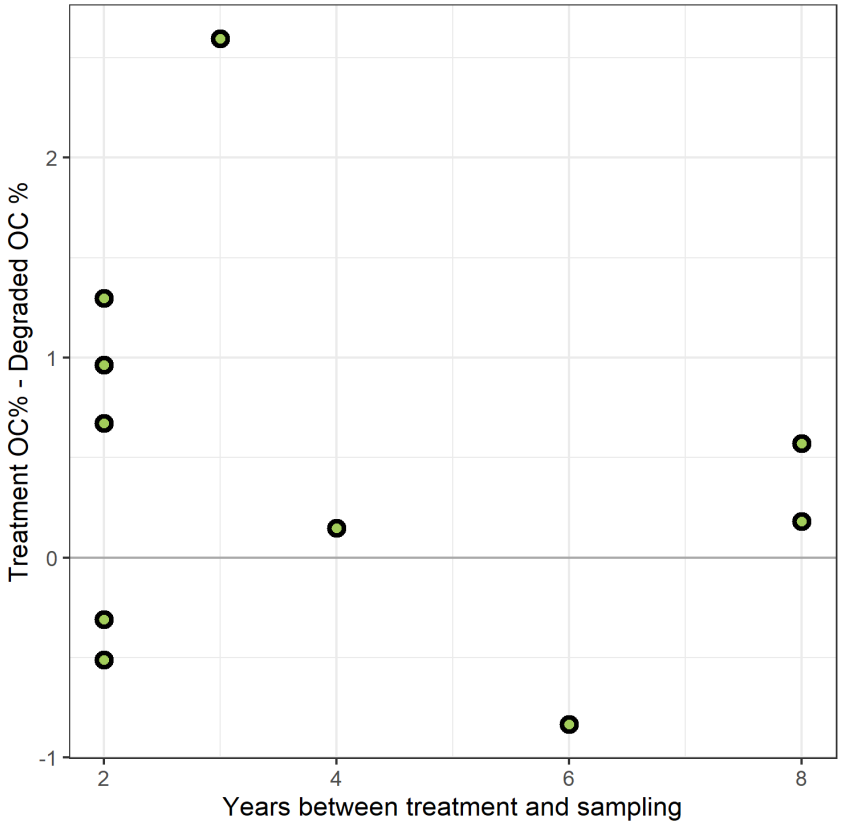

Figure S2. Scatterplot of difference in carbon stocks between treatment and degraded, and time since restoration treatment and sampling. No correlation was found between time since treatment and

Sample I-R1-8, a sample from Indian Ford Creek, a reference site for Whychus Creek, had 11.573 % Organic Carbon.

Figure S3. Photo of a soil sample in the field.